AVANCES EN LAS TECNICAS DE REDUCCION DE TAMAÑO Y CLASIFICACION DE PARTICULAS FINAS
DEL 30 DE SEPTIEMBRE AL 4 DE OCTUBRE DE 1996
DIRECTORIO DE PROFESORES

ING. JORGE ORNELAS TABARES
DEPTO DE EXPLOT DE MINAS Y METALURGIA
DIV INGRIA DE CIENCIAS DE LA TIERRA, FI
EDIF. PRINCIPAL CIUDAD UNIVERSITARIA
COYOACAN
04510 COYOACAN, MEXICO D.F.
550 00 40 FAX 622 08 55

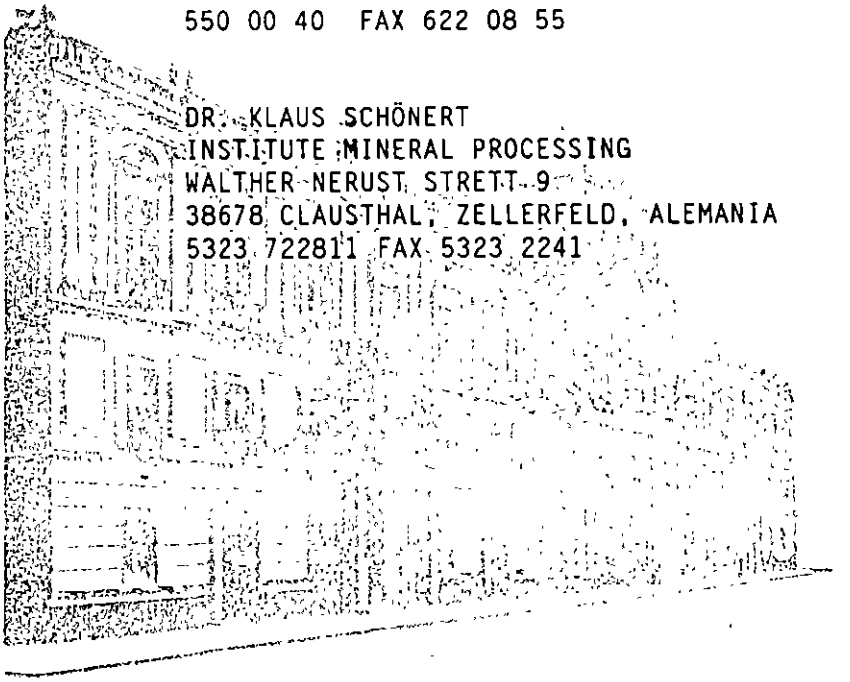

DR. KLAUS SCHÖNERT
INSTITUTE MINERAL PROCESSING
WALTHER NERUST STRETT 9
38678 CLAUSTHAL, ZELLERFELD, ALEMANIA
5323 722811 FAX 5323 2241

DIVISION DE EDUCACION CONTINUA
FACULTAD DE INGENIERIA, UNAM
CURSOS ABIERTOS

CURSO: CURSO NO. 160 AVANCES EN LAS TECNICAS DE REDUCCION DE TAMAÑO Y CLASIFICACION DE PARTICULAS FINAS
FECHA: DEL 30 DE SEPTIEMBRE AL 4 DE OCTUBRE/96

EVALUACIÓN DEL PERSONAL DOCENTE

(ESCALA DE EVALUACIÓN: 1 A 10)

CONFERENCISTA	DOMINIO DEL TEMA	USO DE AYUDAS AUDIOVISUALES	COMUNICACIÓN CON EL ASISTENTE	PUNTUALIDAD
ING: JORGE ORNELAS TABARES				
ING: KLAUS SCHONERT				

Promedio _____

EVALUACIÓN DE LA ENSEÑANZA

CONCEPTO	CALIF.
ORGANIZACIÓN Y DESARROLLO DEL CURSO	
GRADO DE PROFUNDIDAD DEL CURSO	
ACTUALIZACIÓN DEL CURSO	
APLICACIÓN PRACTICA DEL CURSO	

Promedio _____

EVALUACIÓN DEL CURSO

CONCEPTO	CALIF.
CUMPLIMIENTO DE LOS OBJETIVOS DEL CURSO	
CONTINUIDAD EN LOS TEMAS	
CALIDAD DEL MATERIAL DIDÁCTICO UTILIZADO	

Promedio _____

Evaluación total del curso_____

Continúa...2

1. ¿Le agradó su estancia en la División de Educación Continua?

SI ☐ NO ☐

Si indica que "NO" diga porqué: _____

2. Medio a través del cual se enteró del curso:

Periódico *Excélsior*	
Periódico *La Jornada*	
Folleto anual	
Folleto del curso	
Gaceta UNAM	
Revistas técnicas	
Otro medio (Indique cuál)	

3. ¿Qué cambios sugeriría al curso para mejorarlo?

_____

_____

_____

_____

_____

_____

4. ¿Recomendaría el curso a otra(s) persona(s) ?

SI ☐ NO ☐

5.¿Qué cursos sugiere que imparta la División de Educación Continua?

_____

_____

_____

_____

_____

_____

6. Otras sugerencias:

_____

_____

_____

_____

_____

FACULTAD DE INGENIERIA U.N.A.M.
DIVISION DE EDUCACION CONTINUA

AVANCES EN LAS TECNICAS DE REDUCCION DE TAMAÑO Y CLASIFICACION DE PARTICULAS FINAS

PROFESOR KLAUS SCHONERT

1996

INTRODUCTION (1)

Comminution is a very ancient technique, corn, and minerals have been milled since some thousends years with:

Roller mills, cone mills, buhr mills, stamp mills.

The material is stressed between two hard surfaces by compression and shear.

Tumbling mills were developed at the beginning of the last century, the material is also stressed by compression and shear between the tumbling bodies.

Another mode of stressing is that particles collide with a beater or a wall or another particle. This so-called impact stressing is performed in rotor impact mills or jet mills, which are developed about 1870/90 and 1920/30 respectively.

Modern comminution technology is using still these both modes of stressing, however in much more sophisticated designed machines in order to master great mass throughput and to improve the efficiency.

INTRODUCTION (2)

Comminution is a widely uses process, almost all solid materials have to be crushed and ground:
minerals, ores, coal, stones, cement clinker, wood, food stuffs, chemicals, pharmaceuticals, plastics, waste materials etc.

Comminution is a very energy consuming process, about 3.5 % of the produced electrical energy is used for comminution, the main consumers are:

cement industry	0.8 %
mineral processing	0.6 %
wood industry	0.6 %
coal processing	0.2 %

In some cases comminution takes an essential fraction of the production costs e.g.

mineral processing	40 ... 60 %
cement making	25 ... 35 %
polymer powder production	50 ... 70 %

A comprehensive understanding of comminution proccesses and improving them are valuable for the profit of companies, national economy and enviroment protection

CLASSIFICATION OF COMMINUTION MACHINES (1)

Classifying in respect to
(a) particle size of feed and product
(b) desing and operation characteristics

Classification after (a):

- **Crushers**

coarse feed, particles > 100 mm, up to lumps of 1000 mm or even more
size reduction ratio 5 to 15, in special cases with hammer crushers up to 30 ... 50.

- **Grinding mills**

fine feed, particles < 30 mm
product fineness < 1 ... 3 mm, often < 100 µm
mills are often operated in the closed circuit mode in connection with a classifier.

Comminution machines serving in the intermediate are called fine crushers or coarse mills. The classification in respect to the particle size gives a general guidline, however not a scheme with strongly set boundaries.

CLASSIFICATION OF COMMINUTION MACHINES (2)

Classification after (b)

Design and operation characteristics provide a more reasonable classification useful for theory development, investigating fundamental and practical aspects, modelling, machine and process improvements.

Crushers

Jaw crushers
Gyratory crushers
Cone crushers
Roll crushers
Hammer crushers
Impact crushers
Schredders (special designed hammer crusher for waste materials)

CLASSIFICATION OF COMMINUTION MACHINES (3)

Grinding Mills

- **Grinding media mills**

  rod, ball, pebble, autogeneous, semi-autogeneous, stirred, vibration, planetary mill,

The media tumble freely in a container, the particles are to. catch between two media for being stressed.

- **Roller mills**

  roller-table, roller-ring, ball-table, high pressure roller mills

A bed of particles is stressed between a roller or a big ball and a rotating tabel, between a roller and a rotating ring, between two roating rollers. The size reduction occurs mainly by inter-particle breakage.

- **Impact mills**

  rotor impact mills, jet mills

The particles collide with a beater, the mill wall or with another particle, collision velocty 20 to 100 ... 150 m/s, energy introduced either by a rotor or a fluid jet.

- **Hammer mills**

One or two rotors are equiped with swinging hammers, they hit on the particles which either are resting on a stationary plate or are moving freely in the mill chamber, stressing either by a fast compression or by colliding with a hammer.

FUNDAMENTALS

Contents

SCHEME OF COMMINUTION PROCESSES (1)

Any comminution process can be discribed schematically as follows:

- The feed is introduced into the mill chamber.
- Material stressing happens only in locally restricted regions, e.g. in the contact region of two balls or between a roller and the table or at a beater surface.
- The particles have to move into these active volumes, must be stressed there and afterwards have to leave it.
- The product is to discharge out the mill chamber.

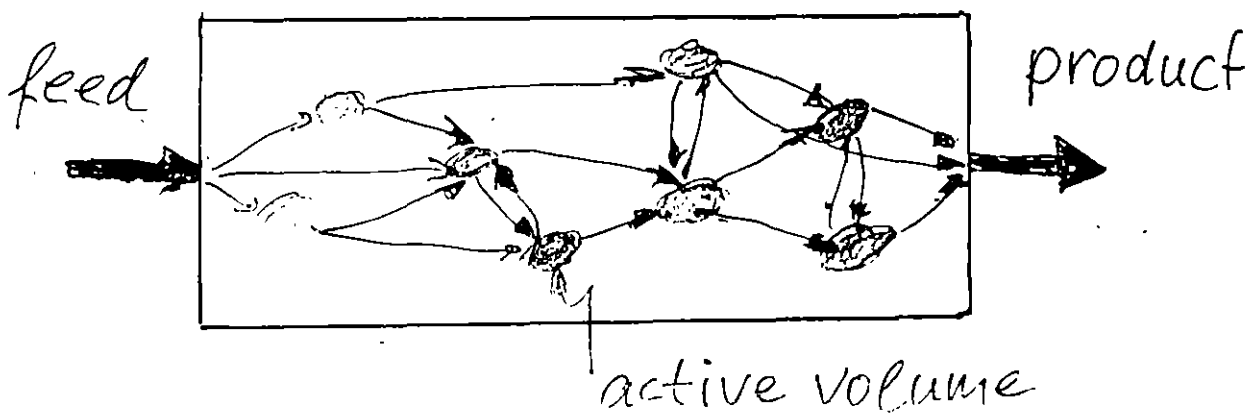

Three areas of fundamentals follows:

(1) material transport phenomena

(2) defining and identificating active volumes

(3) particle breakage phenomena

SCHEME OF COMMINUTION PROCESSES (2)

Fundamental areas

(1) Material transport phenomena:
feeding, stochastical and/or deterministic motion inside the mill, probability for introducing the particles into the active volume (e. g. between two balls), mechanics of the introduction of material into a roller gap, discharging

(2) Defining and indentificating active volumes
geometry of the active volumes, spatial distribution, probability of stressing, stressing intensity spectrum

(3) Particle breakage phenomena
defermation behaviour, fracture physics, single and interparticle breakage, size reduction characteristics

SCHEME FOR COMMINUTION PROCESSES (7)

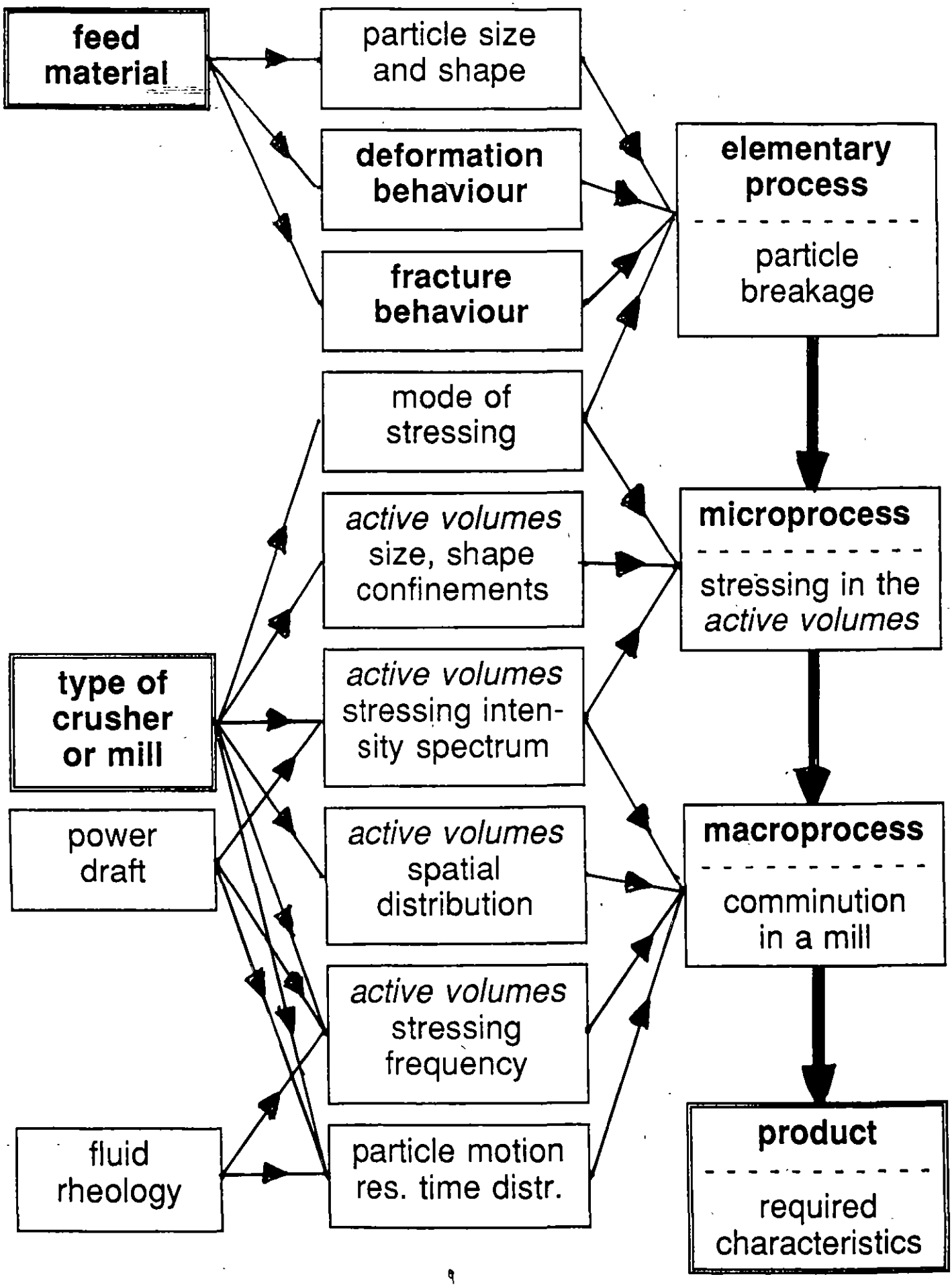

MODES OF STRESSING (1)

Particles or a particle bed can be stressed in different modes, it is reasonable to distinguish in respect to the acting forces and the energy transmission to the particles.

(1) compression - shear stressing
(2) impact stressing
(3) stressing in a shear flow
(4) other methods of energy transmission

(1) Compression - shear stressing between two hard surfaces

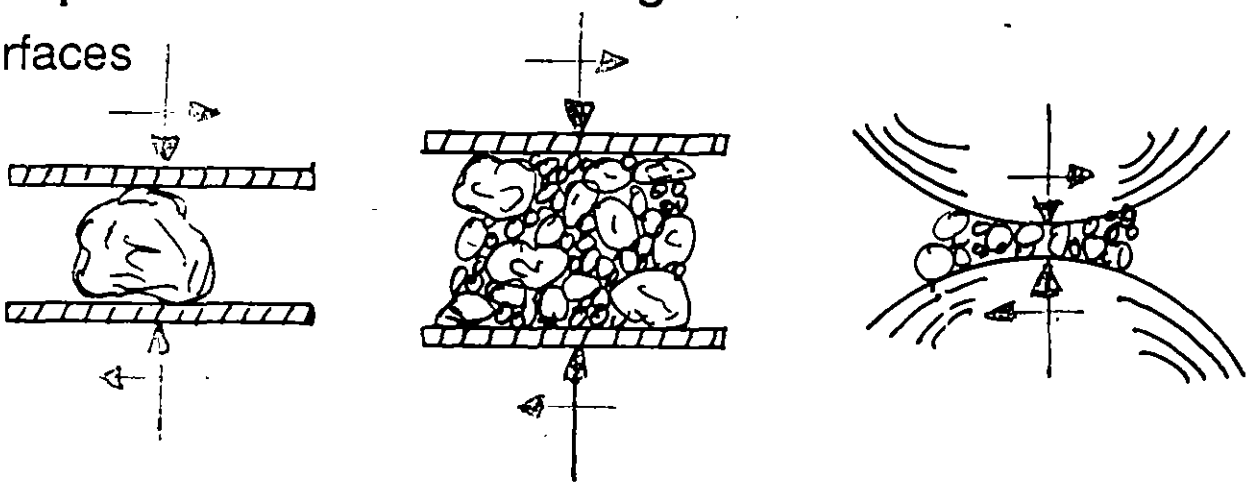

Acting forces are in equilibrium, particle inertia can be neglected, stressing velocity in mills smaller than 1 ... 5 m/s, forces and energy are independent of stressing velocity, stressing intensity is limited by

- available energy (grinding media mills)
- applied force (roller mills)
- given gap width (jaw crushers)

MODES OF STRESSING (2)

(2) **Impact stressing** by a collision with a body or another particle

Contact force in equilibrium with particle inertia, stressing velocity in mills 20 ... 100 (150) m/s, stressing energy equal kinetic energy of the particle

(3) **Stressing in the shear flow** of a highly viscous fluid

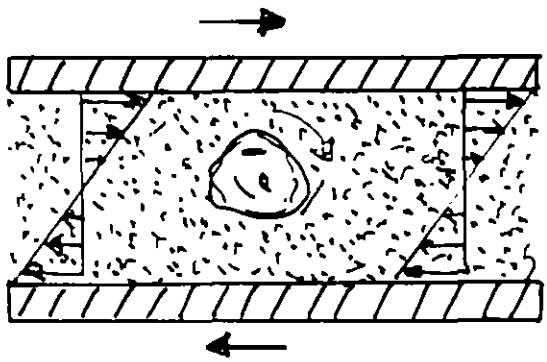

The particle rotates and is subjected to shear, arising stresses are too small to break compact particles however can destroy agglomerates.

(4) **Other methods of energy transmission**

Shock waves, ultrasonic wave field, electrical discharges, heating, heating and quenching. These exotic methods may be applied in very special cases, however are burden with a high energy consumption.

SCHEME OF PARTICLE BREAKAGE (1)

Particle breakage is the elementary process in comminution and can be described as follows:

- The particle is stressed by at least one contact force and is deformed.
- A three-dimensional stress field arises.
- If somewhere the crack criterion is met, then at least one crack is released; mostly many cracks are released.
- After one crack has crossed throughly, the particle is broken
  1 → **breakage point, primary breakage**
- The fragments move sidewards and form a more or less dense pile,
- The stressing continues and some of the primary fragments are broken and so on.
  2 → **secondary breakage**

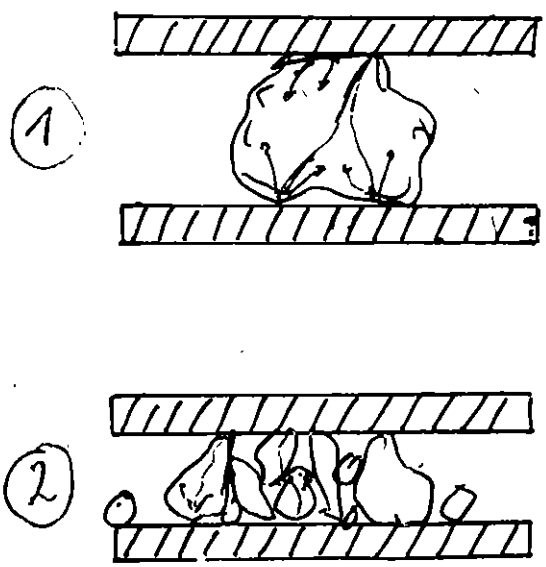

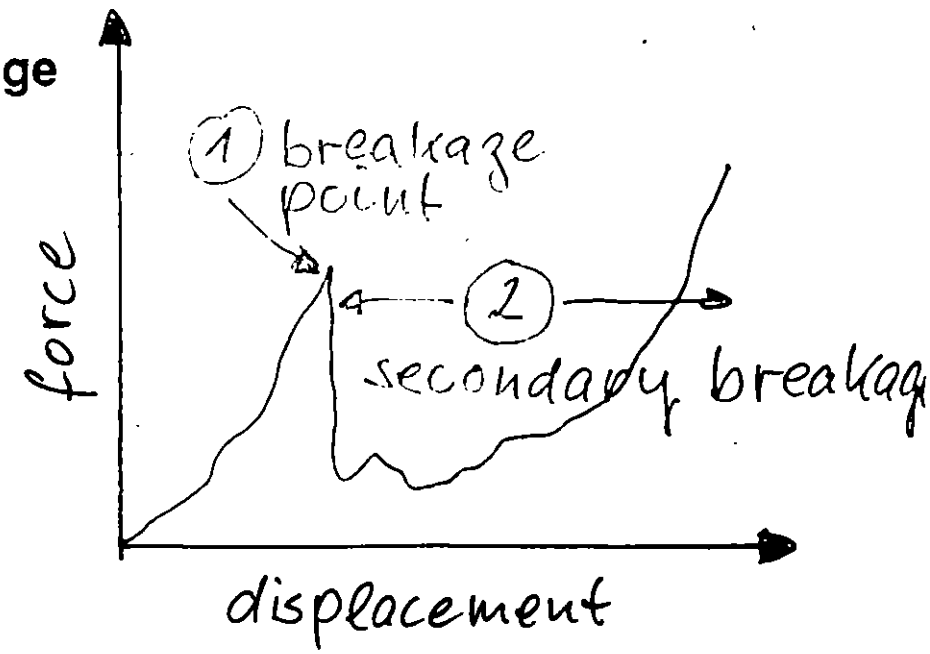

SCHEME OF PARTICLE BREAKAGE (2)

The stress field and the material strength determine the particle breakage. The stressing conditions and the particle properties influence the breakage event.

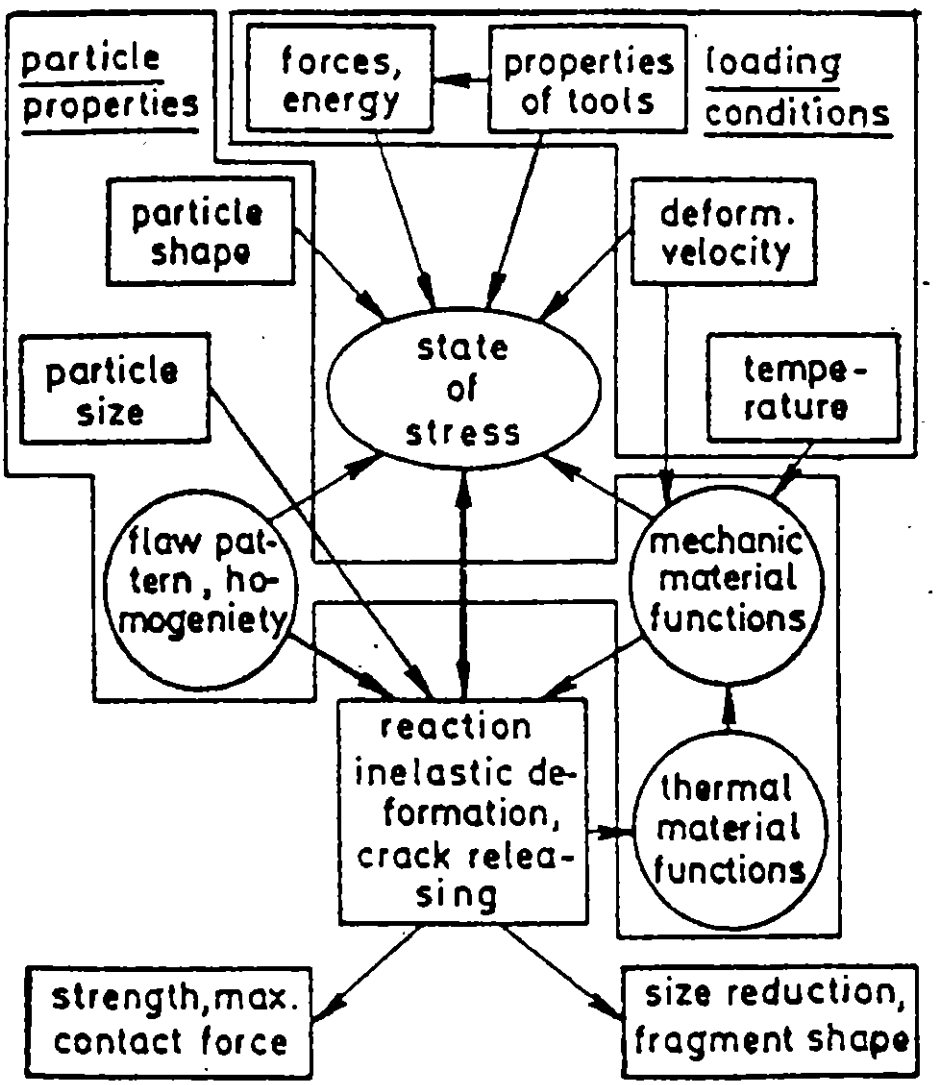

DEFORMATION BEHAVIOUR OF SOLIDS (1)

The release of a crack is caused by a critical stress field situation. The contact forces deforme the particle and cause a strain field. Strain and stress is related to each other by hypothetical material laws (strain-stress relations).

The established strain-stress relations are valid only for small strains and fail at high strains which arises in the critical situations. The deformation behaviour of real materials is complex, nevertheless knowledges on the established relations are helpful for understanding particle breakage.

Three idealized boundary cases.

- elastical deformation (1)
- inelastical deformation

→ elastic-plastic deformation (2)

→ elastic-viscous deformation (3)

DEFORMATION BEHAVIOUR OF SOLIDS (2)

(1) Elastic deformation

- reversible deformation
- no energy dissipation
- independent on strain rate and temperature

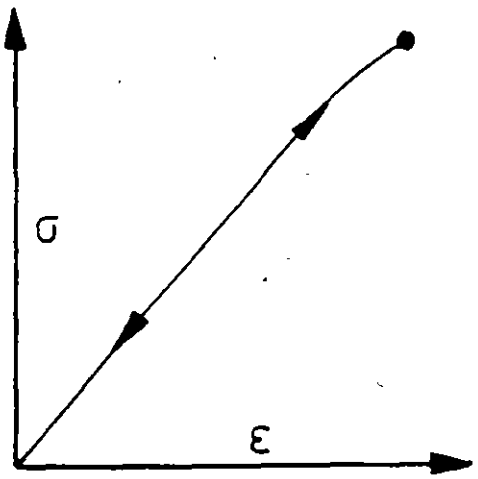

Most simple case:

isotropic linear elasticity.
(Hook´s law)

Stress-strain relation includes only two independent constrants, e. g. Young`s modulus Y and Poisson number ν.

(2) Elastic-plastic deformation

- irreversible deformation
- energy dissipation
- dependent on temperature
- "embrittlement" at low temperature and by multiple stressing
- almost independent on temperature

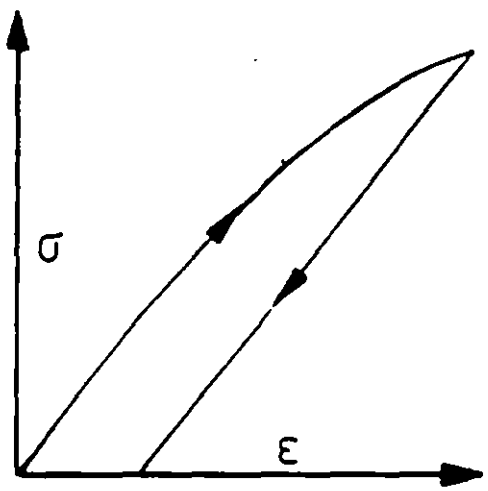

Most simple case:

isotropic ideal elastic-platistic behaviour.

stress-strain relation includes two constants (Y, ν) and a temperature sensitive yield strength $\sigma_y(T)$.

DEFORMATION BEHAVIOUR OF SOLIDS (3)

(3) Elastic-viscous deformation

- irreversible deformation
- energy dissipation
- dependent on strain rate and temperature, the irreversibility decreases as the strain rate raises or the temperature declines.

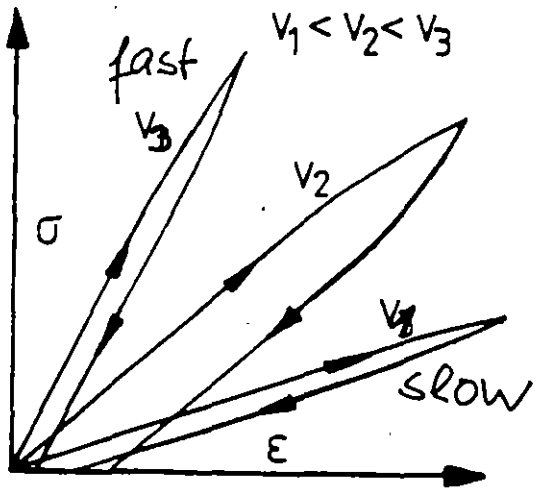

Most simple case:
isotropic linear visco-elasticity

Stress-strain relation includes so-called modulus function, e.g. the strain relaxtion modul function.

DEFORMATION BEHAVIOUR OF SOLIDS (4)

Conclusions for comminution processes

(1) Particles deforming mainly elastically, so-called brittle particles (ores, quartz, calcite, hard coal):

No influence of stressing velocity and temperature,
grinding media and roller mills for hard and impact mills for soft brittle materials

(2) Particles deforming elastic-plastically (soft coal, metalls):

Less influence of stressing velocity, strong influence of temperature, low temperature and multiple stressing advantageously,
grinding media and impact mills

(3) Particles deforming elastic-vicously (polymers):

Strong influence of stressing velocity and temperature, high velocity and low temperature advantageously,
impact mills, cooled impact or vibration mills

FRACTURE PHYSICS (1)

Crack release and propagation is controlled by energy balances.

main energy source : elastic stress field

main energy sink : strong inelastic deformations at crack tip

Energy release rate G

$G = -\partial U_{el} / \partial A_{cr}$ U_{el}: stress field energy; A_{cr}: crack area

most simple case:
uniaxial stressed plate

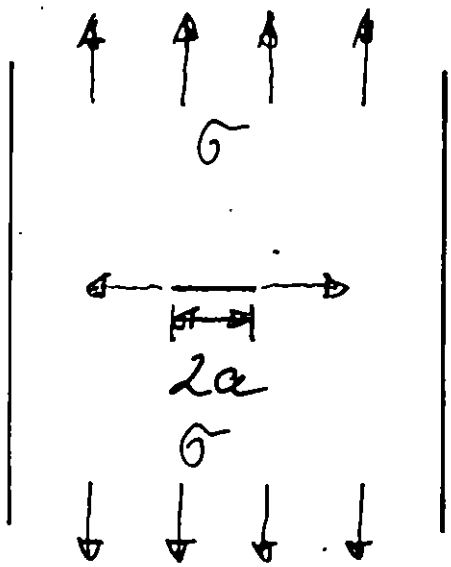

$$G = \pi a \sigma^2 / Y$$

G_c: critical value for crack releasing

Specific fracture energy R

energy consumed by the crack per crack area unit

Differential energy balance for crack releasing

$$G_c = R_o$$

R: specific fracture area energy

glasses	G_c =	1	to	10	J/m^2
brittle polymers	G_c =	10	to	10^3	J/m^2
steel	G_c =	10^3	to	10^5	J/m^2
specific surface energy	γ =	0.01	to	0.5	J/m^2

FRACTURE PHYSICS (2)

The high stress concentration at the crack tip causes strong inelastic deformation in the **crack-zone**, by which the delivered energy dissipates as heat. The size δ of that zone can be estimated:

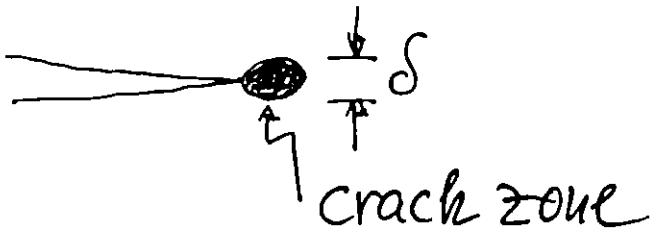

$$\delta \approx 0.4\ G_c\ Y / \sigma_y^2$$

σ_y : yield stress

glases δ = 10 to 100 Å; brittle polymeres δ = 1 to 10 µm

A crack has to cross throughly the particle to break it. In small particles, the elastic stored energy may not cover the energy needed for the total crack path, the crack stops and the particle has to be stressed again

Intergral energy balance

For assuring the breakage of a cylindrical specimen

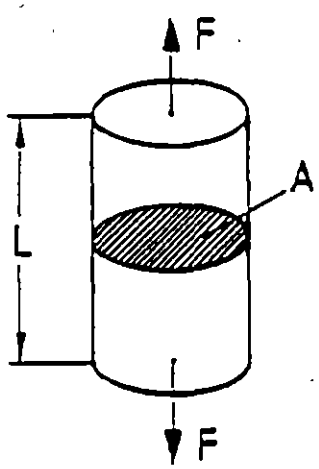

$$(\sigma_{cr}^2 / 2\ Y)\ A\ L \geq \bar{R}\ A$$

$$L \geq 2\ \bar{R}\ Y / \sigma_{cr}^2$$

glasses L > 10 to 100 µm; steel L > 2 to 20 mm

FRACTURE PHYSICS (3)

Conclusions for comminution processes

(1) specfic fracture energy R ecxeeds strongly the specific surface energy γ, therefore γ and its modificating by surfactants has no influence on particle breakage. The so-called Rehbinder-effect does not exist.

(2) The crack zone size determines the smallest fragment size x_{min}, for brittle materials x_{min} = 0.02 to 0.1 µm.

(3) Fracture surfaces are structutally disordered: concentration of dislocations, crystal modifications, amorphous regions, reduced molecular weigth. The enthalpy in the fracture surface region is increased.

(4) The integral energy balance is not satisfied, if the particles become small, multiple stressing has to be performed for particles breakage.

STRESS FIELD IN THE CONTACT REGION (1)

The **Hertz-Huber-Theory** describes the stress field in the contact region of a compressed or impacted sphere for linear elastic behaviour

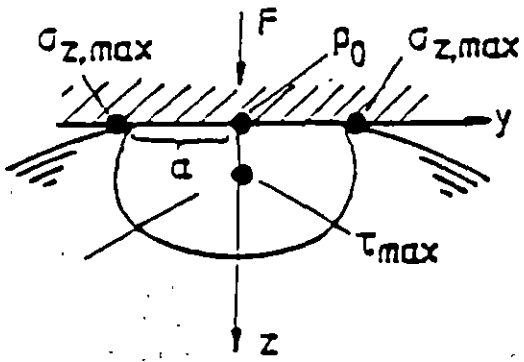

p_o : max. compression stress
τ_{max} : max. shear stress
$\sigma_{z,\,max}$: max. tensile stress
R: sphere radius
F : force
v : impact velocity

Y_s, Y_p, ν_s, ν_p : Young modulus and Possion number of sphere and plate

$p_o : \tau_{max} : \sigma_{z,max} = 1 : (0.2 \text{ to } 0.3) : (0.11 \text{ to } 0.17)$

$$p_o / Y_s = \left\{(\pi/\sqrt{6})\ (1+\kappa)\ \left(1-\nu_s^2\right)\right\}^{-2/3} \left\{F / \pi\ R^2\ Y_K\right\}^{1/3} \quad \text{compression}$$

$$p_o / Y_s = 0.87\,(1+\kappa)^{-4/5}\,(v/c_l)^{2/5} \quad \text{impact}$$

$$\kappa = \left(1-\nu_p^2\right)\ Y_s / \left(1-\nu_s^2\right)\ Y_p$$

$$c_l^2 = \{(1-\nu_s)\ /\ (1+\nu_s)\ (1-2\nu_s)\}\ \{Y_s\ /\ \rho_s\}$$

STRESS FIELD IN THE CONTACT REGION (2)

Evaluation ~~of~~ p_o for glass sphere against steel plate after Hertz Equ.

$Y_s = 70000\ N/mm^2$, $Y_p = 210000\ N/mm^2$

$F/\pi R^2$	:	35	70	140	280	N/mm^2
p_o	:	4100	5170	6520	8210	N/mm^2

v	:	10	30	100	m/s
p_o	:	3990	6300	10500	N/mm^2

molecular strength of glass about 7000 N/mm^2

1mm glass spheres break in compression at $F/\pi r^2$ about 400 N/mm^2 and by impacting at v about 80 m/s, therefore the contact region is deformed inelastically before breakage.

In fine particles of brittle materials the contact region is deformed inelastically, a cone-shaped volume is indented into the sphere and causes ring stresses, which level depends on indentation depth.

STRESS FIELD IN THE CONTACT REGION (3)

Contact forces act obliquely on the particle, therefore it is stressed by normal and tangential forces.

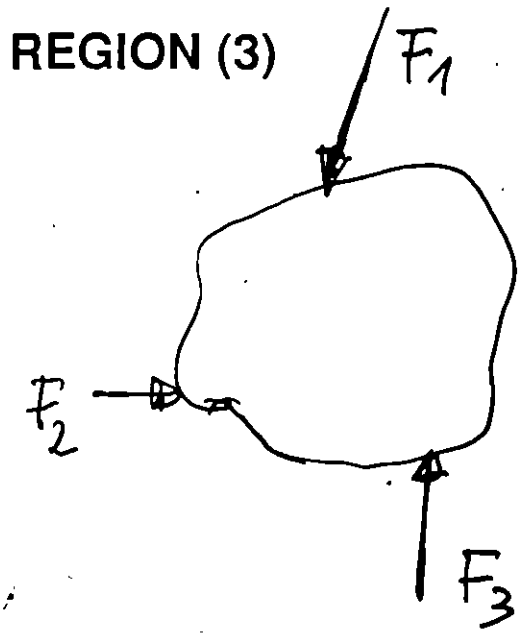

The tangential forces increase the tensile stress, therefore, the particle may fail at a lower normal force. Experiments have shown this effect with glass spheres however not with cement-stone spheres

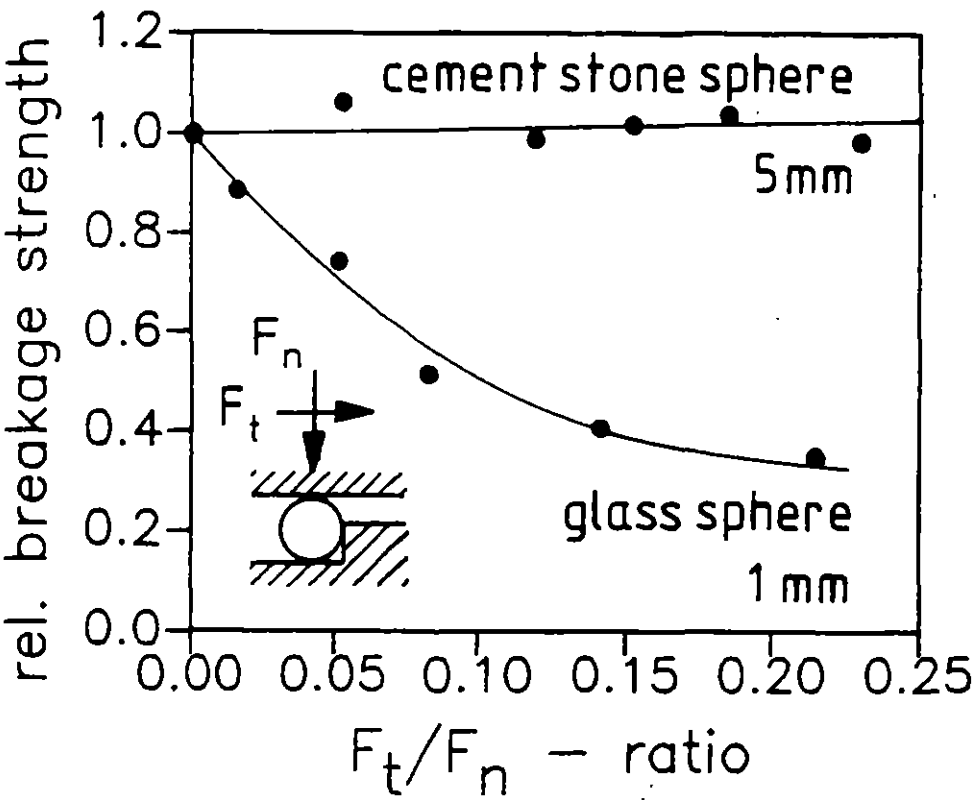

STRESS FIELD IN THE CONTACT REGION (4)

Often is said, impacting causes shock waves in a particle and by that interior cracks. Shock waves are only created if the impact time τ is smaller than the travelling time t_W of the elastic wave through the particle. This time ratio can be calculated with the Hertz equation.

$$\tau / t_W = 5.09\ (1+\kappa)^{2/5}\ (1-\nu_S)^{4/5}\ (1-2\nu_S)^{-2/5}\ (c_l/v)^{1/5}$$

Evaluation for glass sphere against steel plate after Hertz Eqn

v	:	50	100	200	m/s
τ / t_W	:	15	13	11	

impact time much larger than travelling time, inelastic effects in the contact region prolong the impact time ⟶ no wave induced cracks

STRESS FIELD IN THE CONTACT REGION (5)

Conclusion for comminution processes

(1) If the contact region deformes elastically, then maximum tensile stresses at the edge of the contact area, cracks are released there.

(2) The maximum shear stress below the contact center is about twice the maximum tensile stress. If the yield criterion is met before the fracture cristerion, then the contact region deforms inelastically. This effect happens with fine particles. Then cracks are caused by the ring stresses.

(3) Superimposed tangential forces (stressing by friction) support particle breakage only if the contact region does not deforme inelastically. Friction can round particles however cannot break them.

(4) Shock waves are not created by impacting, therefore no wave induced crack releasing.

FRACTURE PATTERN (1)

Cleavage cracks travel perpendicular to the maximum tensile stress, shear cracks parallel to the maximum shear stress.

Principal Pattern I - elastically deformed contact region

ring-shaped surface cracks around the contact area

- divergent cone cracks starting at ring cracks
- breakage by interior cracks on outwardly bended rotational planes starting at divergent cone cracks, onion peel shaped cracks
- cone of fine fragments in the contact region

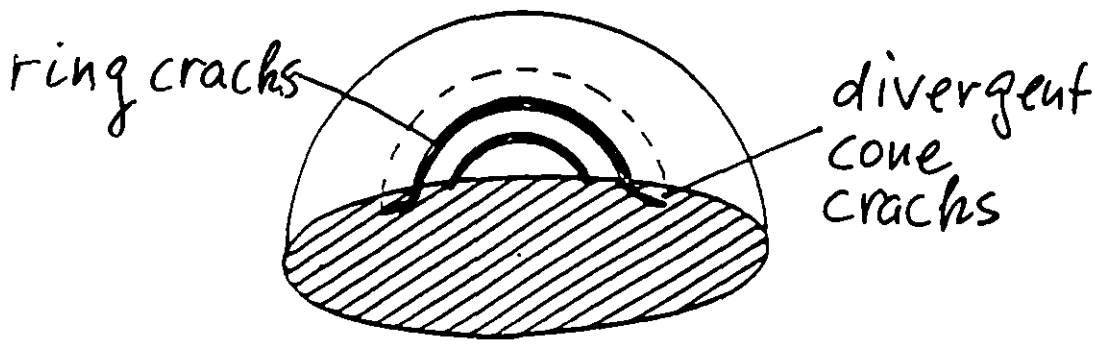

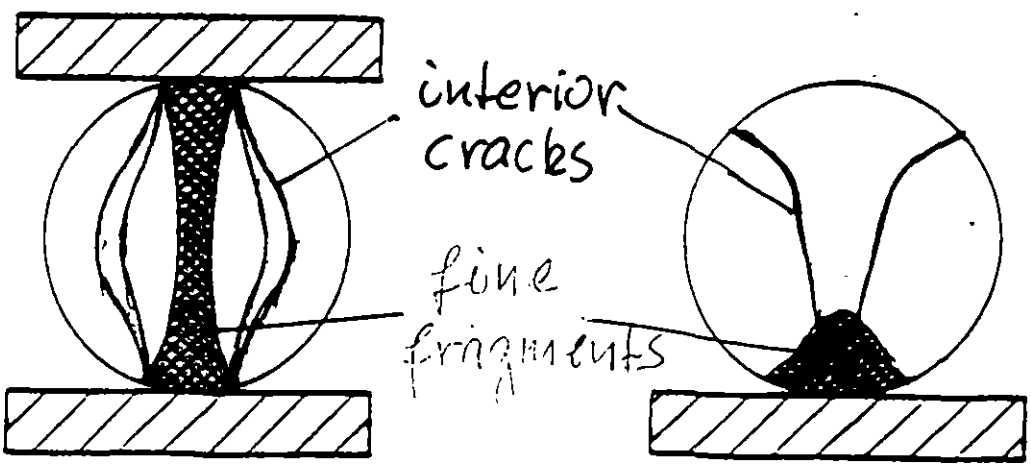

FRACTURE PATTERN (2)

Principal pattern II - inelastically deformed contact region

- indentation of a cone-shaped volume
- breakage by meridional cracks
- unbroken indentation cone

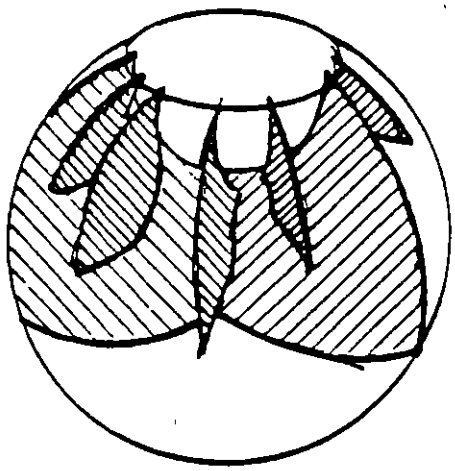

Transition pattern - partly inelastically deformed contact region

- breakage by interior and meridional cracks
- partly broken indentation cone

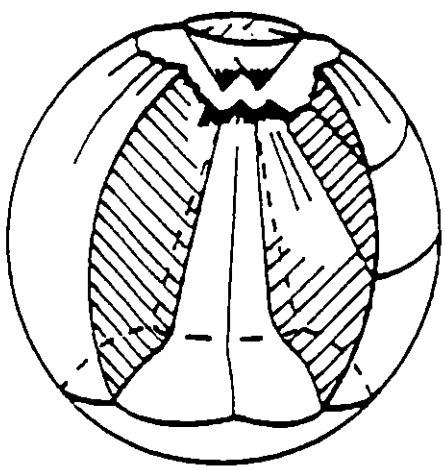

PARTICLE STRENGTH

Measuring the breakage point

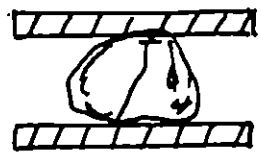

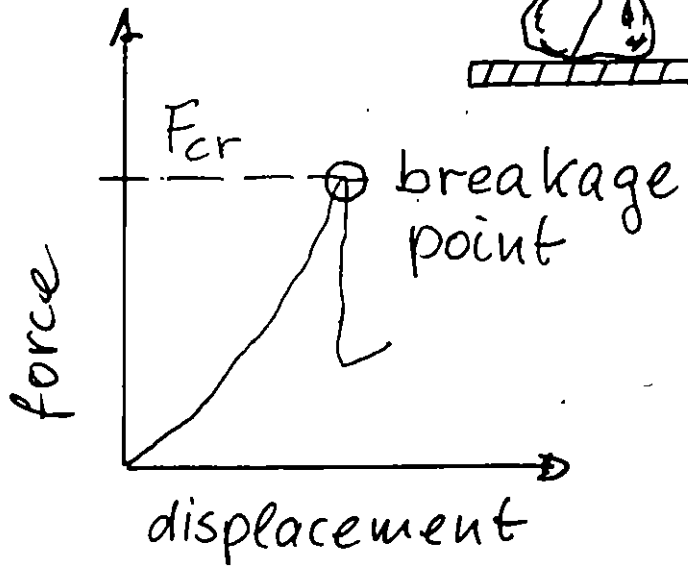

$$\sigma_p = 4\ F_{cr} / \pi\ x^2$$

σ_p: particle strength, x : particle size, F_{cr}: breakage force

Particle strength increases with decreasing particle size, less and smaller material failures, the particle become more homogeneous, the inelastic effects become greater.

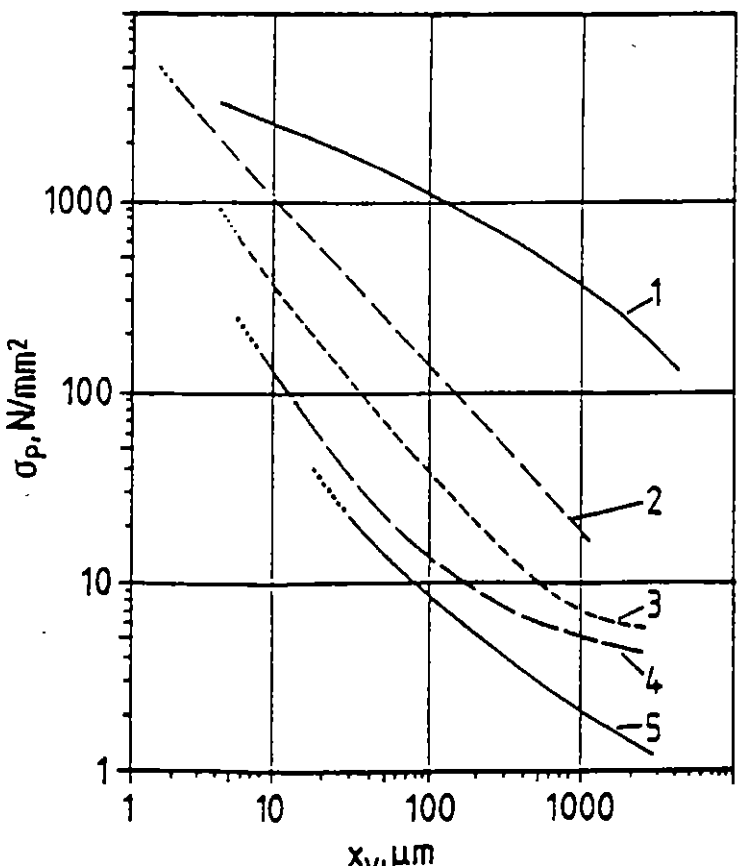

(1) glass beats
(2) crytalline boron
(3) quartz
(4) calcite
(5) black coal

BRITTLE-PLASTIC TRANSITION

The inelastic effect becomes dominantly in very fine particles, even particles of brittle materials do not have a breakage point

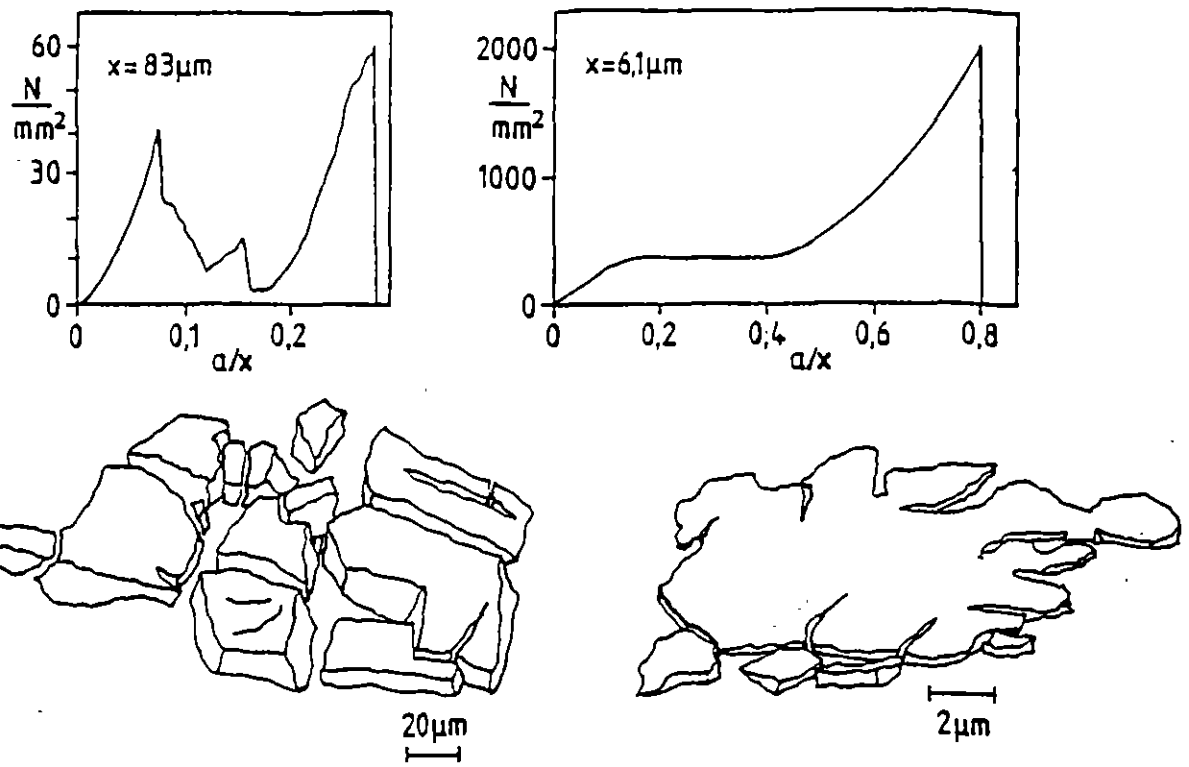

Below the brittle-plastic transition comminution becomes difficulty

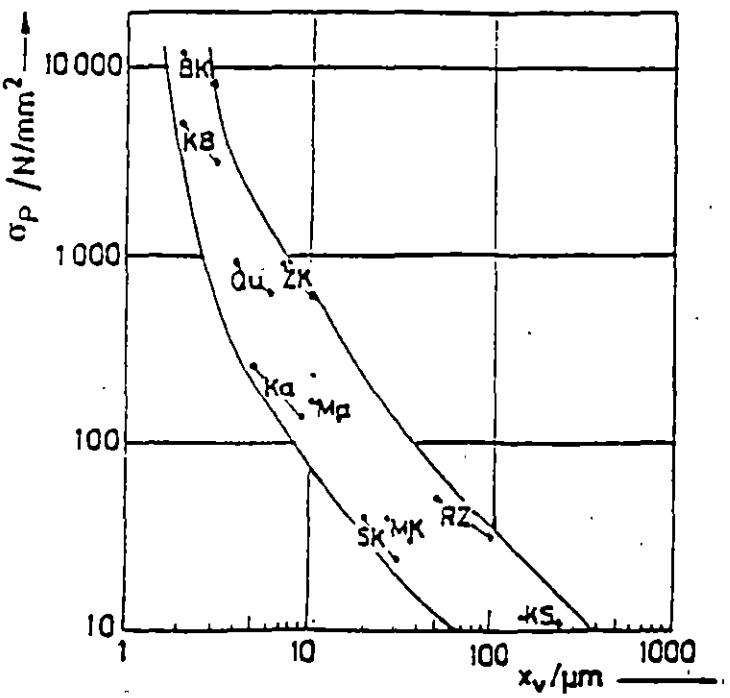

KS calcium chloride
SK black coal
MK coal mixture
RZ sugar
Ka calcite
Ma marble
Qu quartz
ZK cement clinker
KB crystalline boron

SINGLE PARTICLE BREAKAGE (1)

The deformation and breakage is studied in single particle experiments

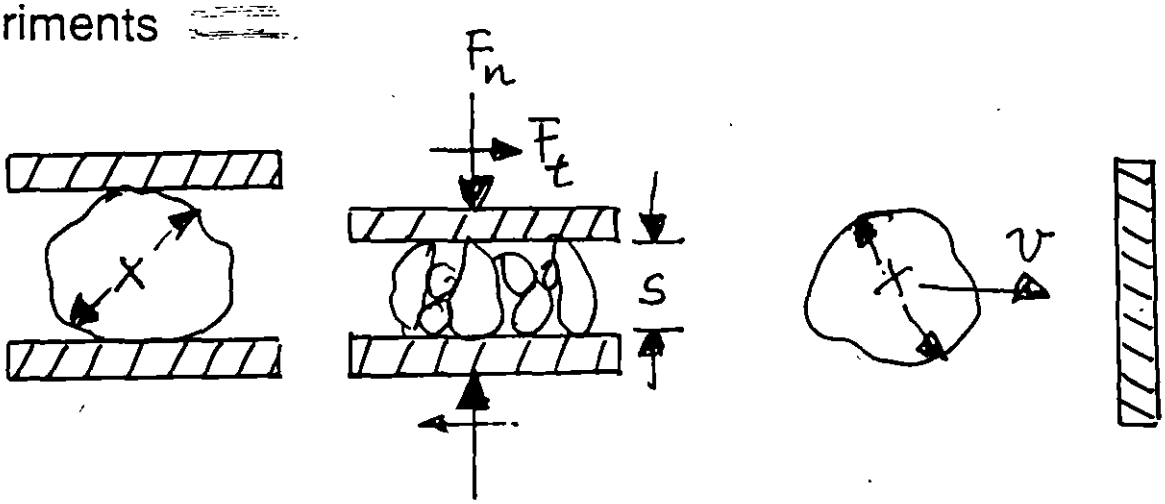

The following characteristics can be measured:

- particle strength (compression)
- particle breakage energy (compression)
- breakage probability (compression, impact)
- specific reaction force (compression)
- product size distribution (compression, impact)
- breakage function (compression, impact)

(1) Particle strength σ_p

force F_{cr} at breakage point related to the nominal cross-section of the particle of size x

$$\sigma_p = 4\ F_{cr} / \pi\ x^2$$

In the fine size range σ_p increases strongly as the particle becomes finer.

(2) Particle breakage energy E_M, E_V

Energy E used up to the breakage point related to the nominal mass or volume of the particle

$$E_M = 6\,E / \rho\,\pi\,x^3 \qquad E_V = \rho\,E_M$$

ρ: density

In the fine size range E_M and E_V increase strongly as the particle becomes finer corresponding to σ_p.

(3) Breakage Probability P

Number N_{br} of broken particles related to number N of stressed particles as a function of the stressing intensity quantified by either particle strength, particle breakage energy, kinetic impact energy or impact volocity

$$P = N_{br} / N$$

The P-distribution shifts to higher intensities and becomes broader with decreasing particle size.

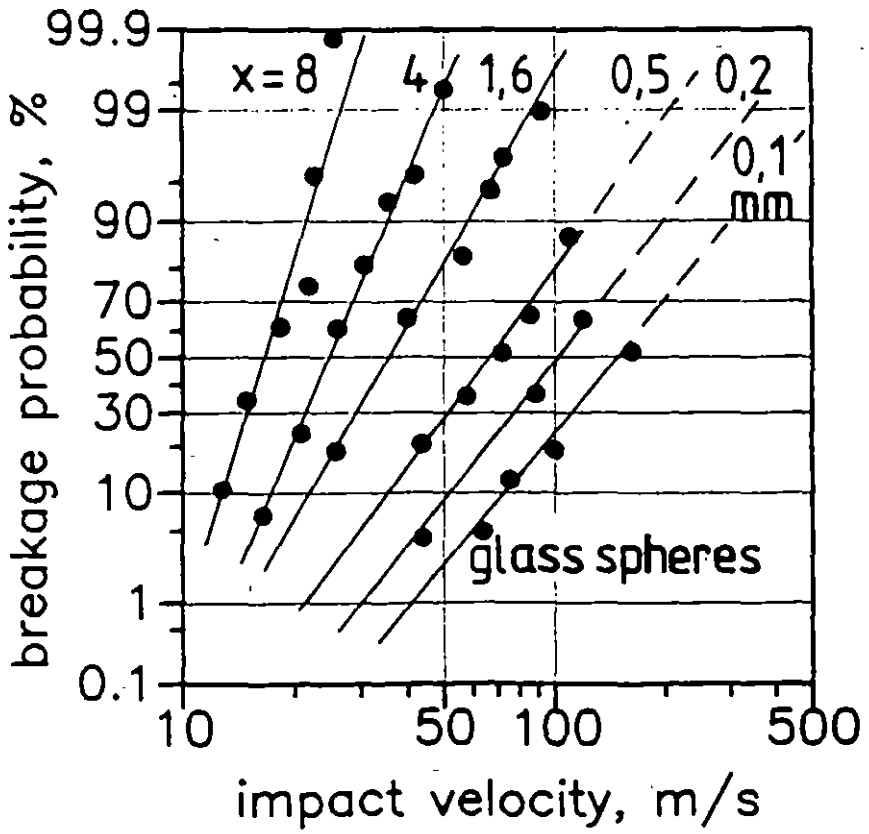

(4) Specific reaction force, F_r

If the stressing is continued beyond the breakage point the fragment pile causes a force F which has to overcome. Relating F to the nominal cross-section of the particle of size x gives F_r.

$$F_r = 4\ F\ /\ \pi\ x^2$$

F_r depends on the gap width s between the compression plates. For a general description s is related to x and this ratio called reduction ratio.
F_r increases with increasing reduction ratio and decreasing particle size.

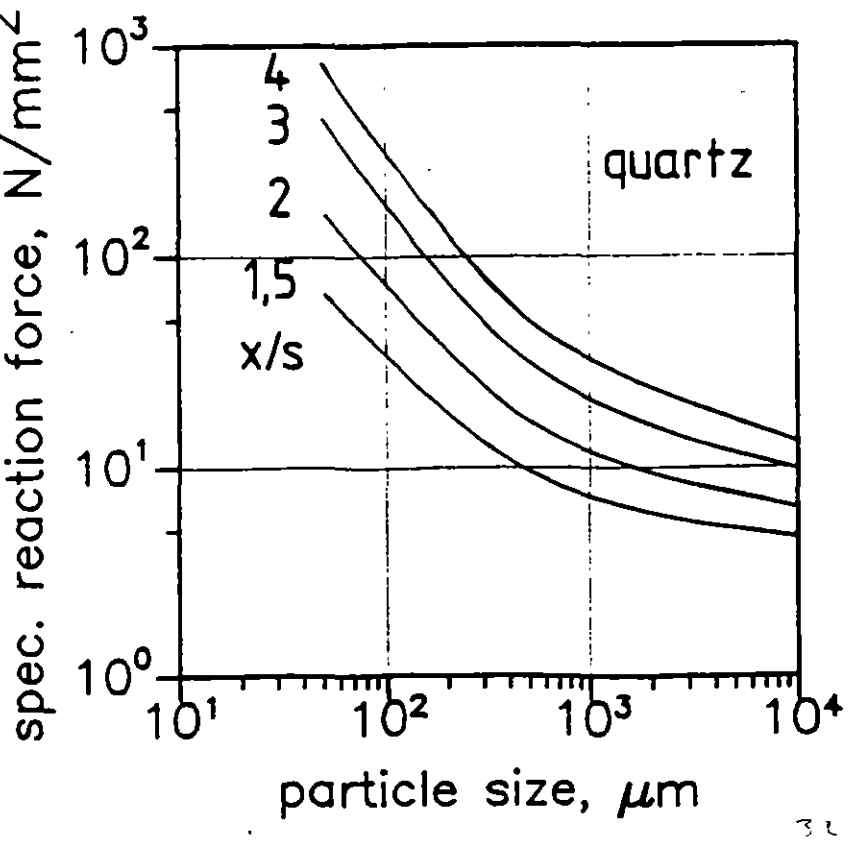

(5) Product size distribution Q(y)

Q(y) represents the distribution of the sample after stressing which depends on the particle size and the stressing intensity.

Compression: Q(y) of brittle materials can be normalized in the size range 50 to 5000 µm as the fragment size y is related to the gap width s.

Impaction: normalizing not possible

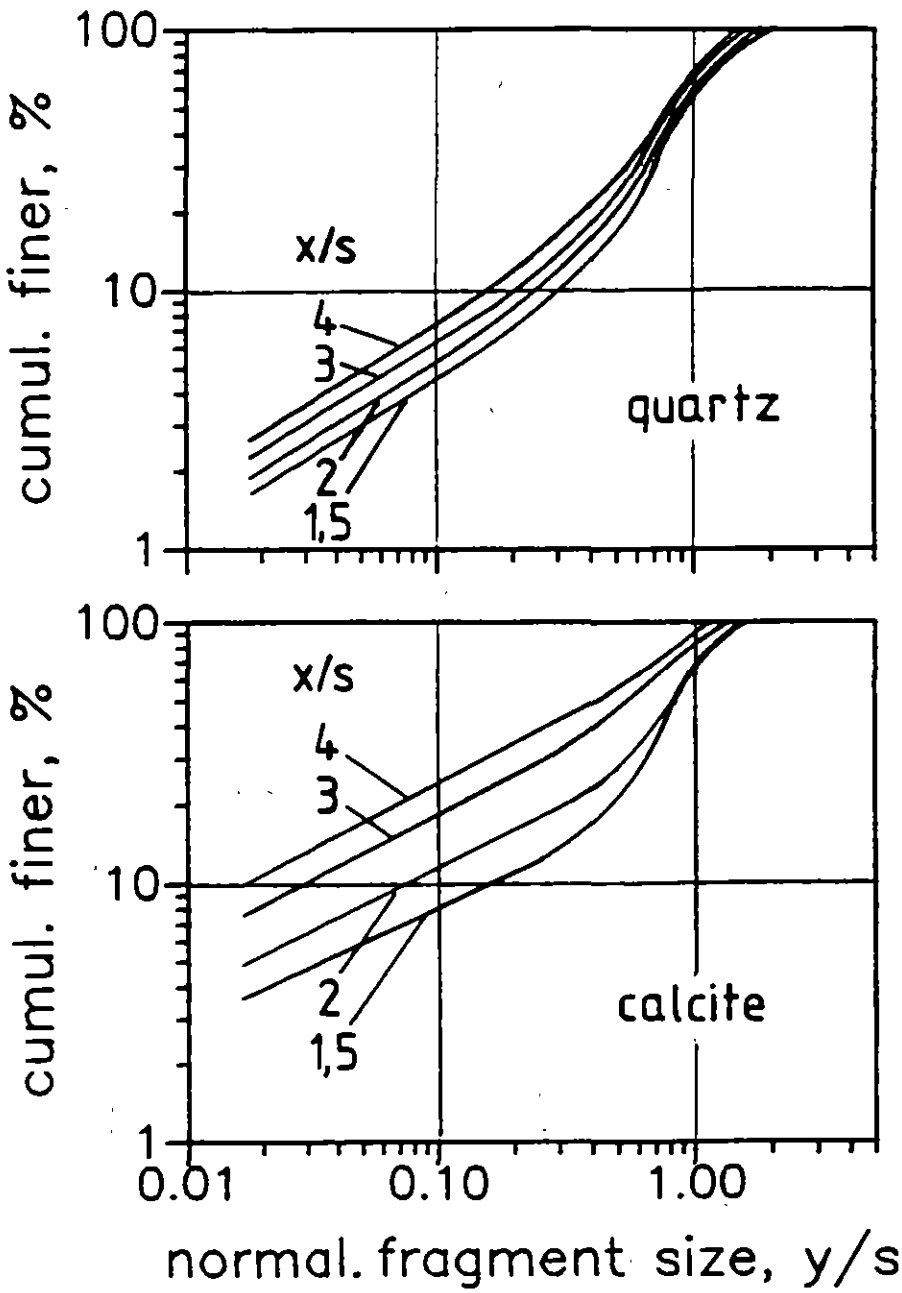

SINGLE PARTICLE BREAKAGE (5)

(6) Breakage function B(y)

B(y) represents the size distribution of the fragments excluding the unbroken particles.

The sample consists of a narrow fraction x_{min} to x_{max}, B(y) follows from

$$B(y) = Q(y) / Q_{(xmin)} \qquad \text{for } y \leq x_{min}$$

compression : $B(y) = Q(y)$ for $x/s > 1.5$

impacting : $B(y) = Q(y)$ for $P = 1$

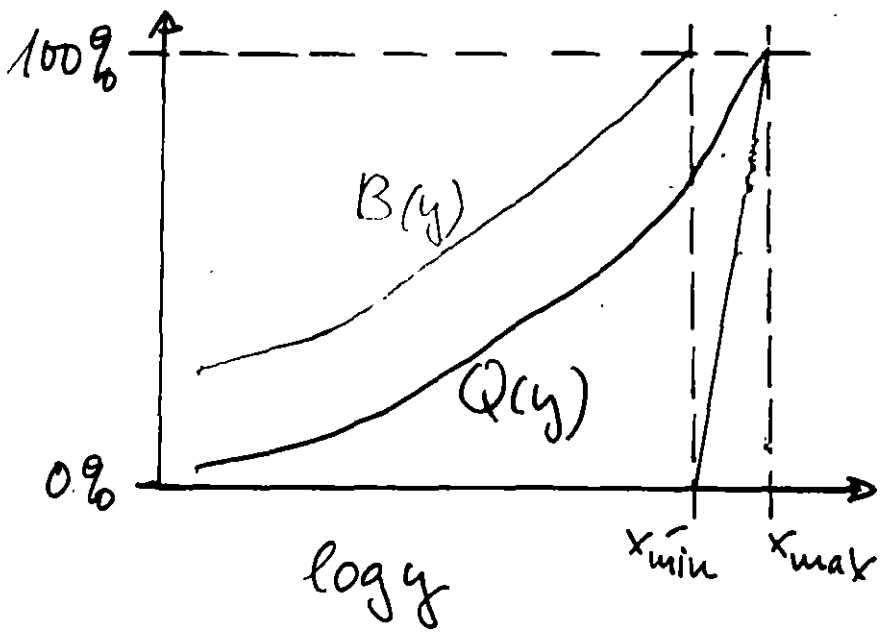

INTERPARTICLE BREAKAGE (1)

The term interparticle breakage means particle breakage inside a particle bed. Never all particles are broken because of the random package structure and the strength distribution. The characteristic features are to study with narrow size fractions in a piston press. The bed size should be that wall effects do not influence the size reduction.

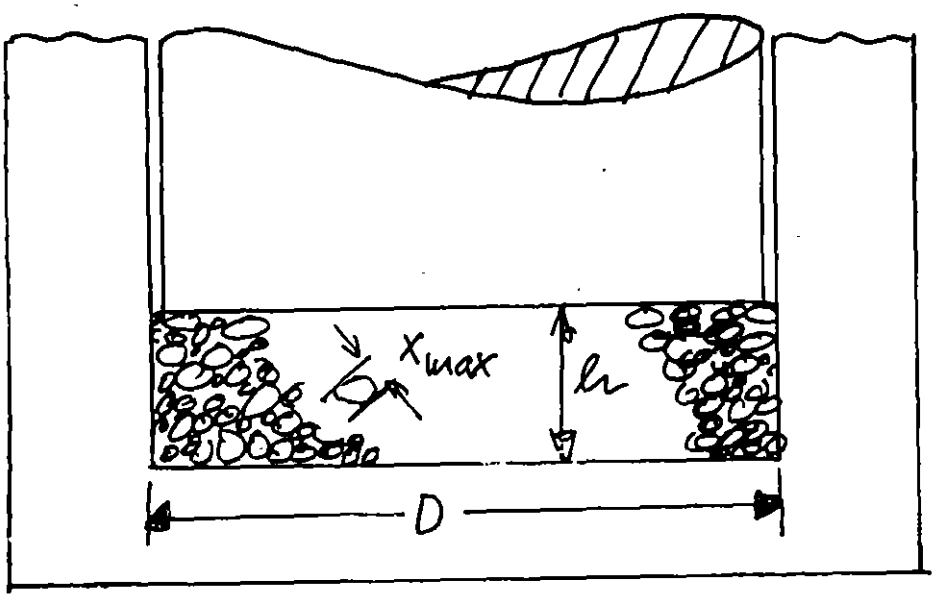

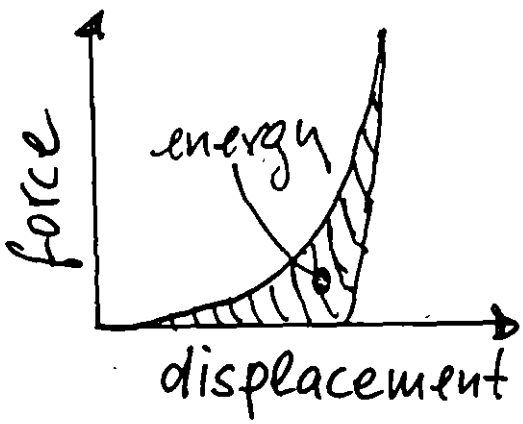

$h > 5 x_{max}$

$D > 3 h$

The stressing intensity can be expressed by the pressur p or the specific energy absorption E_M, E_V.

$$p = F / A \qquad E_M = E / M \qquad E_V = \rho E_M$$

F : press force, A: cross-section of the piston,

E : energy calculated from the compression diagram,

M : particle mass, ρ : density

INTERPARTICLE BREAKAGE (2)

The following characteristics are measured:

- compaction diagram
- product size distribution $Q(y, x, E_M)$
- fraction of broken particles $S(x, E_M)$
- breakage function $B(y, x, E_M)$

Experiments with brittle materials have shown that for general considerations the size reduction date should be discussed in terms of E_M or E_V instead of p.

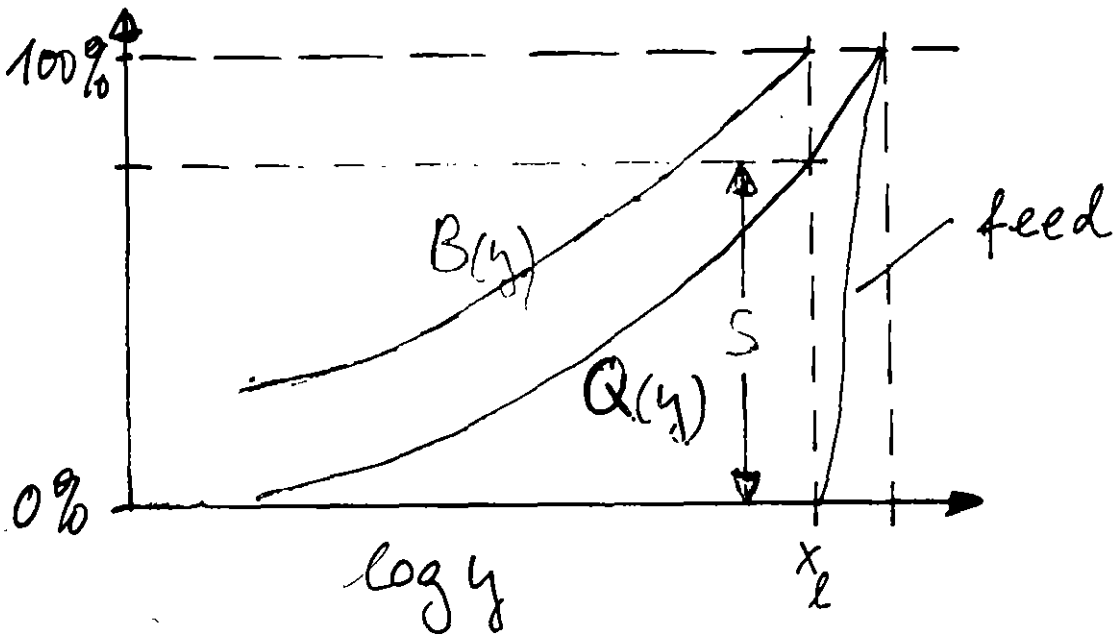

INTERPARTICLE BREAKAGE (3)

(1) Compaction diagram

The compaction diagrams can be generalized as

$$\theta = 1 - \exp\{ - (p/p_c)^n \}$$

p = pressure, p_c= characteristic pressure depending on material and particle size x, n: curve shape fitting parameter depending on material,

θ : normalized compaction, δ_o and δ_s initial and final relative bulk density

$$\theta = (\delta - \delta_o) / (1 - \delta_o) \qquad 0 \le \theta \le 1$$

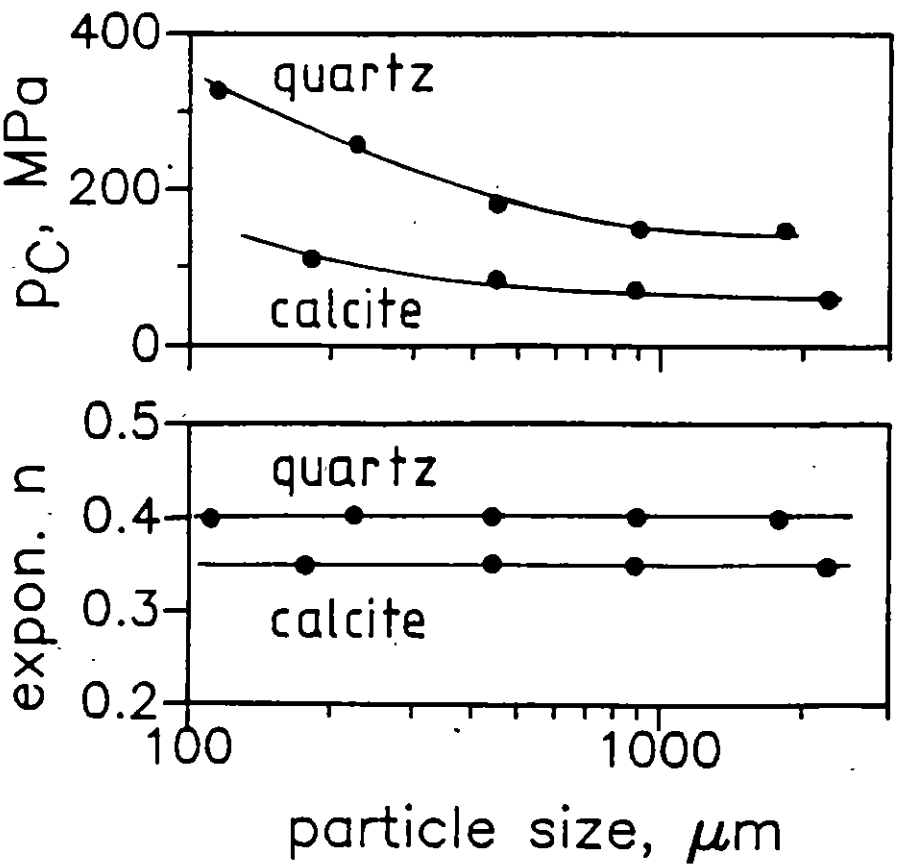

INTERPARTICLE BREAKAGE (4)

Normalized compaction diagram for narrow quartz and calcite fractions in the range 100 µm to 3000 µm

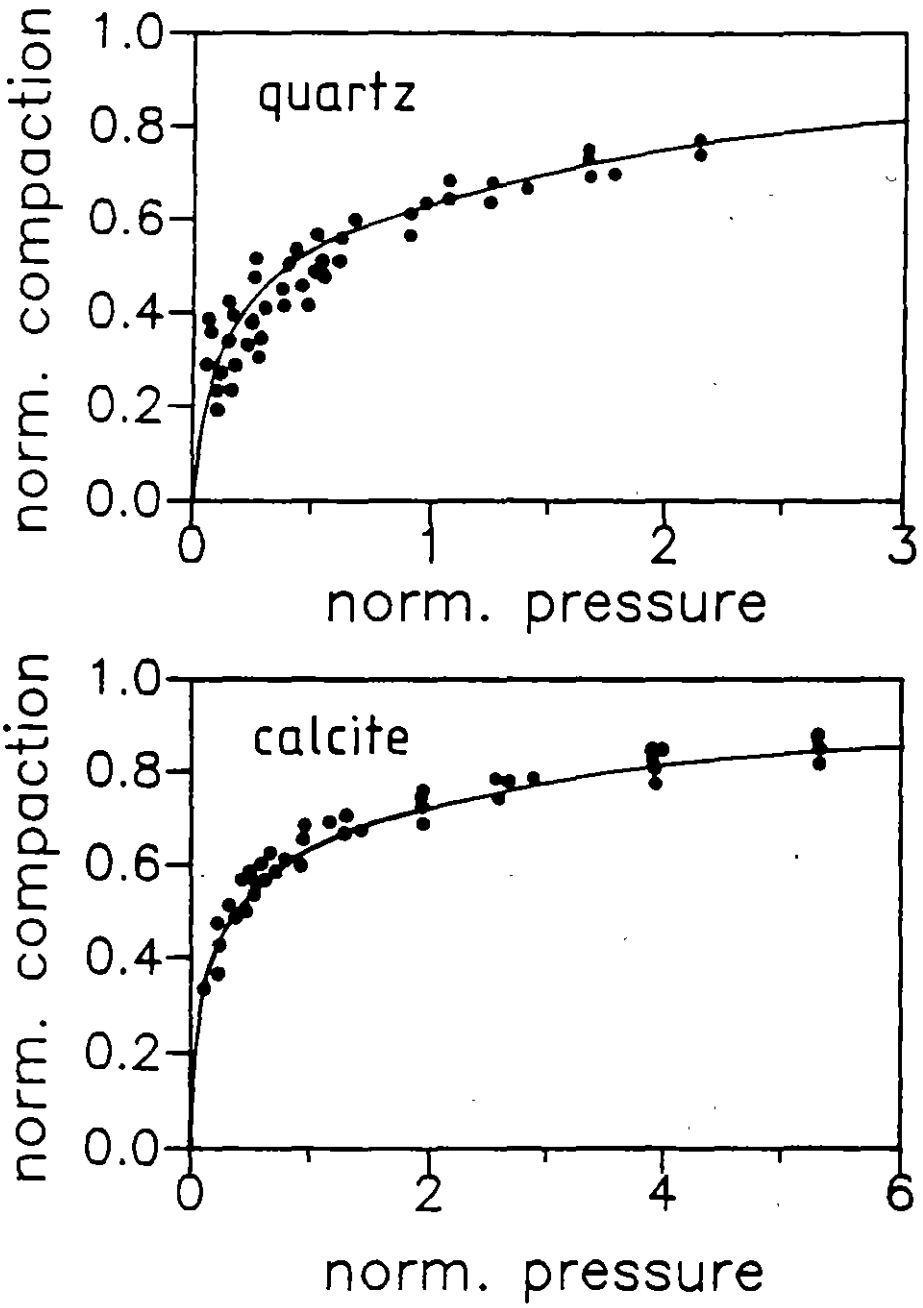

(2) Fraction of broken particles S

S is given by the mass fraction of all fragments smaller than, the lower limit of the feed fraction and depends on material, particle size and energy absorption. S can be generalized as

$$S / S_\infty = 1 - \exp \{ - (E_M / E_{M,c})^\beta \}$$

S_∞ : maximum value for S depending on material,

E_M: energy absorption, $E_{M,c}$: characteristic value of E_M depending on particle size x and material

Narrow quartz fractions in the range 200 to 4000 µm.

$S_\infty = 0.89$ and $\beta = 0.54$

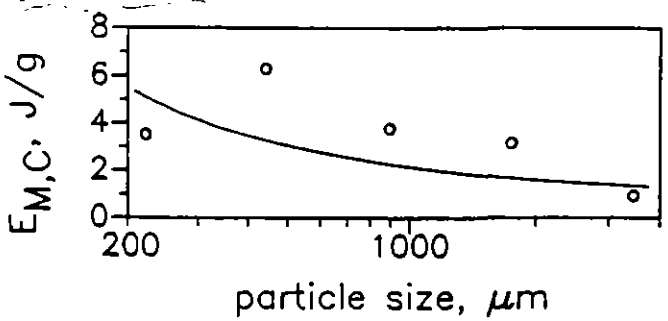

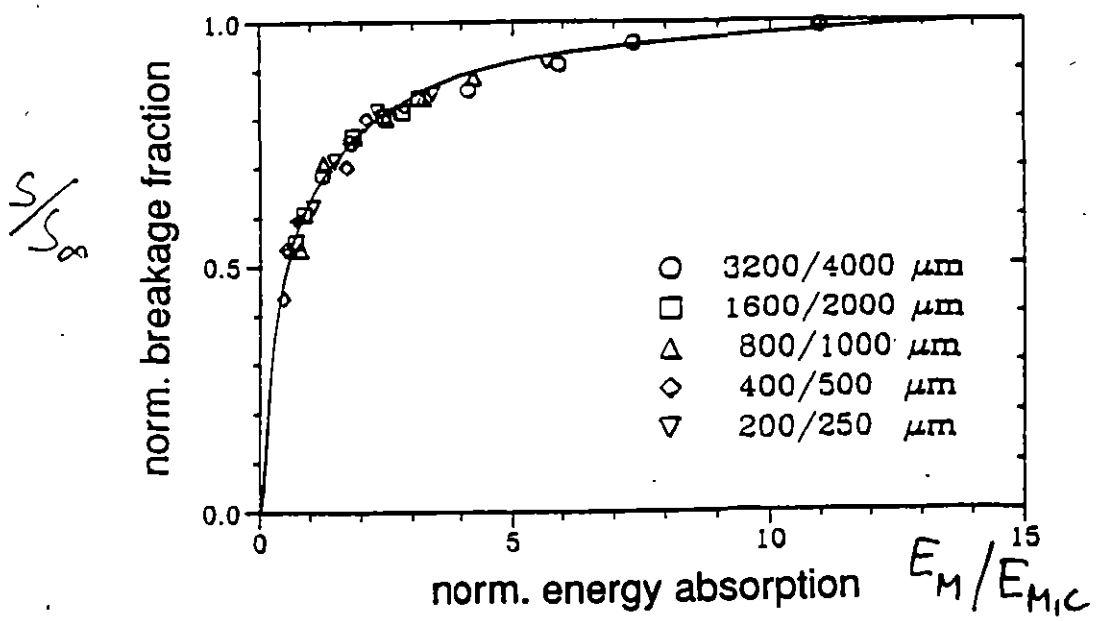

(3) Breakage function B

B represent the size distribution of the fragments, the unbroken particles are excluded. B depends on material, feed size x and energy absorption E_M.

$$B = B(y, x, E_M)$$

Experiments have shown that the breakage function can be approximated by a truncated logarithmical normal distribution.
The transformation is as follows:

y: fragment size, x_l: lower limit of the feed fraction

y_{50}: median value of the fragment size distribution

y_{16}, y_{84}: particle size at which the undersize mass fraction is 16 % and 84 %

$$\xi = y / x_l \qquad \xi_{50} = y_{50} / x_l = \mu$$

$$\eta = \xi / (1-\xi) \qquad \eta_{50} = \mu / (1-\mu)$$

The normal distribution is defined as:

$$h(t) = \left(1/\sqrt{2\pi}\right) \exp\left(-t^2/2\right) \qquad H(t) = \int_{-\infty}^{t} h(\tau)\, d\tau$$

The truncated logarithmic normal distribution follows with:

$$Q(\xi) = H(t) \quad \text{with} \quad t = (1/\sigma)(\ln\eta - \ln\eta_{50})$$

$$\sigma = (1/2)(\ln\eta_{84} - \ln\eta_{16})$$

INTERPARTICLE BREAKAGE (7)

Examples of breakage functions
quartz fractions 200 / 250 µm and 3200 / 4000 µm

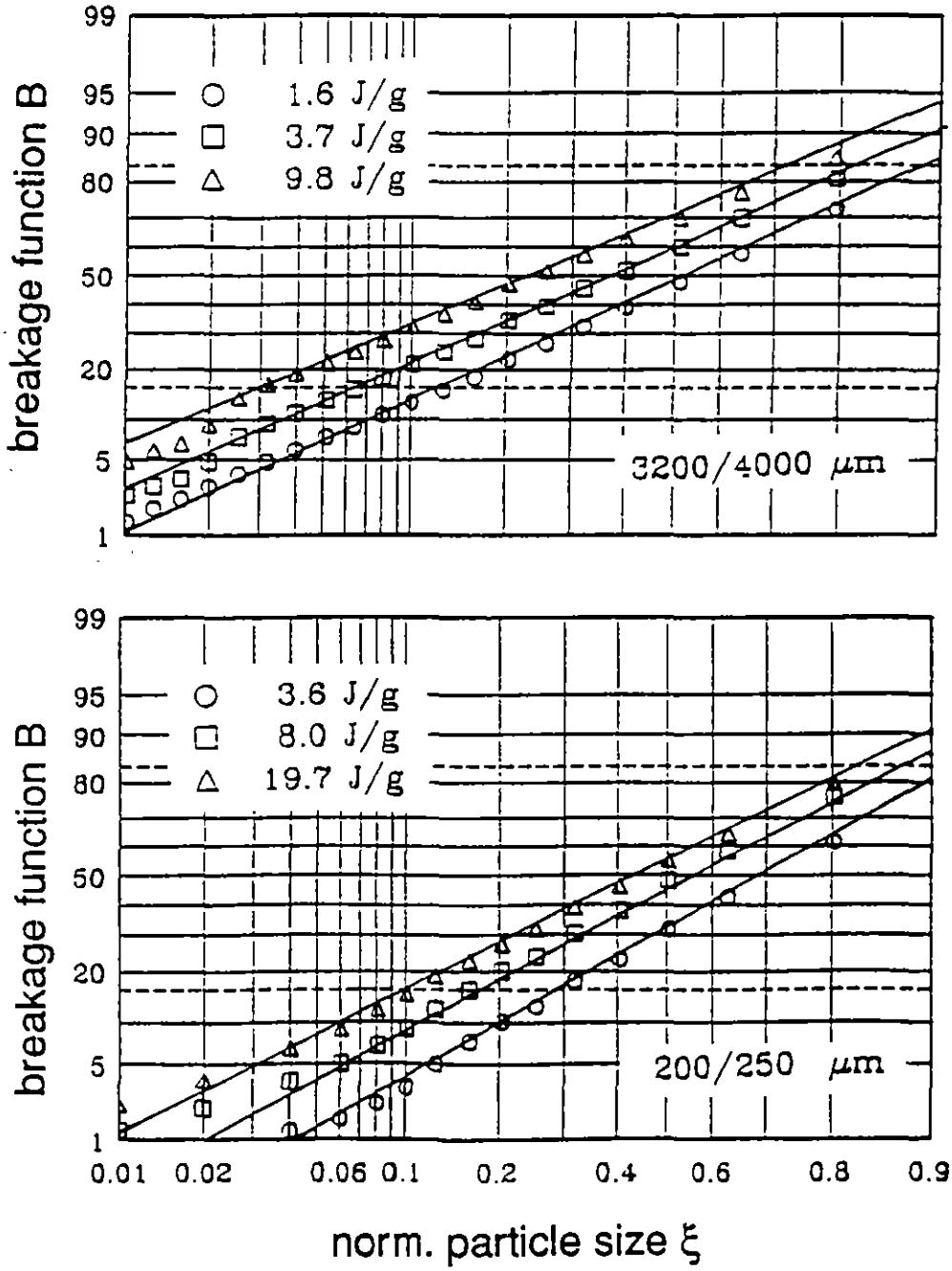

INTERPARTICLE BREAKAGE (8)

The median value μ and the standard diviation σ depend on material, feed size x and energy absorption E_M

$\mu = \mu\ (x, E_M)$ $\sigma = \sigma\ (x, E_M)$

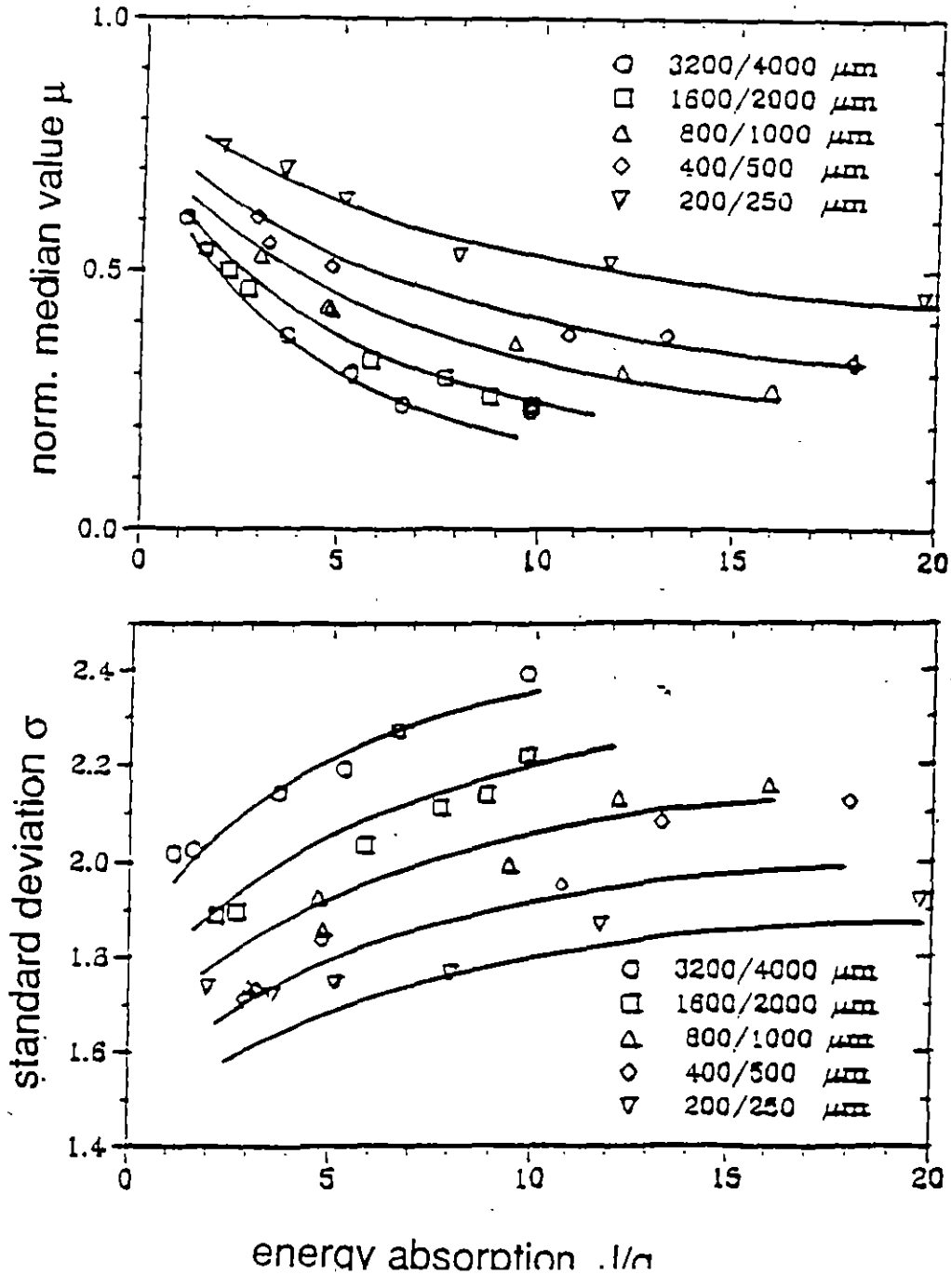

SO-CALLED COMMINUTION LAWS (1)

So-called comminution laws try to relate the energy consumption of a mill to the size-reduction effect, represented by the change either in the size distribution or in the specific surface. Some equations have been published only three should be discussed here.

Rittinger`s law (1867)

Rittinger has proposed the hypothesis that the specific surface S changes proportional to the work-input W.

$$S - S_o = \Delta S \sim W$$

Introducing the mass related values ΔS_M and W_M:

$$\Delta S_M = \text{const } W_M$$

Considering this relation in the term energy utilization which is defined as the quotient of ΔS_M divided by W_M, it follows:

$$EU = \Delta S_M / W_M = \text{const}$$

EU is independent on particle size

SO-CALLED COMMINUTION LAWS (2)

Kick`s law (1885)

Kick has formulated a similarity law for single particle assuming the following:

- geometrical similar particles
- particle strength independent on particle size
- geometrical similar fracture pattern

Based on these assumption it results:

$$EU = \text{const} / x$$

The energy utilization increases as the feed particle becomes finer.

Walker`s equation

Walker has proposed a differential equation approach as usual for chemical reactions.

$$dW_M = -\text{const}\ x^{-n}\ dx$$

intergrating yields:

$$W_M = W_{M,c} \ln (x_F/x_P) \qquad \text{for } n = 1$$

$$W_M = W_{M,c} \{(x_c/x_P)^{n-1} - (x_c/x_F)^{n-1}\} \qquad \text{for } n > 1$$

$W_{M,c}$ and x_c are reference values.

SO-CALLED COMMINUTION LAWS (3)

The Walker equation gives the energy utilization as

$$EU = \text{const}\ x_P^{n-2}$$

From this equation follows Rittinger`s law for n = 2 and Kick`s law for n = 1

Bond equation

Bases on huge experiencies in ball milling Bond has proposed the equation

$$W_M = 10\ W_i \left\{\left(1/\sqrt{P}\right) - \left(1/\sqrt{F}\right)\right\}$$

W_i : Bond index, F : x_{80} of the feed given in µm,
P : x_{80} of the product given in µm

W_i is to measure in a specified lab-scale ball mill with a specified procedure and represents the work-input for F >> P and P = 100 µm.

The Bond equation is identically with the Walker equation setting

$W_{M,\,c} = W_i$, $x_c = 100$ µm, $n = 3/2$

SO-CALLED COMMINUTION LAWS (4)

The validity of these laws have often been discussed controversibly in the past. There are always data available for satisfying each of these laws. It depends on the operation regime which of equation meets the experimental result. The general course of the (EU,ΔS_M)-curve shows a maximum.

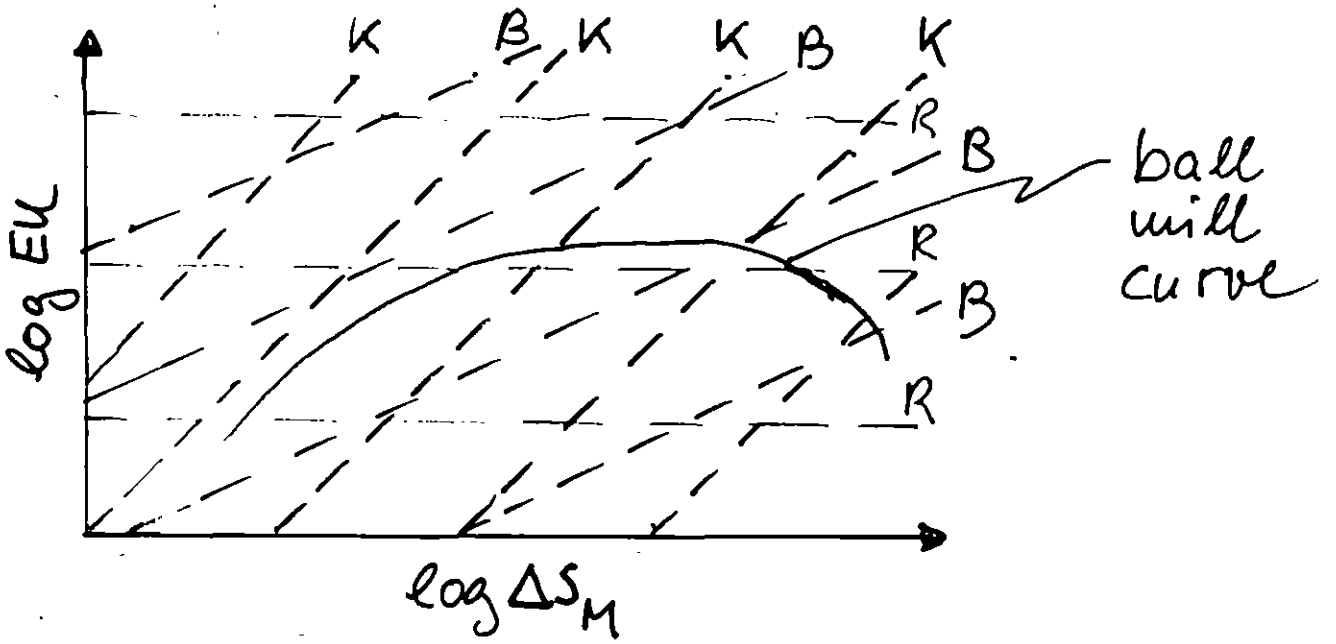

The Bond equation is useful as a first information for scaling-up ball mills. Bond has refined his equation by additional factors considering particular operation and design specification. Manufactures have their own procedures for sizing mills.

Rittinger : $EU = const.$

Kick : $EU = \frac{const}{x} = const \Delta S_M$

Bond : $EU = \frac{const}{\sqrt{x}} = const \sqrt{\Delta S_M}$

EFFICIENCY OF MILLS

Often is said mills have a very low efficiency of 0.1 % or even less. This figure results form the equation:

$$\eta = \gamma \, \Delta S_M \, / \, W_M$$

ΔS_M: specifc surface increase, γ: specific surface energy, W_M: specific work-input

The crack propagation does not depend on γ, therefore the above equation is meaningless.

A technical reasonable definition has to compare the mill work-input with the energy of an ideal comminution process the same size-reduction. Single particle breakage comminutes most efficently, therefore, a cascade of single particle breakage events can be considered as the ideal process.

$$\eta = E_{M,id} \, / \, W_M$$

$E_{M,id}$: specific energy of the single particle breakage cascade evaluated with a cascade model using single particle breakage data.

ball mills	η = 5 ... 10 %
high pressure roller mills	η = 10 ... 20 %

BALL MILLS - INTRODUCTION

Ball mills are the most important members in the group of grinding media mills. They consist of a rotating container with a circular cross-section, mostly clindrical, filled with balls which tumble around and stress the particles by compression and shear. Ball mills are the working horses in comminution of brittle materials. Their advantages are

- simple operation (in principle !),
- wide range of mill sizes up to such for very high capacity,
- insensitive to foreign bodies in the feed,
- easy replacement of worn grinding media,
- dry and wet operation,

however, the disadvantages are

- low efficiency,
- small specific capacity (throughput divided by mill volum)
- high specific wear,
- very noisy in dry milling

Beginning last century small batch mills have been used for grinding minerals and chemicals. Mills for flow-through operation have been developed 1870/90; there were two lines:
(1) peripheral screen discharge mills
(2) axial grate and overflow mills

BALL MILLS - CONTENTS

DENOTATIONS

The following denotations are used in the following .

Mill

D: interior diameter, L: length, V: interior volume, n: speed, n_c: critical speed, ω: angular velocity, M: mill charge, T: torque, P: powder draft

Balls

d: diameter, m: mass, ρ_B: density, M_B: ball charge, ε_B: porosity of ball charge

Material

x: particle size, $Q_f(x)$ and $Q_p(x)$ feed and product size distribution, ρ_M: density, M_M: material charge, ε_M: porosity of material charge, $\dot{M}$: mass throughput,

wet grinding : M_S: slurry charge, ρ_S: slurry density, μ_S: slurry load on mass basis, δ_S: slurry load on volum bases

Dimensionless parameters

Dimensionless parameters are useful for general considerations.

relative speed $z = n / n_c$; $\boxed{n_c = (1/\pi)\sqrt{g/2D}}$

$R\omega_c^2 = g$

ball filling ratio $\varphi_B = M_B \,/\, (1-\varepsilon_B)\delta_B V_B$

material filling ratio

$$\varphi_M = (M_M / M_B)\,(\rho_B / \rho_M)\,\{(1-\varepsilon_B)/\varepsilon_B(1-\varepsilon_M)\}$$

slurry filling ratio

$$\varphi_S = (M_S / M_B)\,(\rho_B / \rho_S)\,\{(1-\varepsilon_B)/\varepsilon_B\}$$

CHARGE MOTION (1)

The torque draft T and by that the power density P/V is determined by the charge motion which depends on

- relative speed z,
- ball and material (slurry) filling ratio φ_B and φ_M (φ_S),
- ball to mill diameter ratio (d/D),
- liner geometry, lifting bars.

Four principle motion regimes can be distinguished

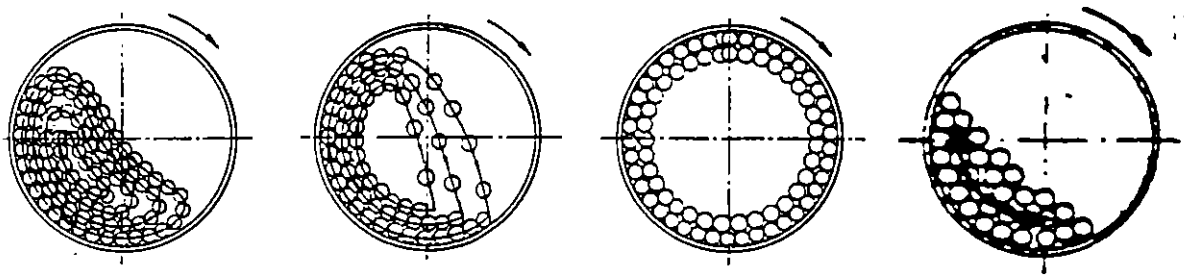

cascading cateracting centrifuging oscillating

Proper operations in cascading and cateracting regime, in centrifuging regime no power draft, oscillating causes rotational oscillations in the drive system.
The actual motion can be a mixture between either cascading and cateracting or cateracting and centrifuging.

CHARGE MOTION (2)

The theory of charge motion was treated in many early papers. ~~Three~~ Four features should be disussed:

- single ball approach (Fischer, Davis)
- momentum exchange between the up-flying balls (Steiger)
- surface contour of the cascading charge (Barth, Uggla)
- oscillating (Rose)

The theoretical approvaches of Fischer, Davis,Steiger, Barth und Uggla assume no slip between the mill wall and the ball charge. This can only be assured with lifter bars. In mills with smooth liners, the slip depends on the (D/d)-ratio and can be neglected for (D/d) > 40. In lab-scale mills with smooth liners the charge always slips.

CHARGE MOTION (3)

Angle of ejection and impinging

The angle of ejection α_o is defined that there the balls loose the contact with the wall, α_o follows from the force balance:

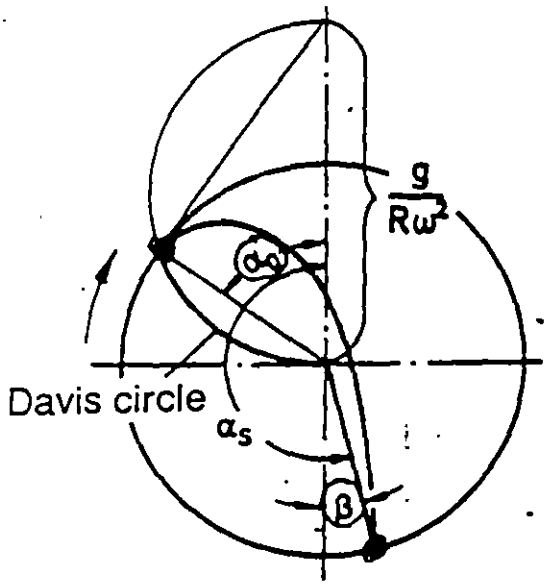

$$\cos\alpha_o = \omega^2 R / g = z^2$$

A single ball would move on a parabolic path and meets the shell at impinging angle β_{FD}.

$$\beta_{FD} = \pi - 3\alpha_o = \pi - 3 \arccos z^2$$

In reality a row of balls is ejected. On the rising fly path the velocity slows down, therefore the balls stay in contact and push each other (momentum exchange) which lengthens the fly path to the impining anlge β_S.

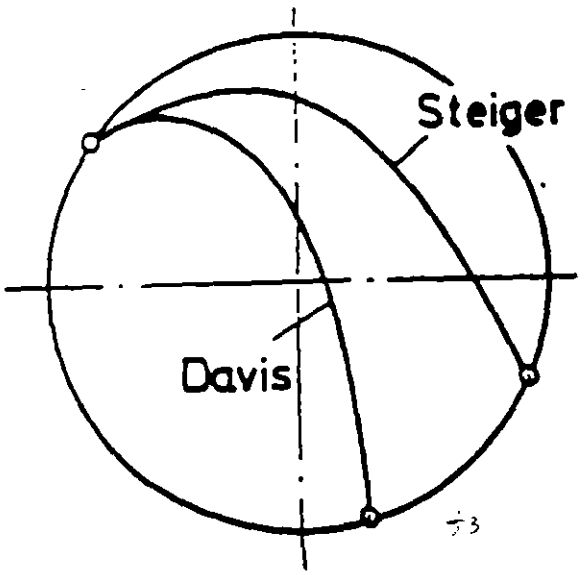

z	0.6	0.7	0.75	0.8
α_o	69	61	56	50
β_{FD}	-27	-2	13	29
β_S	33	45	69	78

So-called optimum speed

The parabolic path of a flying single ball and the falling height h from the summit to the impinging point can be calculaded.

$$h/D = (9/4)\ \sin^2\alpha_o\ \cos\alpha_o = (9/4)\ z^2\ (1-z^4)$$

(h/D) rises to a maximum at

$$z_{opt} = 0.76 \longrightarrow \boxed{n_{opt} = 0.76\ n_c}$$ so-called optimum speed

Experiences show optimum operation in the speed range 0.65 to 0.75 depending on material feed size, wanted size reduction, mill desing (L/D-ratio, linear geometry), wet or dry operation.

Cascading contour

For calculating the cascading contour a force balance including centrifugal, gravity and friction force is to consider. The result show this contour as a part of a logarithmical spiral depending on φ_B, z and the internal friction μ in the charge.

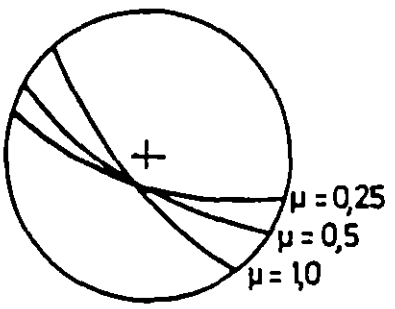

$\frac{n}{n_c} = 0{,}7 \quad \varphi_B = 0{,}4$

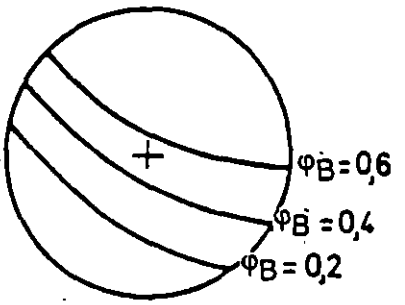

$\frac{n}{n_c} = 0{,}7 \quad \mu = 0{,}5$

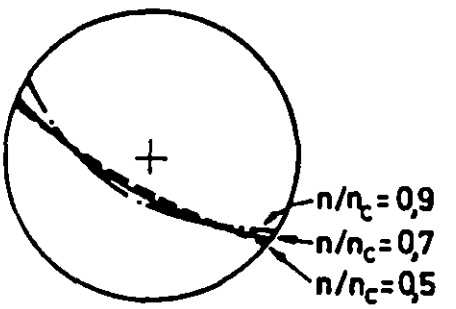

$\varphi_B = 0{,}4 \quad \mu = 0{,}5$

Charge oscillation

Charge oscillation have to be avoided otherwise the drive system can be damaged. Rose has shown that oscillation is function of ($\varphi_B \mu$) and (D/d); μ = friction coefficient charge against the wall. The oscillating frequency is about the same as the critical speed:

$\omega_{osc} \approx \omega_c$

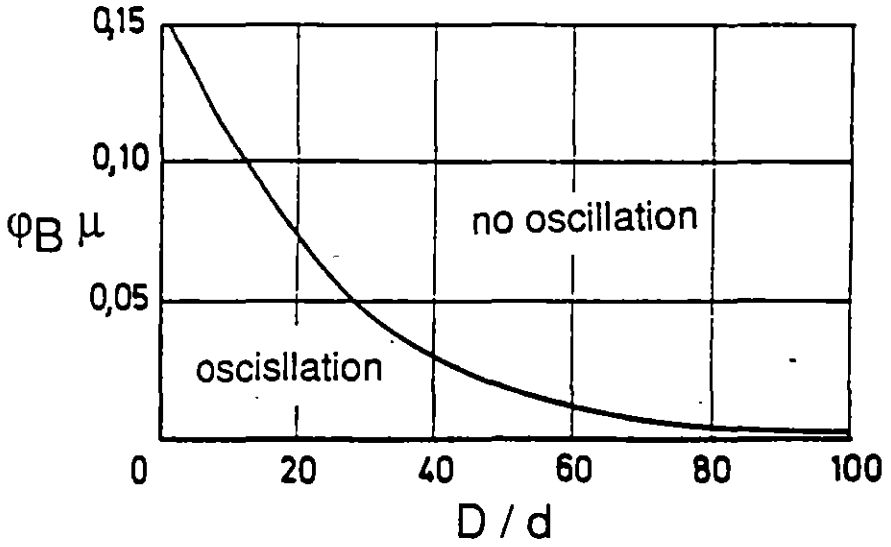

Ball charge motion model

A charge motion model can be calculated using ball ejection equation, fly path equation after Steiger, cascading contour after Barth-Uggla and the partition of the charge in respect to flying and not-flying balls.

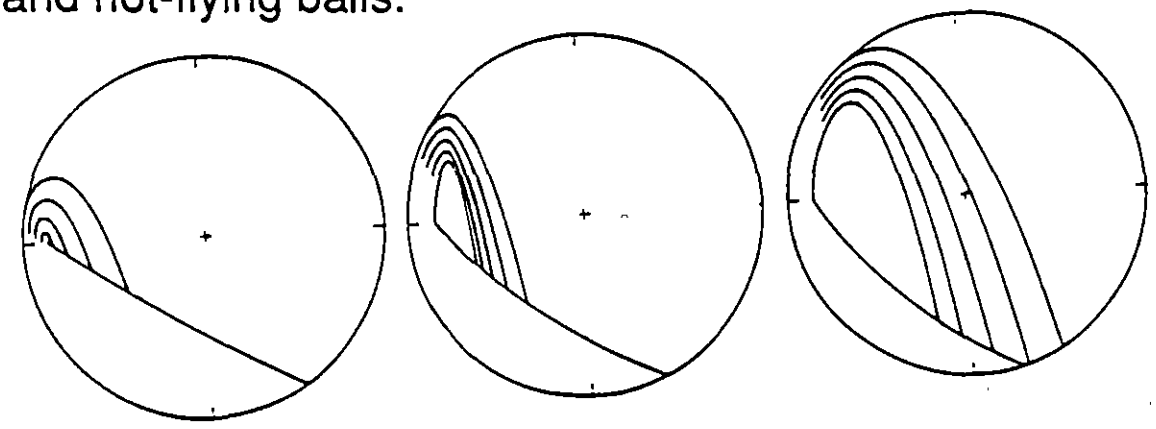

φ_B = 0.23, z = 0.35 φ_B = 0.23, z = 0.65 φ_B = 0.23, z = 0.80

POWER DRAFT (1)

The power draft is always an essential characteristic of a machine. Emperical relations are given and used. An engineer should know the background; helpful are equation in dimensionless terms.

$$P = T\,\omega = 2\,\pi\,n\,T$$

$T = M\,g\,a^*$ $\quad a^*$ = lever arm

$M = M_B + M_M = M_B\,(1+\gamma)$

$M_B = \delta_B\,(1-\varepsilon_B)\,\varphi_B\,V$

$a = a^* / D$

$n = z\,n_c = (z/\pi)\,\sqrt{g/2D}$

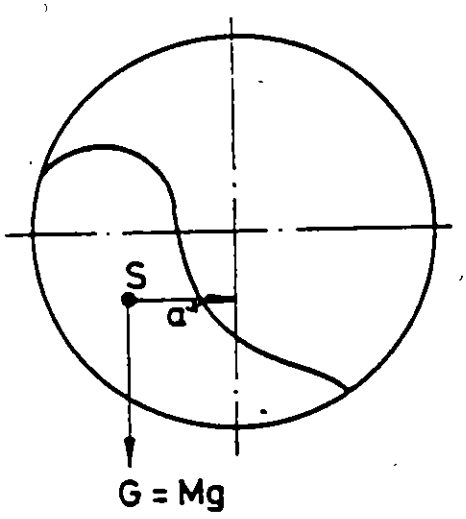

Introducing all these relation into the torque equation yields to

$$P = p\left(\varphi_B, a, z, \gamma, \varepsilon_B\right)\,g^{1.5}\,\rho_B\,L\,D^{2.5}$$

$$p = \left(\sqrt{2}\pi/2\right)\,(1+\gamma)\,\left(1-\varepsilon_B\right)\,\left(a\varphi_B z\right)$$

P = power factor • power term

The power is proportional to the "power term" only as long as the "power fractor" is constant. The problem arises how the dimensionless power factor depends on the operation condition.

$$p = 1.11\,(1+\gamma)\,(1-\varepsilon_B)\,(a\,\varphi_B z)$$

The mass ratio γ can be rewritten as:

$$\gamma = (\rho_M/\rho_B)\,\varepsilon_B\,\gamma_M\,\{(1-\varepsilon_M)/(1-\varepsilon_B)\}$$

With $\varepsilon_M = \varepsilon_B = 0.4$, $\varphi_M = 1$, $\rho_M = 7800$ kg/m^3 (steel), $\rho_M = 3100$ kg/m^3 (cement clinker) it results $\gamma = 0.16$. The operation conditions do not effect strongly γ and γ does not influence strongly p. The essential term in p is the product ($a\ \varphi_B z$). As already shown a depends on φ_B and z.

$$a\ \varphi_B\ z = a(\varphi_B,z)\ \varphi_B\ z = f(\varphi_B,z)$$

$f(\varphi_B,z)$ is not a simple function with the following properties.

- $f = 0$ for $\varphi_B = 0$ or $\varphi_B = 1$ or $z = 0$ or z large
- cuts $f(\varphi_B, z = \text{const.})$ and $f(\varphi_B = \text{const.}, z)$ have a maximum
- $f(\varphi_B,z)$ - plane has a maximum in the range φ_B around 0.35 and z around 0.70.

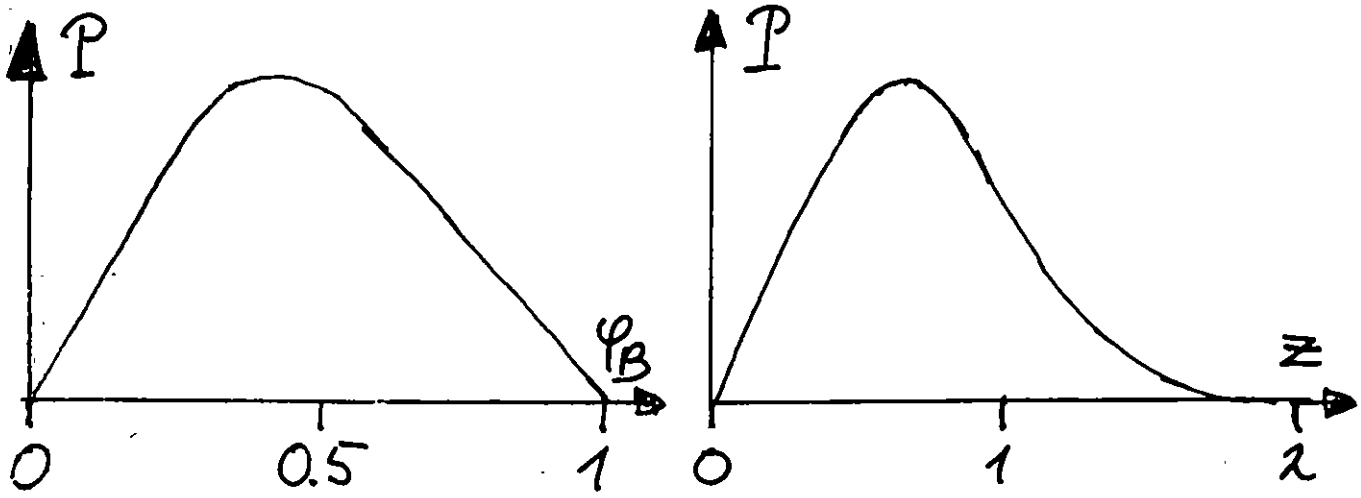

POWER DRAFT (3)

The power equation gives guideline for scaling-up. A mill in proper operation runs in the range of the p-maximum in which p does not change strongly, then

$$P \propto g^{1.5}\ \rho_B\ L\ D^{2.5}$$ if $p = const.$

The power and also the capacity of a ball mill increase more than proportional to the mill volume

The power fractor can be evaluated inserting:

$\varepsilon_B = 0.4, \gamma = 0.16, \varphi_B = 0.35$ and

(az) = (1/4) 0.6 ... (1/3) 0.7 = 0.15 ...0.23 ≈ 0.19

p = 0.05

The power equation can be rearanged as

$$P = k\ M_B\ \sqrt{D}$$

this form is often used for empirical equations, e.g. Blanc-Eckardt equation. The factor k has the dimension ($kW/kg\ m^{-1/2}$) and is given to be 0.006 to 0.007 for z = 0.75, φ_B around 0.35 and (ρ_M/ρ_B) around 0.3.

MILL SIZING (1)

Mill sizing has to solve the problem how a given material can be ground with the wanted throughput to the demanded product. Each manufacture has his own procedure. The general background should be discussed.

(1) The specific work-input W_M has to be determined by an established test procedure, e.g. Bond procedure (Bond index,Bond equation)

(2) Mass throughput $\dot{M}$ and W_M gives the required power draft of the mill independent on the circuit mode.

$$P = W_M \dot{M}$$

(3) The term $(LD^{2.5})$ can be calculated from the power equation

$$L D^{2.5} = \lambda D^{3.5} = P / p g^{1.5} \rho_B \qquad \lambda = L / D$$

(4) The mill diameter D can be calculated for each chosen (L/D)-ratio which follows from experiences. This ratio is limited bacause the wanted mass flow through the mill must be guaranteed. An additional equation for considerng this point is given in (5).

MILL SIZING (2)

(5) The mean residence time τ of the material is given by:

$$\tau = M_M / \dot{M} \longrightarrow M_M = \tau \dot{M}$$

$$M_M = \mu \rho_M L D^2$$

$$\mu = (\pi/4) \varphi_B \varepsilon_B \varphi_M (1-\varepsilon_M)$$

This is the second equation for calculating L and D.

$$W_M \dot{M} = p g^{1.5} \rho_B L D^{2.5}$$

$$\tau \dot{M} = \mu \rho_M L D^2$$

$$D = \left\{ (\mu/p) (\delta_M/\delta_B) \left(W_M / g^{1.5}\tau\right)\right\}^2$$

$$L = (1/p) \left(\dot{M} W_M / g^{1.5}\rho_B D^{2.5}\right)$$

The calculation of D and L needs beside W_M and $\dot{M}$ the mean residence time τ as the third value which has to be determined experimentally or to be chosen.

BALL SIZE (1)

A good size-reduction performance needs proper chosen ball sizes. A optimum ball size exists because firstly the ball must weigth enough to break the particle and secondly the number of balls should be as many as possible. The optimum size depends on

- material to be ground (particle strength),
- particle size,
- mill diameter,
- ball density.

Some emperical equations have been published, that one of Bond reads for steel balls:

$$d = 0.024\,(\rho_M\ W_{Mi} / z)^{1/3}\ x^{1/2}\ D^{-1/6}\ \text{mm}$$

units, ρ_M: kg/m^3, W_{Mi}: kWh//t, x: µm, D: m

Most equations can be written in the general form

$$d \propto x^q / D^p \quad \text{with} \quad q=0.2 \ldots 1 \quad \text{and} \quad p=1/6 \ldots 1/3$$

Ball mixtures are advantages for a size-reduction ratio larger than ten. General guidline is to take as much as possible of the small balls optimized in respect to the fine grinding part in the mill and add as few a possible large balls which assure the breakage of the coarse particles.

BALL SIZE (2)

In long ball mills the balls should be seperated in respect to size that the large ones are in the front section and the small ones in the rear. For this reason so-called classifying liners have been developed.

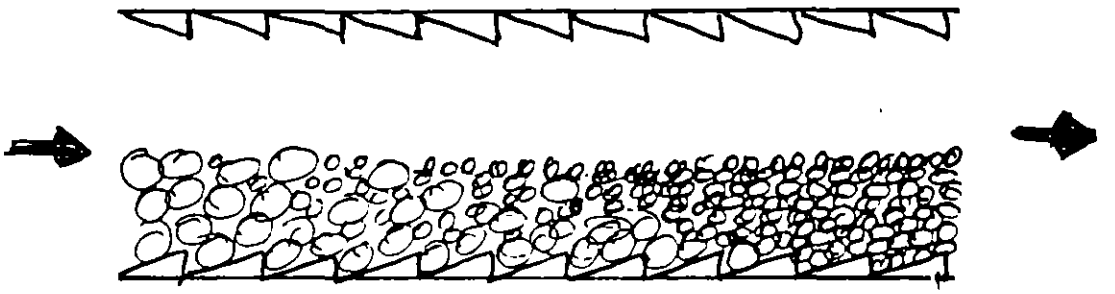

The ball classification can be explained as follows:
The larger balls move more probably to the mill wall and were transported by the screw-like positioned classifying liners towards the front. The small balls stay more probably in the charge interior and flow towards the end due to the overall flow equilibrium.

WEAR (1)

Balls and liners are worn. The ball wear reduces the size-reduction effect because ball charge and ball size become smaller. To overcome this problem balls have to be refilled. The basis for each refilling program is the wear kinetics, often written in the form:

$$- dm / dt = k\ d^n$$

k and n are to determine experimentally, n = 2 means a wear proportional to the ball surface and n = 3 proportional to ball volume or mass. The measured values of n are in the range between 2 and 3.

In practical application the specific wear is considered, defined either as

w_m = mass of worn material / mass of milled material or

w_e = mass of worn material / energy used for grinding.

w_m and w_e are related mutually by the specific work-input W_M

$$w_m = w_e W_M$$

The mass related wear is a useful term only if different ball materials are to compare as the same feed material is ground to the same product. The energy related wear is a more general term.

WEAR (2)

The wear depends on the feed material, the ball material and the size-reduction ratio. Balls wear much more in wet than in dry grinding because no powder adhere on the balls and protects them. Typical values are:

dry grinding	w_m =	10 to	300	g/t
wet grinding	w_m =	300 to	2000	g/t

dry grinding coal	w_e =	0.5 to	5	g/kWh
dry grinding cement clinker	w_e =	1 to	20	g/kWh
wet grinding iron ores	w_e =	10 to	100	g/kWh

The **relative charge wear rate** $\Delta M_B / M_B t$ is defines as:

charge weight lost per time/initial charge weight

$$\Delta M_B / M_B \; t = \left\{4p / \pi\varphi_B\left(1-\varepsilon_B\right)\right\} \; g^{1.5} \; w_e \; D^{0.5}$$

$p = 0.05$, $\varphi_B = 0.35$, $\varepsilon_B = 0.4$, $w_e = 10$ g/kWh,
$D = 4$ m

$\longrightarrow$ rcwr = 0.46 % per day which is 10 % in 22 days

ROLLER MILLS - INTRODUCTION (1)

The common characteristic of roller mills is that a particle bed passes the gap between one roller and a rotating grinding path/or between two rollers and is stressed there. The grinding path can be the surface of a pan, table, bowl, ring. The ball bearing mill is also count to this group because of the same stressing mechanism.

The stressing of a particle bed causes firstly a consolidation of the package, secondly particle beakage and thirdly agglomeration and even briquetting. Middle hard materials (calcite) agglomerate easier and at lower pressure but hard materials (quartz, magnetite) need much higher pressure and form weak agglomerates.

In roller-grinding path mills mostly such a pressure is applied that agglomeration just is avoided. A particular 2-roller mill was developed for a very high pressure, the material leaves the gap as dense flakes, which has to be deglomerated afterwards to liberate the produced fine material. This mill is called high pressure roller mill (HPR-mill).

ROLLER MILLS - INTRODUCTION (2)

History

Pan mills have been used since at least two thousands years. The first engineeringly designed pan mill was the Chilean mill (1830/50). The "arrestre" is a simple forerunner used in Mexico for grinding and amalgamation of gold ores. In the last quarter of the 19. century the Griffin mill (one pendulum roller), the Raymond-Bradley mill (3 to 4 pendulum roller), ring mills (Maxecon, Kent, Sturtevant) and bowl mills have been developed. Nowadays the grinding path is mostly flat or sligthly conical table. Roller-table mills are equipped with an interior air classfier, which causes a high interior material circuit flow. Huge mills with a capacity of some hundreds of tons per hour are manufac-tured. ~~cutores~~. The HPR-mill was introduced 1985. Modern designed large ring-roll mills are manufactured recently.

ROLLER MILLS - CONTENTS

DENOTATIONS

The following denotations are used:

Mill

D: roller diameter, D_T: table diameter, L: roller length, n: roller speed, n_c: critical value of n, n_T: table speed, u: peripheral roller velocity, s: roller gap, F: milling force, T: roller torque, T_T: table torque, P: power draft

Material

x: particle size, $Q_f(x)$ and $Q_p(x)$ feed and product size distribution, ρ_M: density, $\dot{M}$: mass throughput, δ_0 and δ_s: initial and maximum solid fraction per volume in the bed.

Characteristical and dimensionless parameters

Such parameters are useful for general considerations.

specific grinding force $F_{sp} = F / D\ L$

specific torque $T_{sp} = T / D^2 L$

relative gap with $\sigma = s / D$

relative speed $z = u / u_c \qquad u_c = \sqrt{g D / 2}$

specific throughput $\nu = \dot{M} / \rho\ D\ L\ u$

PRINCIPAL - DESIGN OF ROLLER-TABLE MILLS

In a roller-table mill the grinding work and an air classifyer are integrated in one housing. The grinding work consits of a rotating flat or slightly conical table and two to four rollers. The material is fed with a screw feeder to the center of the table, moves outwards by the centrifugal force, is stressed by overrolling and flows over the table rim into the ring-shaped gap between table and housing. A strong air stream carries the material upwardly. The coarser particles fall down to the table, the finer particles are carried up to the classifier which only let pass the product. The reject falls also down to the table. The interior material circuit is 10 to 20 times larger than the mill throughput.
The rolls are pressed upon the particle bed by a hydraulic force system. Two motors drive the grinding table and the classifyer rotor; a fan produces the air stream.
The product is separated from the air by cyclons and dust filters.

D_T	=	0.4	to	6 m
$D/_{DT}$	=	0.45	to	0.55
L/D	=	0.3	to	0.4
P_{table}	=	50	to	5000 kW
$\dot{M}$	=	1	to	500 t/h

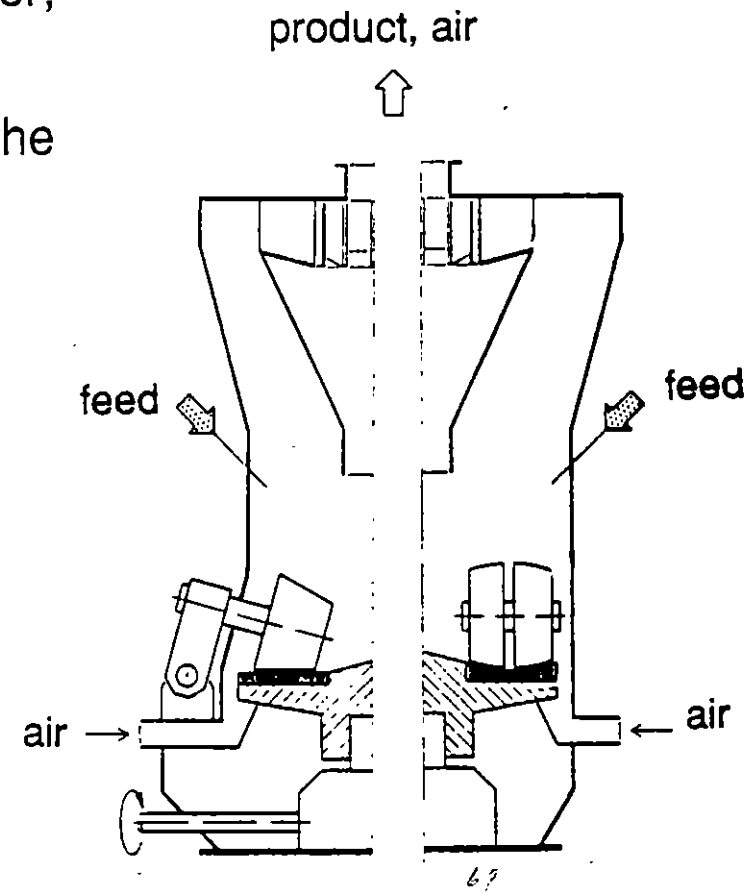

PRINCIPAL DESIGN OF HPR-MILLS

High pressure roller mills consits of a strong frame work with two rollers and the hydraulic force system. The bearing blocks of one roller are fixed and those ones of the other roller can move linearly. The force acts on the movable bearing blocks and presses that roller against the particle bed. The material flows from a vertical silo into the gap between the rollers. In the upper part of the gap the material is accelerated and the particle stream is narrowed. In the lower gap the particle bed is stressed in such an extent that flakes are performed. Both rollers run with the same peripheral velocity.

The roller surface is smooth or roughly structured by on-welded chevrons. The working gap is determined by the compaction behaviour of the material and the mass flow which is introduced into the compaction zone and depends on the outer and inner friction.

D	=	400	to	2000 mm
L/D	=	0.3	to	1
s/D	=	0.008	to	0.025
u	=	0.3	to	2.0 m/s
P	=	200	to	4500 kW
$\dot{M}$	=	20	to	1000 t/h

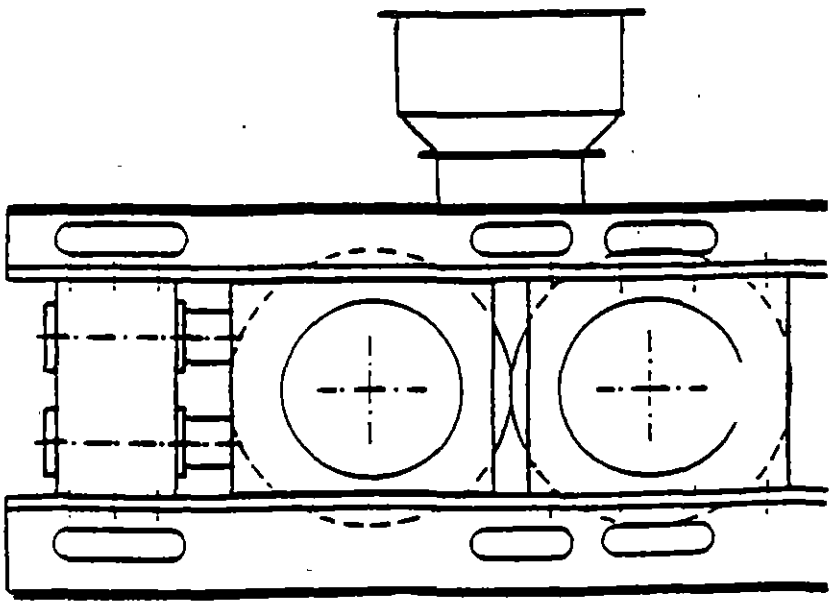

PRESSUR AND ROLLER MILL PERFORMANCE (1)

With increasing pressure p the energy absorption $E_{M,\,pb}$ of the particle bed and the amount of produced fine material f increases. However, f does not raise proportional with $E_{M,\,pb}$, therefore the efficiency declines. The recirculating load k in a roller-table mill or in a HPR-mill circuit is inversely proportional to f.

$$k = 1 / f$$

The recirculating load determins the mass flow $\dot{M}_c$ in the circuit.

$$\dot{M}_c = k\,\dot{M}$$

$\dot{M}$ = circuit throughput

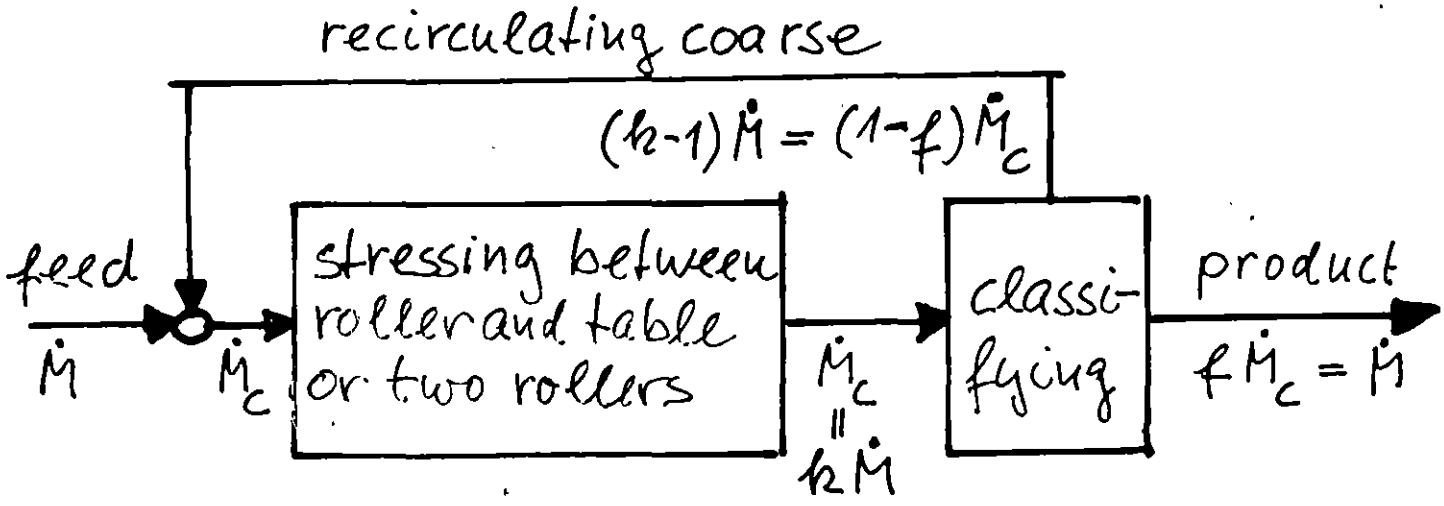

The size of mill, classifier and transporting equipements increase with raising k and therefore the capital costs too. It may be reasonable to apply a higher pressure to minimize the comminution costs although the size-reduction efficiency becomes smaller. This problem can be studied by stressing a particle bed in a piston press.

PRESSURE AND ROLLER MILL PERFORMANCE (2)

Experimental set-up

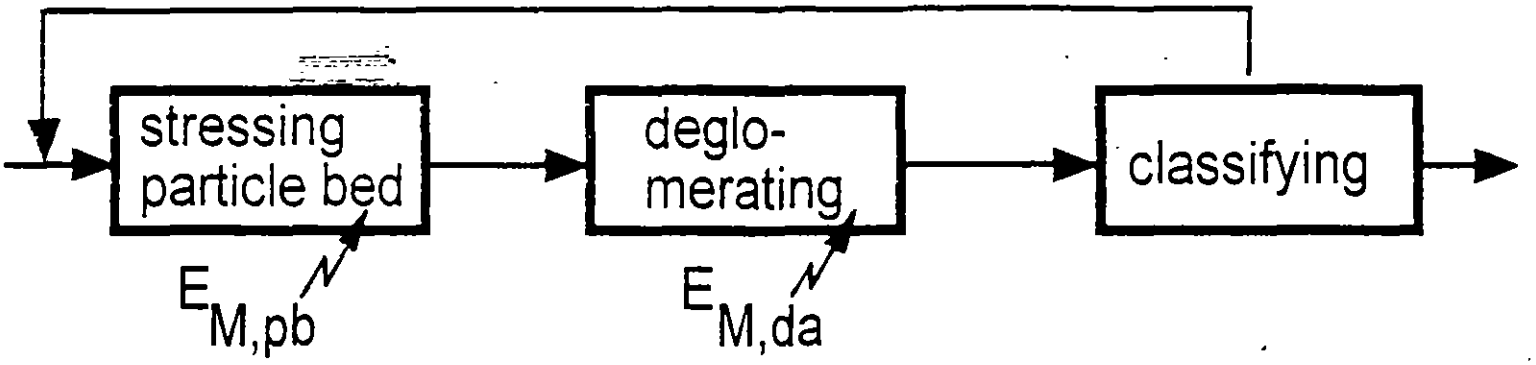

$E_{M,pd}$: energy absorption of the particle bed, k = 1/f : circuit factor, $E_{M,da}$: energy consumption for deglomerating, W_M : specific work-input for comminution and deglomeration

$$W_M = k \left\{ E_{M,pb} + E_{M,da} \right\}$$

Example: Grinding a cement clinker fraction 2.0 / 2.5 mm to a product with a specific surface of 2200 cm^2/g, $E_{M,da}$= 1.4 kWh/t

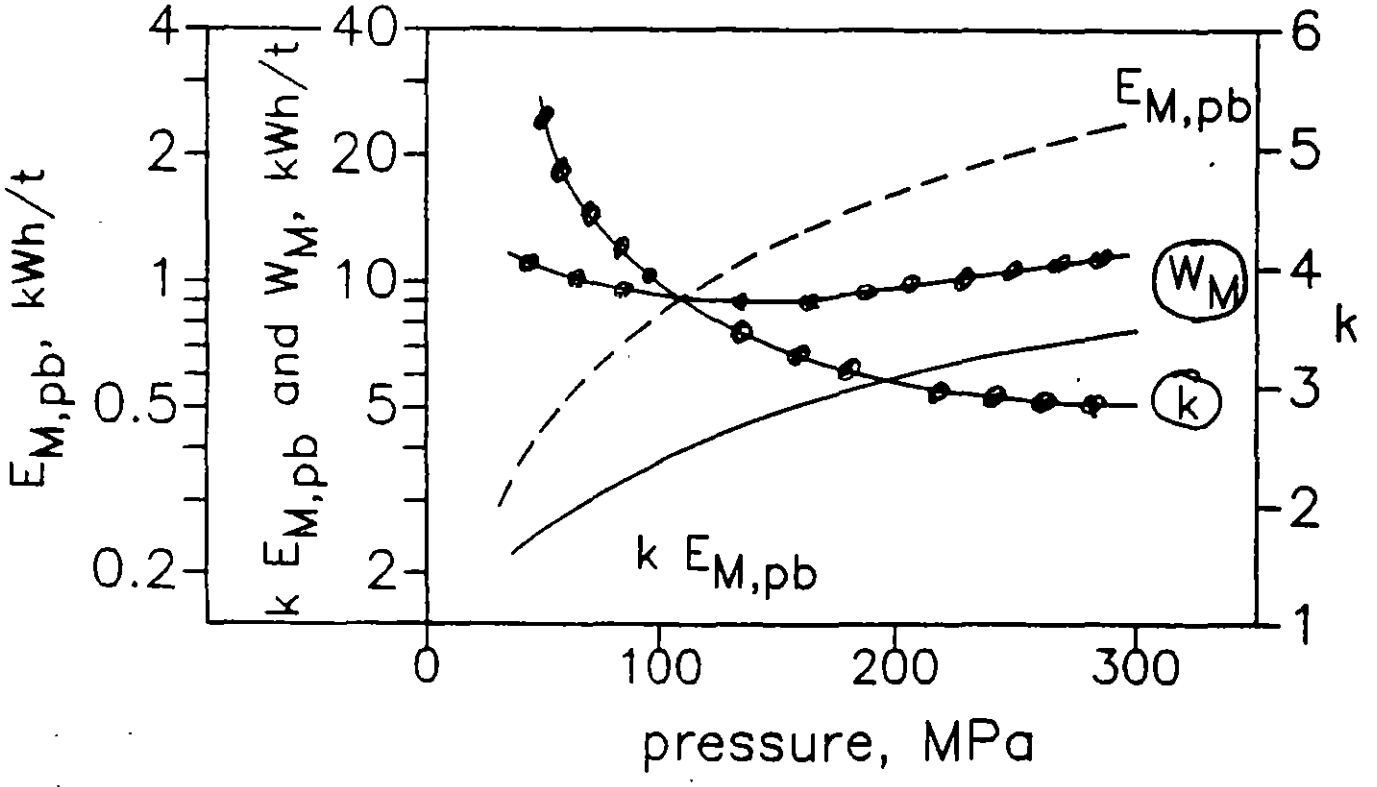

W_M almost independent on p, however k decreases from 30 at 50 MPa to 3 at 200 MPa.

POWER DRAFT OF ROLLER-TABLE MILLS (1)

The power draft is always an essential characteristic of a machine. Emperical equations are given and used. An engineer should know the background; equation in dimensionless terms are helpful.

The mill motor drives the table. The grinding force F acts on the roller and cause a torque if a material bed is introduced into the gap (without material no power draft !).

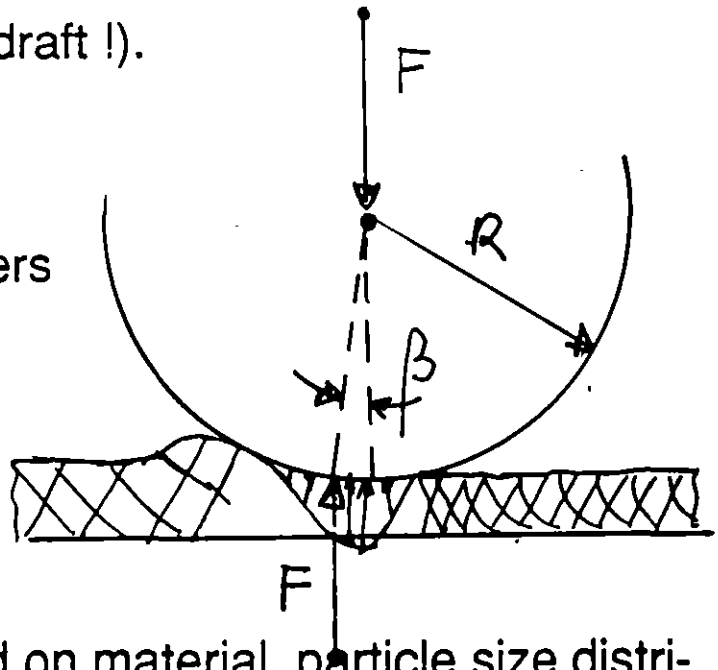

$$P = T_T \, \omega T = 2 \, \pi \, n_T \, T_T$$

$T_T = N \, T$ N: number of rollers

$$T = F \, R \, \sin \beta = \beta \, F \, (D/2)$$

$$\boxed{P = (\pi \, N \, \beta) \, F \, D \, n_T}$$

The force acting anlge β depend on material, particle size distribution of the introduced bed and is unknown. For generalizing the power equation, it should be considered that the size-reduction is determined by the pressure upon the bed. In different sized mills the average bed pressure $\bar{p}$ should be the same if the same size -reduction ist to perform.

$$\boxed{\bar{p} = k \, F \, / \, D \, L}$$

POWER DRAFT OF ROLLER-TABLE MILLS (2)

$P = (\pi N \beta) F D n_T \qquad \bar{p} = k F / D L$

$$\boxed{P = (\pi N \beta / k) (n_T \bar{p} L D^2)}$$

Introducing the relative speed z_T of the table.

$$P = \left(N \beta / \sqrt{2 k}\right) \bar{p} \left(L D^2 / \sqrt{D_T}\right) z_T \sqrt{g}$$

The term $\left(L D^2 / \sqrt{D_T}\right)$ is constant if mills are designed geometrically similar:

$$\boxed{P = p(N, \beta, k, z) \left(\bar{p} D_c^{2.5} \sqrt{g}\right)}$$

$$\boxed{p = \sqrt{2} N \beta^{z/} 2 k \qquad D_C = \left(L^2 D^4 / D_T\right)^{1/5}}$$

P = power fractor • power term

The power is proportional to the "power term" only as long as the "power factor" is constant. Usually D_c = (0.4 to 0.6) D.

An average force acting anlge $\bar{\beta}$ can be estimated with for torque and the grinding force.

$$T = (\$D/2) \sum_{i=1}^{N} \beta_i F_i = (D/2) \bar{\beta} \sum_{i=1}^{N} F_i = (D/2) \bar{\beta} F_{tot}$$

$$\boxed{\bar{\beta} = 2 T / D F_{tot}}$$

MECHANICS OF HPR-MILLS (1)

Stress field in the roller surface

The compaction of the particle bed causes a stress field in the roller surface with radial, peripheral and axial principal stresses σ_r, σ_p, σ_a: The stresses σ_p and σ_a arise because the cross-strain behaviour of steel and the particle bed differ. If the material slip on the roller then an additional shear in slip direction is causes, τ_p and τ_a. All these stresses depend on the anlge α and the axial position l.

$\sigma_r = \sigma_r(\alpha,l)$; $\sigma_p = \sigma_p(\alpha,l)$; $\sigma_a = \sigma_a(\alpha,l)$;

$\tau_p = \tau_p(\alpha, l)$; $\tau_a = \tau_a(\alpha,l)$

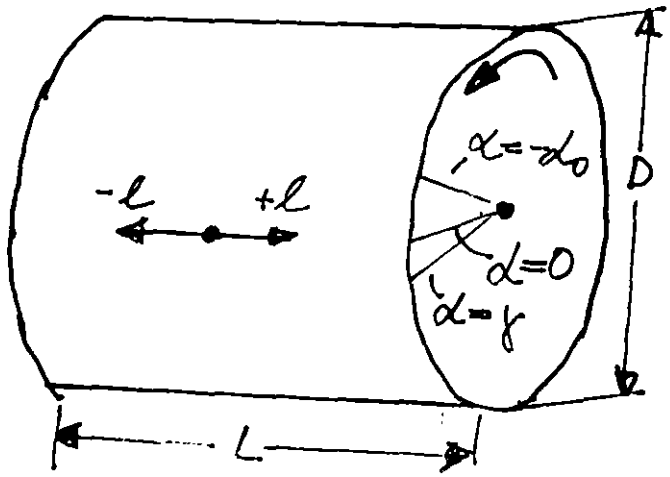

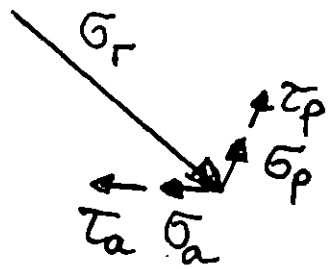

For simplification the averages of σ_r and τ_p over the roller length are considered in the following.

$$p(\alpha) = (1/L) \int_{-L/2}^{+L/2} \sigma_r(\alpha,l)\, dl$$

$$\tau(\alpha) = (1/L) \int_{-L/2}^{+L/2} \tau_p(\alpha,l)\, dl$$

The stresses σ_p and σ_a are internal stresses and do not affect the euqilibrium of outer forces.

MECHANICS OF HPR-MILLS (2)

The compaction begins at the compression angle α_o. The pressure p increases to a maximum at α around -1° and declines to zero at the relaxation angle γ. The peripheral stress σ_p acts firstly oppositly to the rotation, reaches an extremum, passes zero, then acts with the rotation, reaches a second extremum and declines to zero at γ. Measurements have shown that α_0 is in the range -12° to -8° and γ between +3° and +6°.

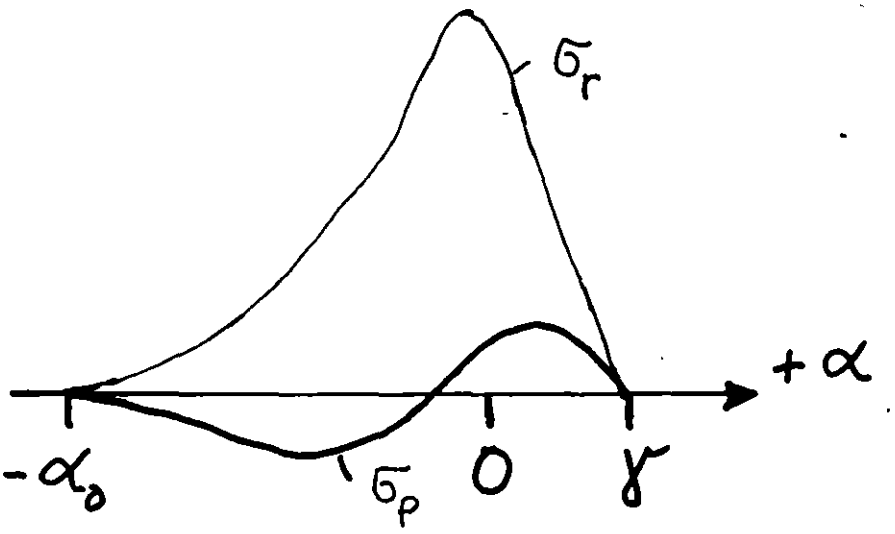

Slip is caused only if (σ_p/σ_r) is larger than the coefficient of friction μ. Then the slip induced shear τ_p is equal to $(\mu\ \sigma_r)$. Measurements indicates that slip may exist only in the relaxation zone.

MECHANICS OF HPR-MILLS (3)

Specific grinding force F_{sp} and maximum pressure p_{max}

The grinding force F is related to the p(α) - and τ(α) - function by an intergral expression:

$\tau(\alpha) \neq 0$ only if $\sigma_p/\sigma_r > \mu$.

$$F = (L\,D/2) \int_{-\gamma}^{\alpha_0} \{p(\alpha)\cos\alpha + \tau(\alpha)\sin\alpha\}\, d\alpha$$

Because α is at the maximum 12^0, it can be set:

$\cos\alpha = 1$ and $\sin\alpha = \alpha$.

The function p(α) can be expressed by p_{max} f(α). The slip induced shear τ(α) can be written as (μ(α) p (α)). The above equation is rearranged.

$$F = (L\,D/2)\, p_{max} \int_{-\gamma}^{\alpha_0} f(\alpha)\, \{1+\alpha\mu(\alpha)\}^{*}\, d\alpha$$

Normalizing the ~~angle~~ angle α with α_0: $q = \alpha / \alpha_0$; $k = \gamma / \alpha_0$

$$F = (L\,D/2)\, p_{max}\, \alpha_0 \int_{-k}^{1} f(q)\, \{1+q\,\mu(q)\}\, dq$$

$$F_{sp} = F / L\,D = p_{max}\, \alpha_0\, I_F$$

$$I_F = (1/2) \int_{-k}^{1} f(q)\, \{1+q\,\mu(q)\}^{*}\, dq$$

$$p_{max} = F_{sp} / \alpha_0\, I_F$$

* this term is only in that α-range or q-range to consider in which $\sigma_p/\sigma_r > \mu$

MECHANICS OF HPR-MILLES (4)

$$p_{max} = F_{sp} / \alpha_0 \; l_F$$

The factor l_F depends mainly on the $p(\alpha)$-function shape and by that on the material, the (D/x_{max})-ratio and the roller surface structure. Measurements have shown that $(1/\alpha_0 \; l_F)$ is between 20 and 40.

If $(\alpha_0 \; l_F)$ is constant then the maximum pressure p_{max} is proportional to the specific grinding force F_{sp} which, therefore, is the appropriate parameter for characterizing the applied force and comparing HPR-mills of different size.

MECHANICS OF HPR-MILLS (5)

Specific torque T_{sp} and maximum pressure p_{max}

The total torque T of both rollers is related to the p(α) - and τ(α) - function by an intergral expression:

$\tau(\alpha) \neq 0$ only if $\sigma_p / \sigma_r > \mu$!

$$T = 2\left(LD^2/4\right) \int_{-\gamma}^{\alpha_0} \{p(\alpha)\cos\alpha + \tau(\alpha)\}\, d\alpha$$

Because α is at the maximum 12^0, it can be set:

$\cos\alpha = 1$ and $\sin\alpha = \alpha$

The function p(α) can be expressed by p_{max} f(α). The slip induced shear τ(α) can be written as (μ (α) p(α)). The above equation is rearranged.

$$T = \left(LD^2/2\right) p_{max} \int_{-\gamma}^{\alpha_0} f(\alpha)\, \{\alpha + \mu(\alpha)^{*}\}\, d\alpha$$

Normalizing the ~~angle~~ angle α with α_0 : $q = \alpha / \alpha_0$; $k = \gamma / \alpha_0$

$$T = \left(LD^2/2\right) p_{max}\, \alpha_0^2 \int_{-\gamma}^{1} f(q)\, \{q + (\mu(q) / \alpha_0)\}\, dq$$

$$T_{sp} = T / LD^2 = p_{max}\, \alpha_0^2\, I_T$$

$$I_T = (1/2) \int_{-k}^{1} f(q)\, \{q + (\mu(q) / \alpha_0)^{*}\}\, dq$$

$$p_{max} = T_{sp} / \alpha_0^2\, I_T$$

* this term is only in that α-range or q-range to consider in which $\sigma_p / \sigma_r > 0$

MECHANICS OF HPR-MILLS (6)

$$p_{max} = T_{sp} / \alpha_0^2 \, I_T$$

The fractor I_T depends on the $p(\alpha)$ - function shape and also on the compression anlge α_0 if the material is slipping. Therefore the material, the (D/x_{max}) - ratio and the roller surface structure influences I_T. Measurements have shown that
$(1 / \alpha_0^2 \, I_T)$ is between 700 and 1300.
If $(\alpha_0^2 \, I_T)$ is constant then the maximum pressure p_{max} is proportional to the specific torque T_{sp} which, therefore, is the appropriate parameter for charcterizing the resulting torque and comparing HPR-mills to different size.

Force acting angle β

The force acting angle follows directly from the measured grinding force F and torque T.

$$T = F \, D \, \sin\beta = \beta \, F \, D \qquad \beta = T / F \, D = T_{sp} / F_{sp}$$

The (α_0 / β) - ratio is given by

$$\alpha_0 / \beta = I_F / I_T$$

Measurements have shown β is between 1.7^o and 3.4^o and (α_0 / β) between 3 and 6; β decrease with raisings force.

THROUGHPUT OF HPR-MILLS (1)

Three regions of the space between the rollers can be distinguished:

- **Acceleration zone** in which the particles are accelerated and the material stream is narrowed both caused by friction forces between rollers and material, therefore slip on the roller and inside the bed exists.
- **Compaction zone** beginning at the compression angle α_0, i.e. no slip or only little slip just at the end, however very high compaction ($\delta > 0.85$) provokes slip.
- **Relaxation zone** between $\alpha = 0$ and $\alpha = \gamma$, the compacted bed respectively the flakes expand, the expansion is 10 to 40 %, slip exists.

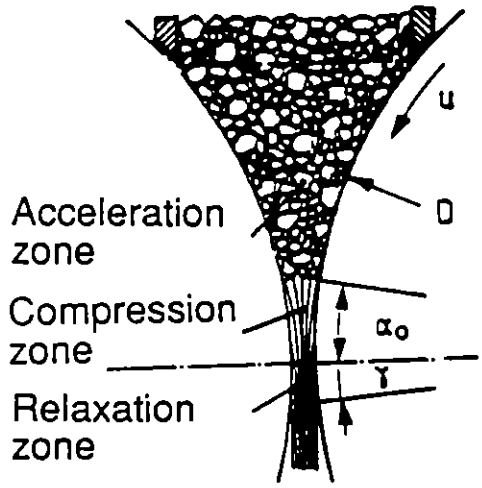

The throughput $\dot{M}$ is determined by the material flow through the entry of the compaction zone at α_0 and also equal to the material flow through the smallest gap at $\alpha = 0$.

$$\dot{M} = \delta_0 \rho h L w_0 = \delta_s \rho s L w_s$$

h: entry width, w_o and w_s average material flow velocity at α_0 and $\alpha = 0$

THROUGHPUT OF HPR-MILLS (2)

If slip can be neglected then $w_0 = w_s = u$, the specific throughput ν reads.

$$\nu = \dot{M} / \rho \, L \, D \, u = \delta_0 \, (h / D) = \delta_s \, (s / D) = \delta_s \, \sigma$$

$$h = s + D \, (1 - \cos\alpha_0) = s + (D\alpha_0^2 / 2)$$

$$\boxed{\nu = \delta_0 \left\{ \sigma + \left(\alpha_0^2 / 2 \right) \right\} = \delta_s \, \sigma}$$

Regarding the maximum feed particles x_{max} two situations are to consider:

- $x_{max} < s$, a particle bed exists in the entry , δ_0 is about the relative bulk density δ_B, $\delta_0 \approx \delta_B = 0.5$ to 0.6
- $x_{max} > 2s$, the maximum particles contact directly both rollers, $\delta_0 < 0.50$

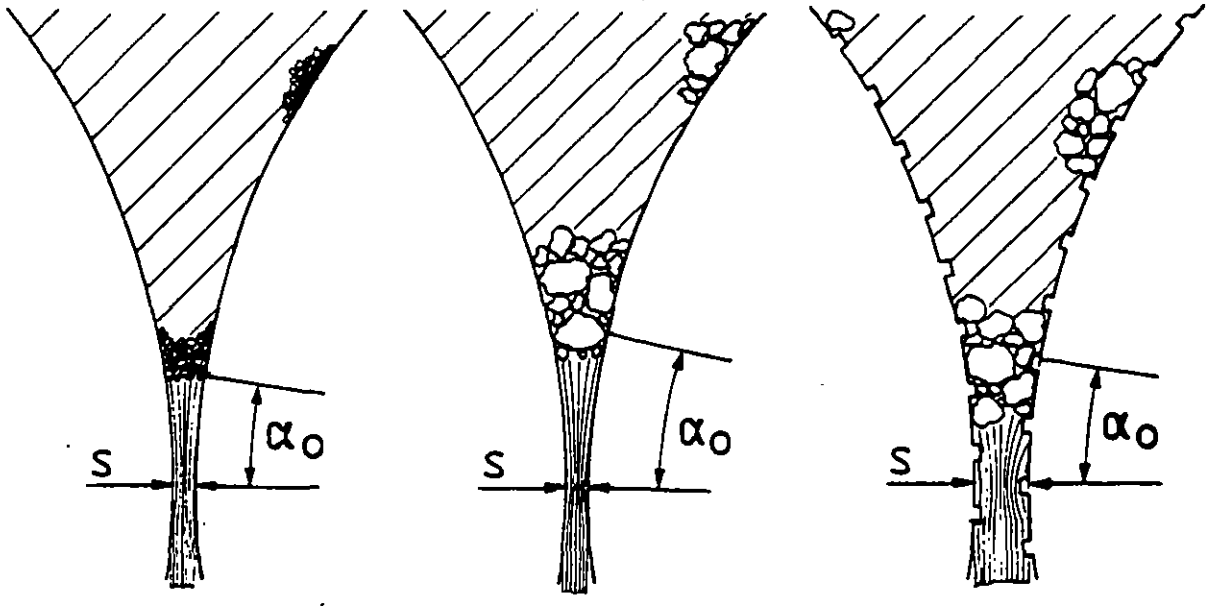

THROUGHPUT OF HPR-MILLS (3)

The relative gap width σ results from the equilibrium of the particle bed reaction and the grinding force and can be influenced only a little. Usually the grinding force is chosen that δ_S is 0.7 to 0.8.

Introducing a **particle bed** than δ_0 is predetermined by δ_B depending on p. s. d., therefore α_0 is the dominant factor which depends on the inner and outer friction and these both increase as

- feed finer
- p. s. d. wider
- particle shape more edged
- moisture raises in hydrophilic feed
- moisture declines in hydrophobic feed
- roller surface rougher

Feeding a coarse material then the **direct contacts** determine the compression angle α_0.

$$\cos\alpha_0 = (D+s) / (D+x_{max}) = (1+\sigma) / (1+(x_{max} / D))$$

It can be shown that in this situation σ and δ_0 are correlated to each other and the grinding force F affects the throughput which decreases as F is increased.

THROUGHPUT OF HPR-MILLS (4)

Throughput characteristics

$\dot{M} = \delta_s \sigma \rho D L u$

The ($\dot{M}$, u)-function represents the throughput characteristic.

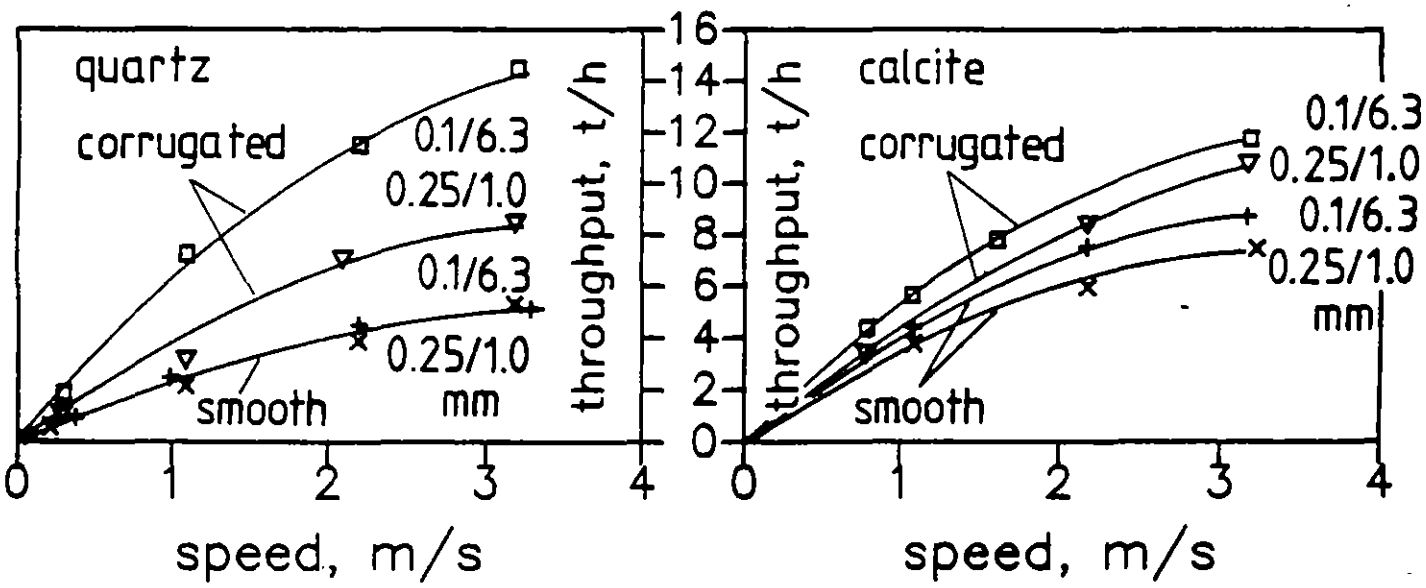

- The throughput raises proportional to the velocity only at low speed, at higher speed the curves bend downwards.
- The material influences strongly the throughput.
  smooth rollers: higher throughput with calcite than with quartz; no particle size influence with quartz, however with calcite $\dot{M}$ increases as x_{max} becomes coarser.
  corrugated rollers: higher $\dot{M}$ than with smooth rollers, much stronger size influence with quartz than with calcite, higher $\dot{M}$ with coarse quartz than coarse calcite feed.

THROUGHPUT OF HPR-MILLS (5)

Explanations:

(1) The **material influence** is due to the material hardness. Softer materials (calcite) tend to adhere on the roller surface, therefore the friction increases and by that $\dot{M}$. The furrows of the corrugated surface is partly filled with calcite and the effect of the corrugation is reduced. Harder materials (quartz) clean the surface.

(2) **Moisture** increases the inner friction of hydrophilic materials, $\dot{M}$ increases as long as the volumetric water content is smaller than δ_S. A moist hydrophobic feed (coal) causes a slippy film on the roller, which reduces friction and by that the throughput.

(3) The underproportionality of $\dot{M}$ over u has two reasons.

• The **acceleration effect** is causes by the centrifugal acceleration which reduces the particle contact force on the roller and by that the friction force. This effect is independent on particle size.

•The **backflow effect** is caused by the air expelled from the voids as the bed is compacted. Most of the air flows upwards and can loosen the bed above α_0 or even fluidize partly, if the particle are fine enough. The throughput begins to oscillate and breaks down as the speed is further increased. This effect depends strongly on the particle size.

THROUGHPUT OF HPR-MILLS (6)

Grinding force and throughput

In principle the grinding force influences the throughput. The package situation in the gap determines the force sensibilty. If $x_{max} < s$ then $\dot{M}$ is almost independent on F; size-reduction and throughput are decoupled. As particles contact directly the rollers, that is $x_{max} > 2s$, then $\dot{M}$ declines with raising force.

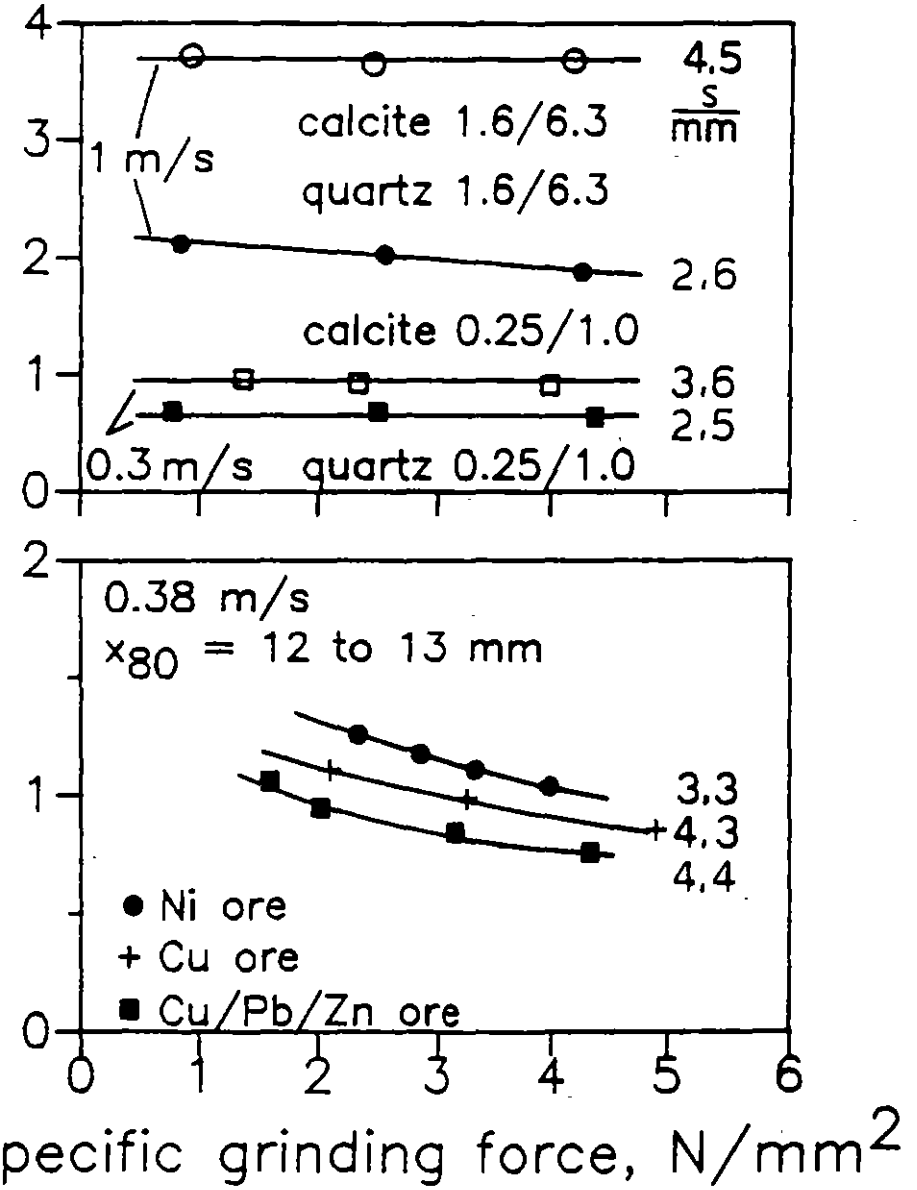

Throughput number and throughput elasticity

The acceleration effect is caused by the centrifugal force which acts on the particles moving along the rollers, therefore the square of the speed should be introduced into the throughput relation.

$$\dot{M} = C_1 u - C_2 u^2$$

The specific throughput reads:

$$\nu = \nu_0 - (1/\kappa)\, z$$

$z = u / u_c$: relative speed, $u_c = \sqrt{g D/2}$, ν_0 : throughput number, κ: throughput elasticiy

A straight line in the (ν, z) - diagram proves the idea of the acceleration effect.

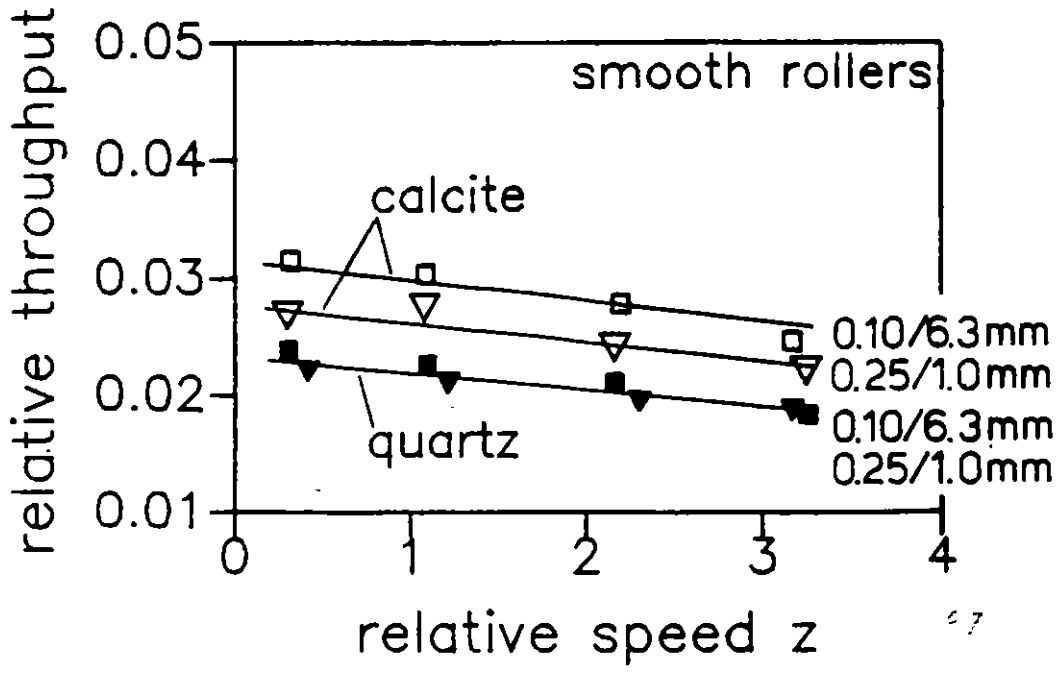

PARTIKELBEWEGUNG IN DER BESCHLEUNIGUNGSZONE

$D = 200\,mm$

$u_c = \sqrt{gD/2} \approx 1\,m/s$

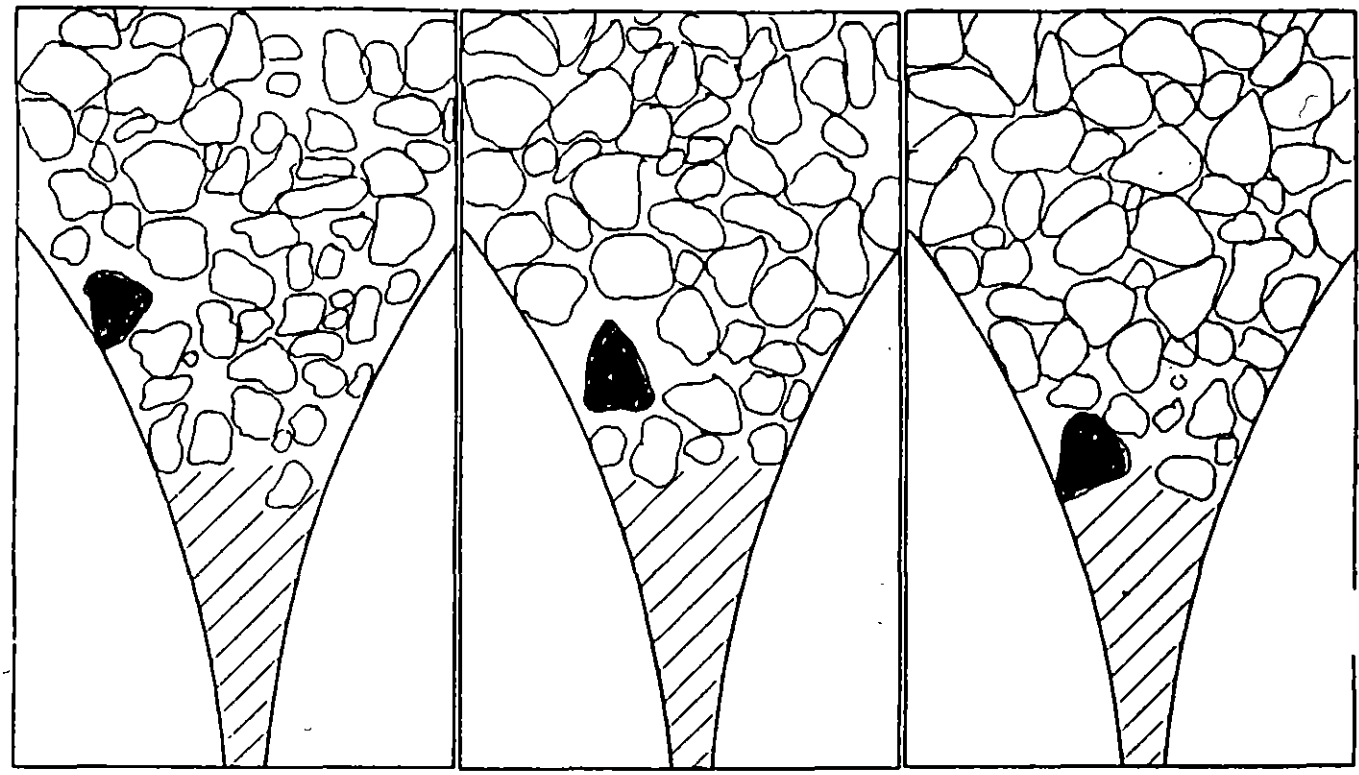

glatte Walzen, $u = 2\,m/s$

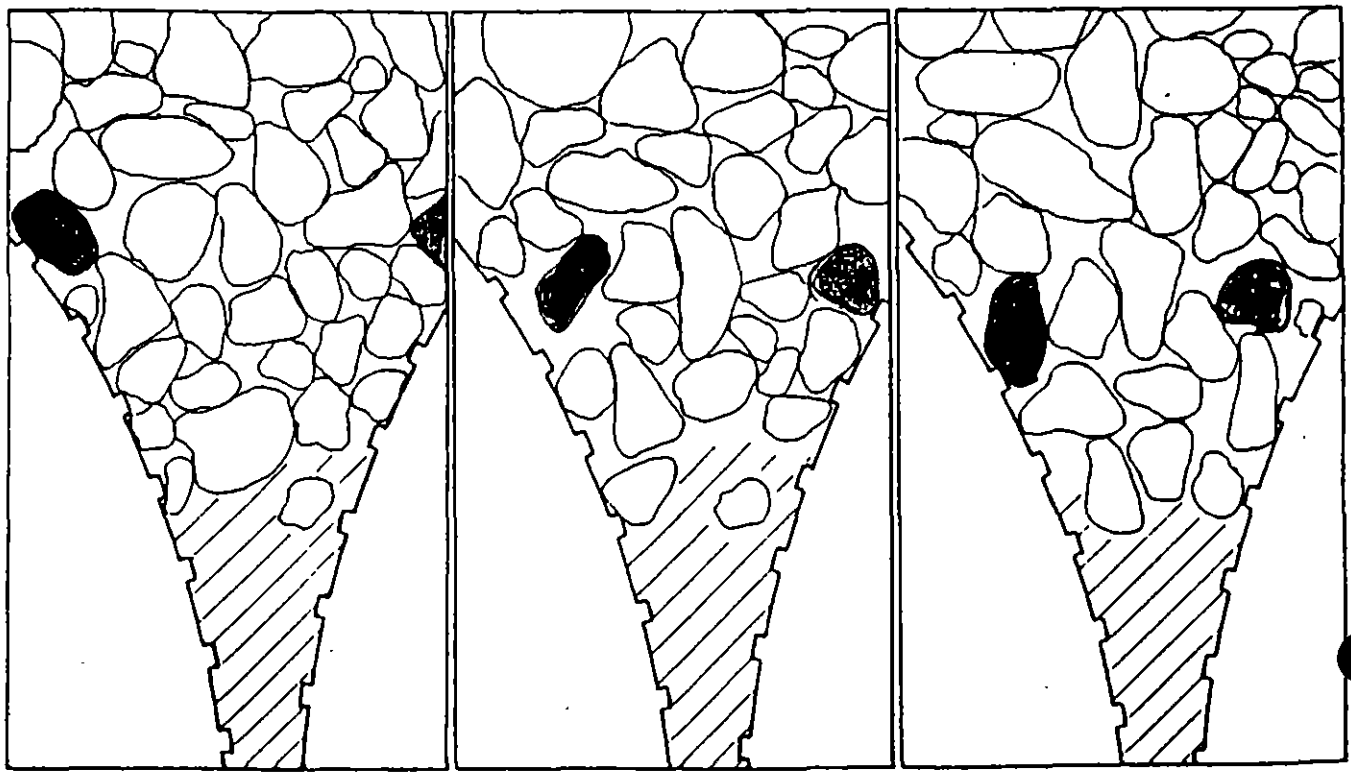

profil. Walzen, $u = 1\,m/s$

$u = 1\,m/s$

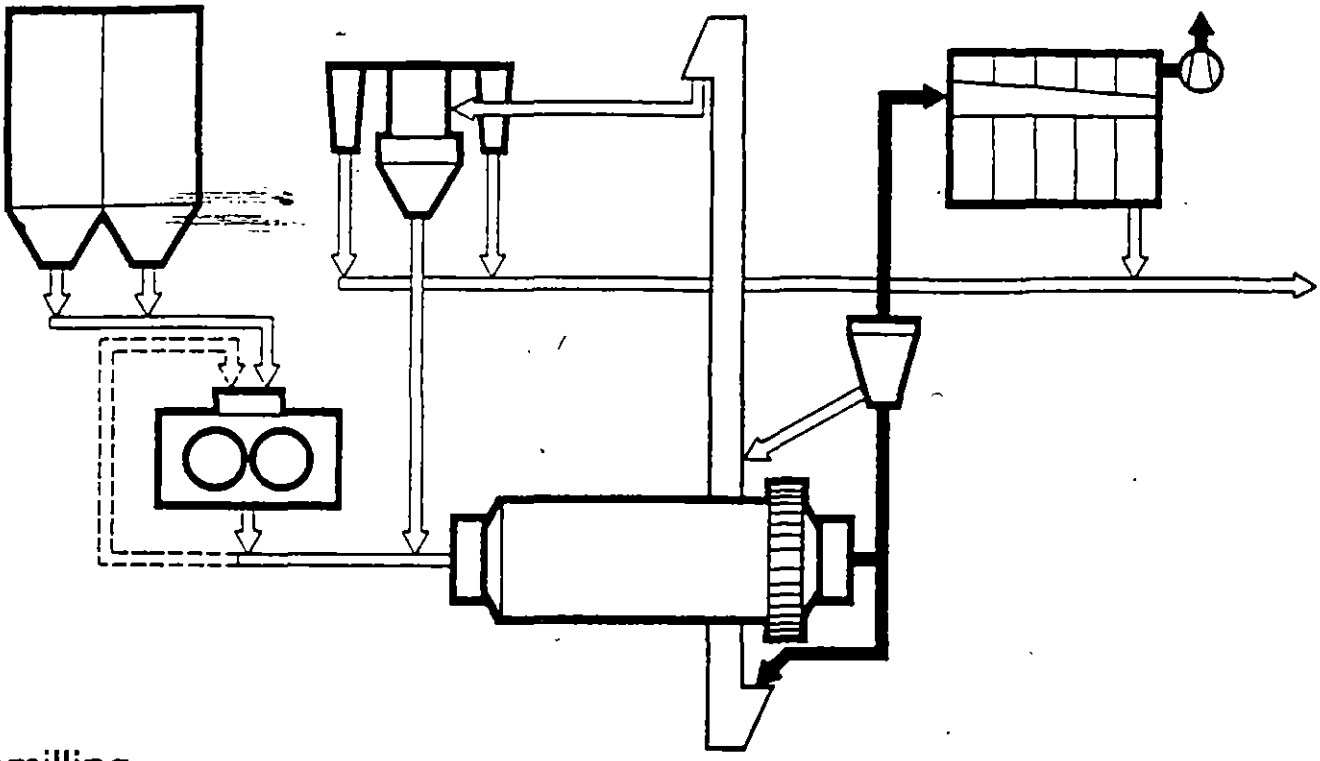

Premilling

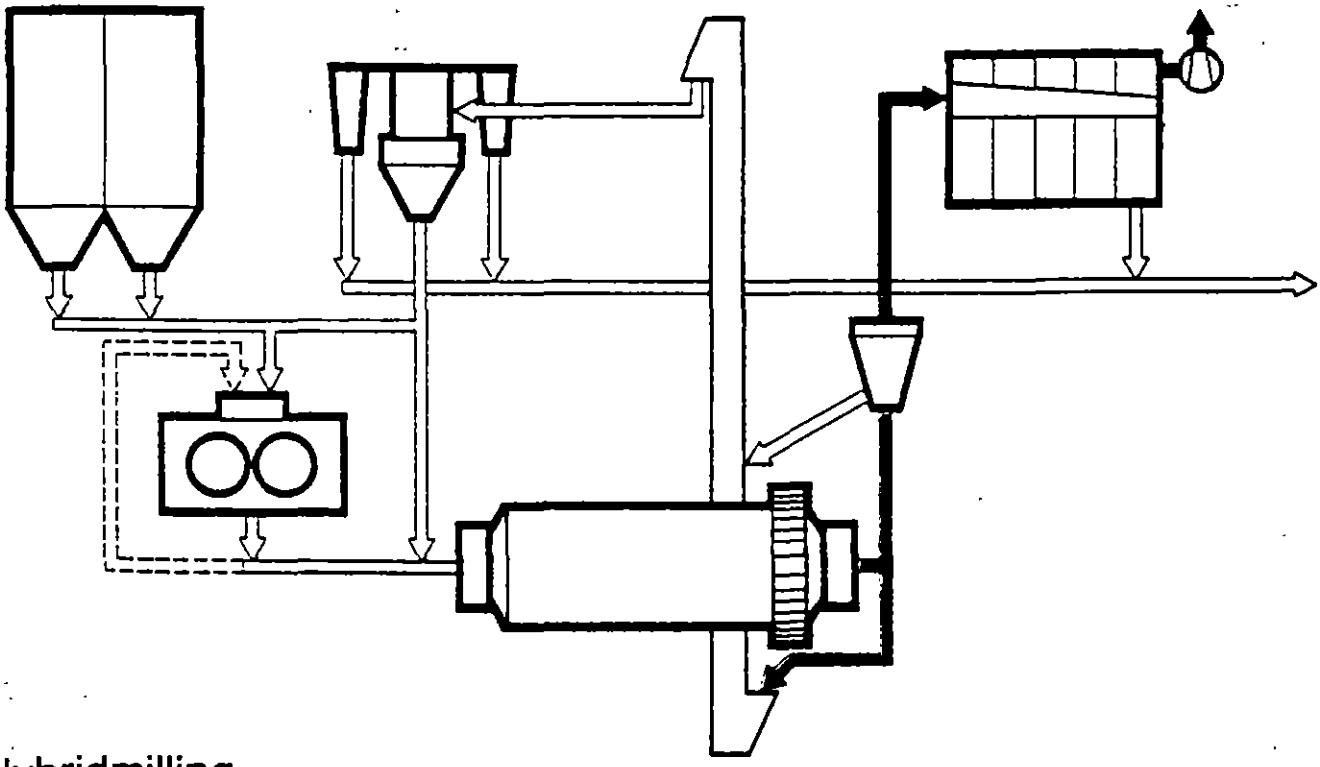

Hybridmilling

STIRRED MILLS - INTRODUCTION (1)

Stirred mills belong to the main group of grinding media mills. They consits of a cylindric (mostly circular) vessel filled almost completely with balls and a stirrer which introduces the energy to the balls. The ball are very small 0.2 to 3 mm in diameter. Theses mills are most capable for very fine grinding below about 30 µm or even microfine grinding below some microns. They are operating wet in batch or through-flow mode. The suspension is pumped into the mill and discharged through a screen with quadratic or slit-shaped apertures or through a ring slit between a rotating plate and a ring. The high power density can cause strong temperature raise and requires cooling of the vessel.

Stirred mills are classified in respect to the stirrer peripheral velocity and to a particular geometric extension characterizing the process volume.

- **low speed mills,** peripheral velocity 1 to 4 m/s, often also called attritor
- **high speed mills,** pheripheral velocity 8 to 12 m/s, that the usual range
- **gap mills,** width of process volume only some millimeter however at least 5-times the ball diameter
- **tower mills,** mill length much larger than diameter, tower mills use larger balls of 1 to 20 mm and run with low speed.

STIRRER MILLS - INTRODUCTION (2)

Advantage: The only mill for microfine wet grinding
Disadvantage: High wear with abrasive feed, then coating of stirrer and mill wall with plastics or rubber, reduced heat transfer, for avoiding contamination larger particles of the feed material are used as media (autogenous grinding).

Histrory

Using a stirrer vessel for grinding was firstly proposed 1928.
These so-called attritors are slow speed mills
In the forties high speed mills have been developed using rounded quartz sand as grinding media. They have been called sand mills.
The development of modern high speed mills began in the fifties.

Tel.05321/64064 Fax 64074

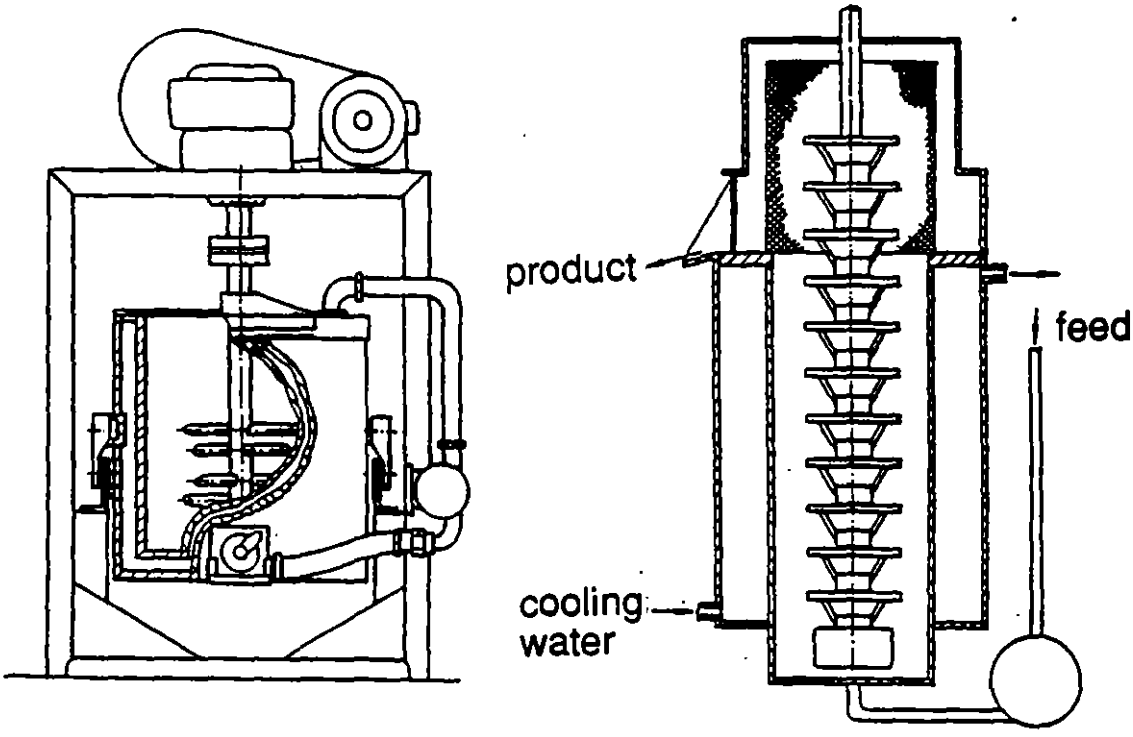

Attritor Sand Mill

TYPICAL DESIGN FEATURES OF STIRRED MILLS (1)

The **orientation of the mill** can be horizontal or vertical. The horizontal orientation is advantageous for large mills because the power peak at starting is reduced. The vertical orientation reduces the media lift which causes pressing of the balls against the discharging apertures.

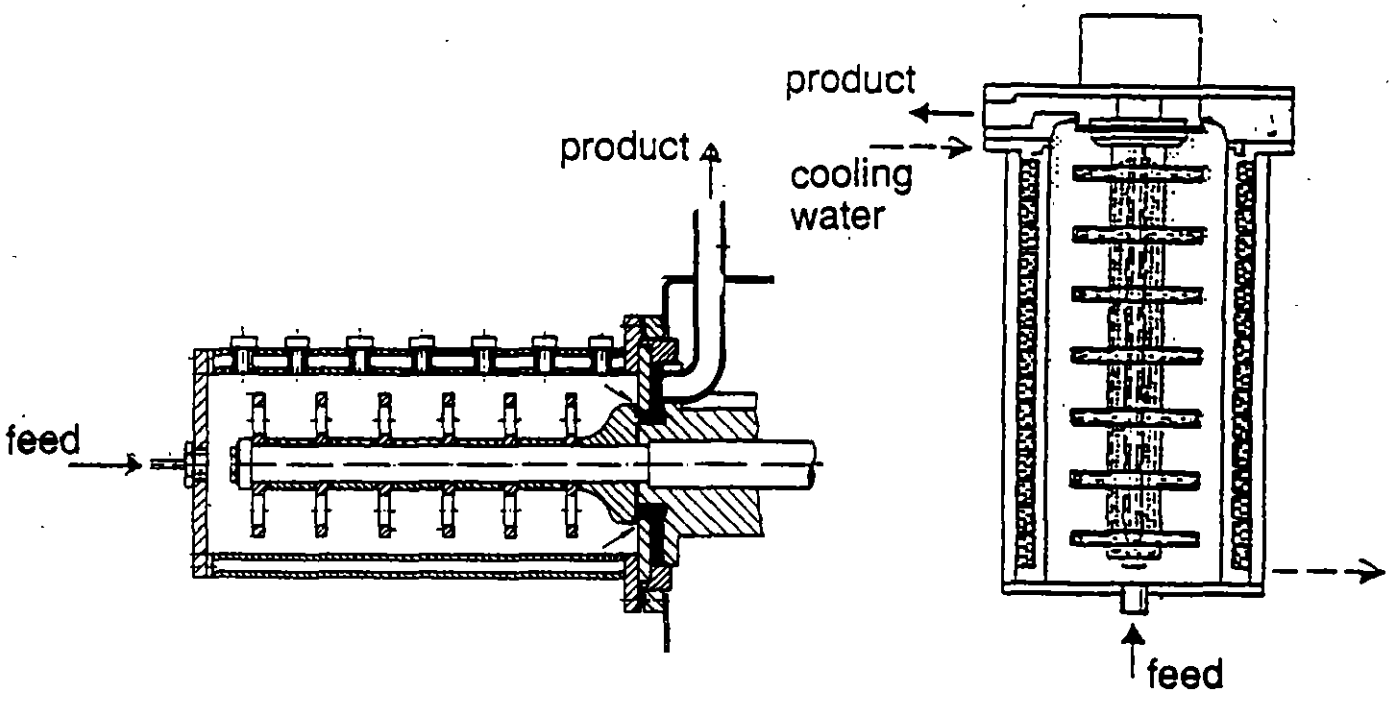

The **length to diameter ratio** is usually between 1 and 4, at very big mills it can be up to 6. If required that the temperature raise should be constant, then the power has to be proportional to vessel wall, $P \propto A$. If required that the specific work-input should be constant, then the power has to be proportional to the throughput, $P \propto \dot{M}$. With these condition follows:

Throughput proportional to $(\text{volume})^{2/3}$ if $(L/D) = \text{const.}$

TYPICAL DESIGN FEATURES OF STIRRED MILLS (2)

Quite different **stirrer elements** have been tried. The shape of the elements determine the torque and by that the power draft and the power density which dominates the size-reduction effect. Nowadays discs with circular holes are mainly used because they are the best compromise in respect to power density and wear. Stud discs are used if a very high power density is required and the feed is less abrasive.

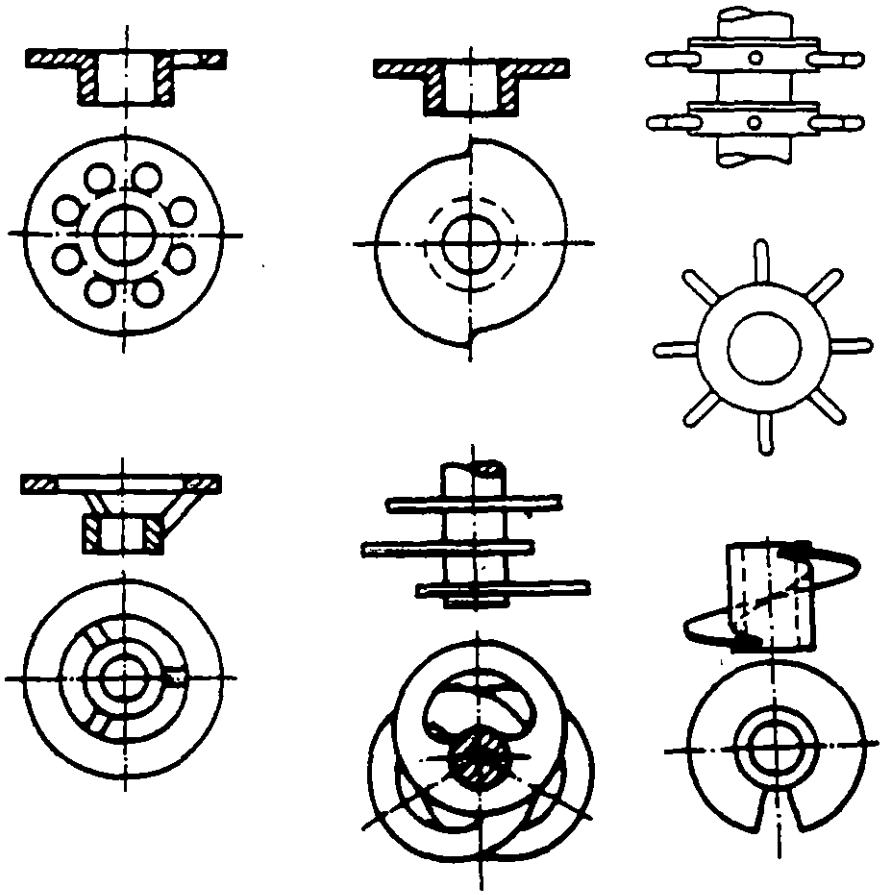

The **ball filling ratio** is chosen about 0.8 of the free mill volume which is the mill volume minus the stirrer volume.

TYPICAL DESIGN FEATURES OF STIRRED MILLS (3)

The **media separator** at the outlet have to hold back the ball charge in the mill whereas the slurry is discharged. A cylindrical screen is the most simple separator for balls larger than 1 mm. Mills with a screen are called open mills. The carge forms a trompe which could be disadvantageous because air is introduced into the slurry and bubbles are created. To avoid this effect the mill must be closed. The slurry discharge is achieved through a so-called friction slit or through a metallic slit screen filter.

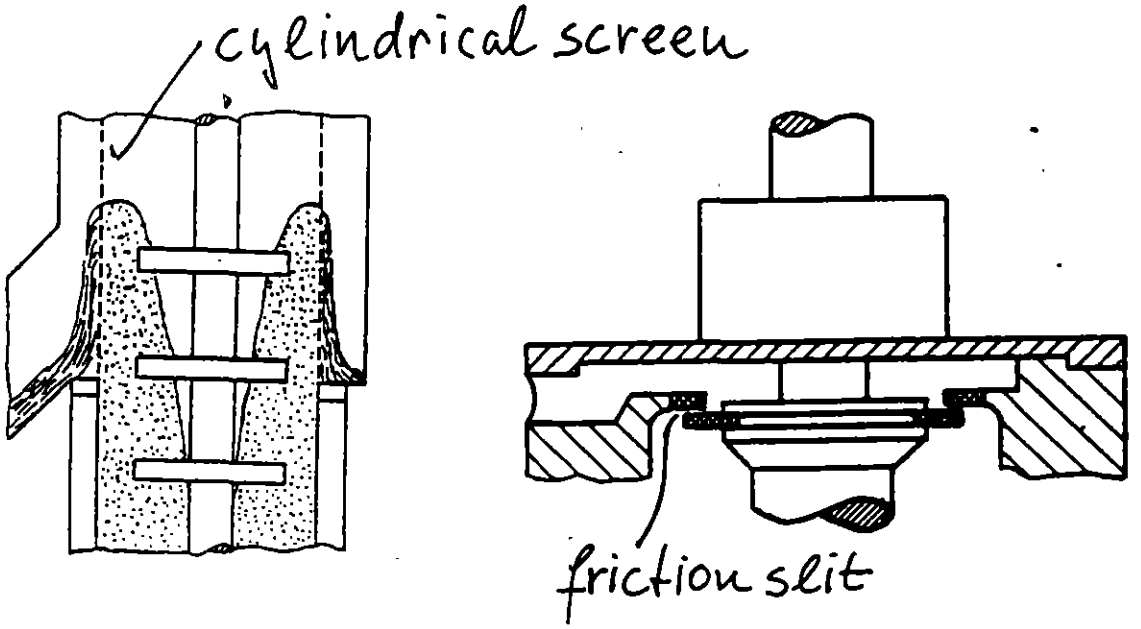

The friction slit consists of a rotating disc mounted on the stirrer shaft and equiped with a wear resistive material and a ring of such material. The rotation helps to reject the balls. The minimum gap width is 100 µm. In full size mills a friction slit should not be used for balls smaller than 0.5 mm.

Slit screen filter are manufactured with slit down to 50 µm.

TYPICAL DESIGN FEATURES OF STIRRED MILLS (4)

Grinding media of different materials and sizes are used: glass, aluminium oxide, zirconium silicate, zirconium oxide, steel, hardened steel. The sizes are between 0.2 and 5 mm.

CHARGE MOTION (1)

The stirrer causes a 3-dimensional flow pattern of the charge. The tangential motion dominates and creates centrifugal forces. The tangential velocity depends on the radial and axial position and has a maximum at the stirrer tips and a minimum at the wall and causes a radial secondary flow which is directed outwardly in the disc region and inwardly in the middle region between two discs.

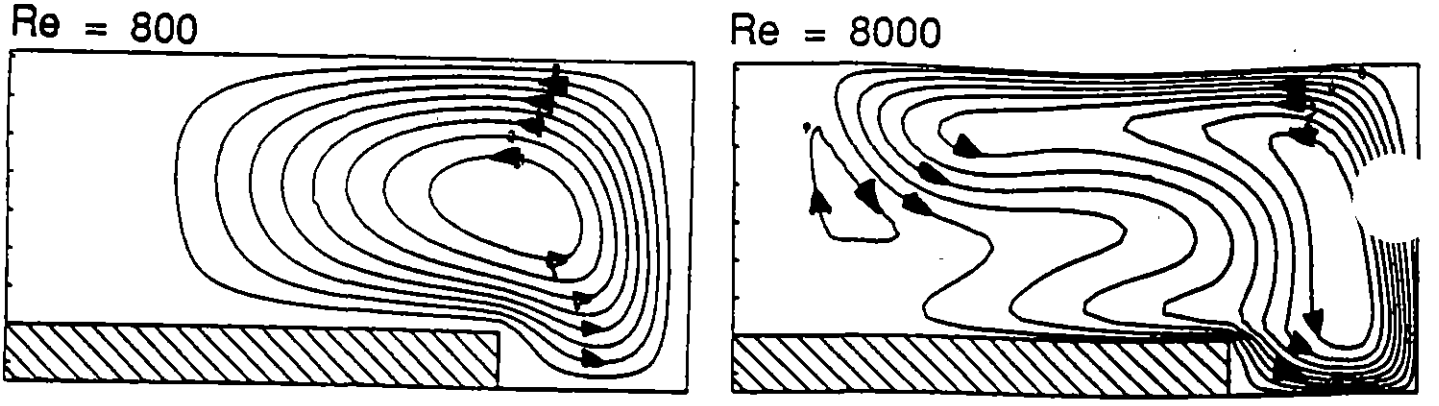

Flow lines of the fluid

Because of the 3-dimensional flow pattern, the balls slip against each other which causes as well particle stressing by compression and shear as exchanging of particles and fragments in the contact region between the balls. This relative movement of the balls is essential for the size-reduction.

CHARGE MOTION (2)

With a sophisticated model the local energy dissipation in the flow pattern has been calculated. The maximum values arise in a small region at the outer part of the discs and in a small region at the wall opposite the discs. This means the size-reduction is mainly performed only in a small fraction of the mill value.

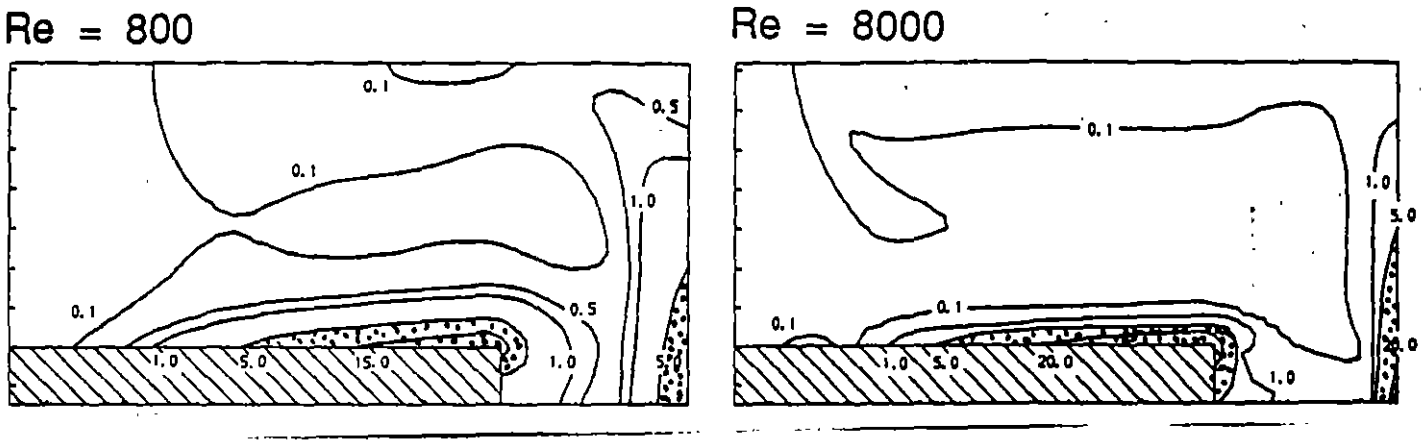

Lines of equal relative energy dissipation in the fluid

regions with over 5

The centrifugal acceleration is between 50 g and 2000 g which is much higher than the gravity acceleration, therefore the flow pattern is not much influenced by the mill orientation.

The centrifugal forces push the charge outwards; a cylindrical region around the shaft is free of balls. To avoid a short flow of the suspension from the inlet to the outlet, the discs should not have openings in this region.

POWER DRAFT OF STIRRED MILLS (1)

The power draft is an essential characteristic of a machine. Equations for the different types of sitrred mills are not known. The general background is discussed.

$$P = T\,\omega = 2\,\pi\,n\,T = 2\,u\,T / D_s$$

The torque is caused by the drag force F acting on the stirrer and depends on particular design of it, the slurry density ρ^*, balll diameter, filling ratio and the peripheral velocity u. The flow is turbulent, therefore the drag force is proportional to the rotor velocity square.

$$F = \text{const}\ \rho^*\ A\ u^2$$

A: surface of all stirrer elements, z: number of elements, D_s, D_i: diameter of the stirrer and the shaft, l: spacing of the elements. For geometrical similar mills, that is

$z = L / l$, $D_s \propto D_i$ and $l \propto D_s$,

the surface A can be expressd as:

$$A = \text{const}\ L\ D_s$$

$$T = F\ D_s = \text{const}\ \rho^*\ L\ D_s^2\ u^2$$

$$P = p\ \rho^*\ L\ D_s^2\ u^3$$

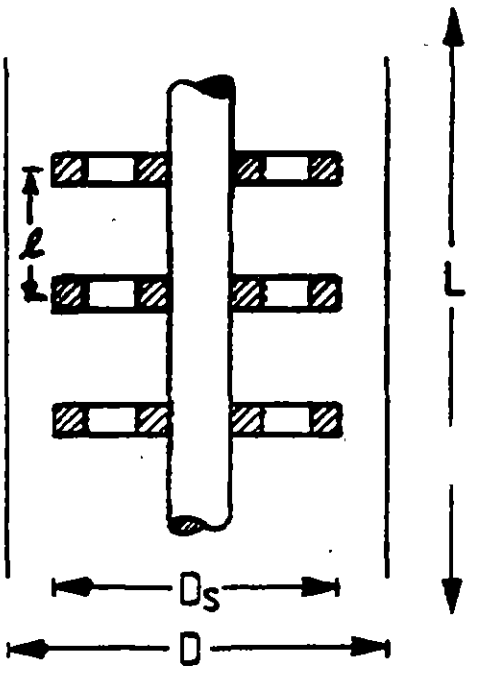

POWER DRAFT OF STIRRED MILLS (2)

$$P = p \cdot \rho^* \cdot L \cdot D_S^2 \cdot u^3$$

The power factor p depends only on mill and stirrer design, ball diameter and filling ratio and can be easily determined experimentally. p should be constant for geometrical similar mills. If the disc spacing l is not proportional to the mill lenght L, then p is to assume being proportional to z.

The ball size has a minor influence as long as it is not variated in a large extend.

The suspension throughput begin to influence the power if the charge is pressed against the media separator, however this situation is not a proper operation.

For mills with usual disc stirrer in proper operation, the power factor p is about 0.05.

Tel.05321/64064 Fax 64074

BALL SIZE

The ball size influences the size reduction. The example for grinding calcite 30/100 µm in a disc stirrer mill shows clearly the situation.

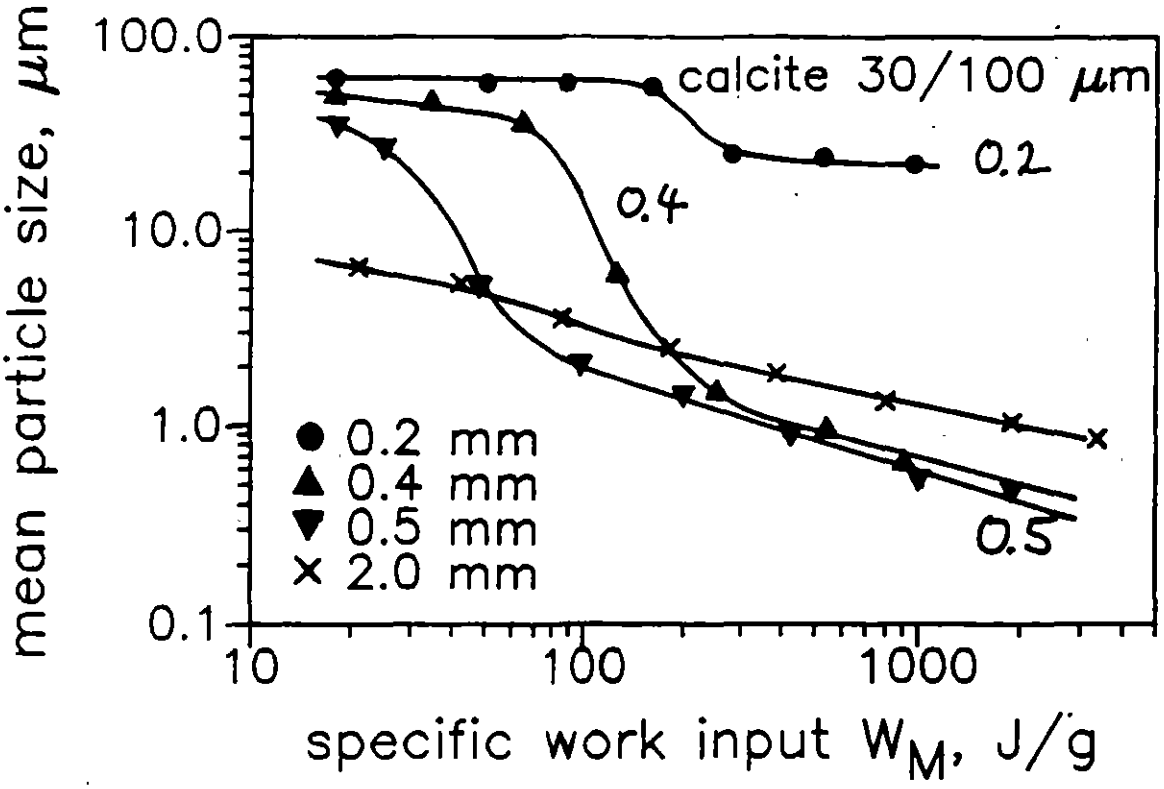

The very small balls of 0.2 mm are inefficient. The balls of 2 mm break the feed particles rapidly, however need in the mircrofine range much more energy than the 0.4/0.5 mm balls.

The selection of the optimum ball size is very important for an effective operation. In comparing different types of mills the ball size effect have strictly to be considered.

PAUL RADDATZ Gibraltar
Tel. 053 21/6 40 64 Fax 6 40 74

SPECIFIC WORK-INPUT

The size-reduction depends in principle on many operation parameters as e. g. speed, ball size, filling ration, suspension throughput, suspension load, mill size, stirrer design. However the specific work-input expressed by W_M or W_V is the dominant factor as a mill is operated in proper condition.

W_V = work-input related to the particle volume

P: power draft, P_0: power draft of the empty mill, $\dot{V}$: suspension throughput, [redacted]: volumetric feed load c_V

$W_V = (P - P_0) / c_V \dot{V}$

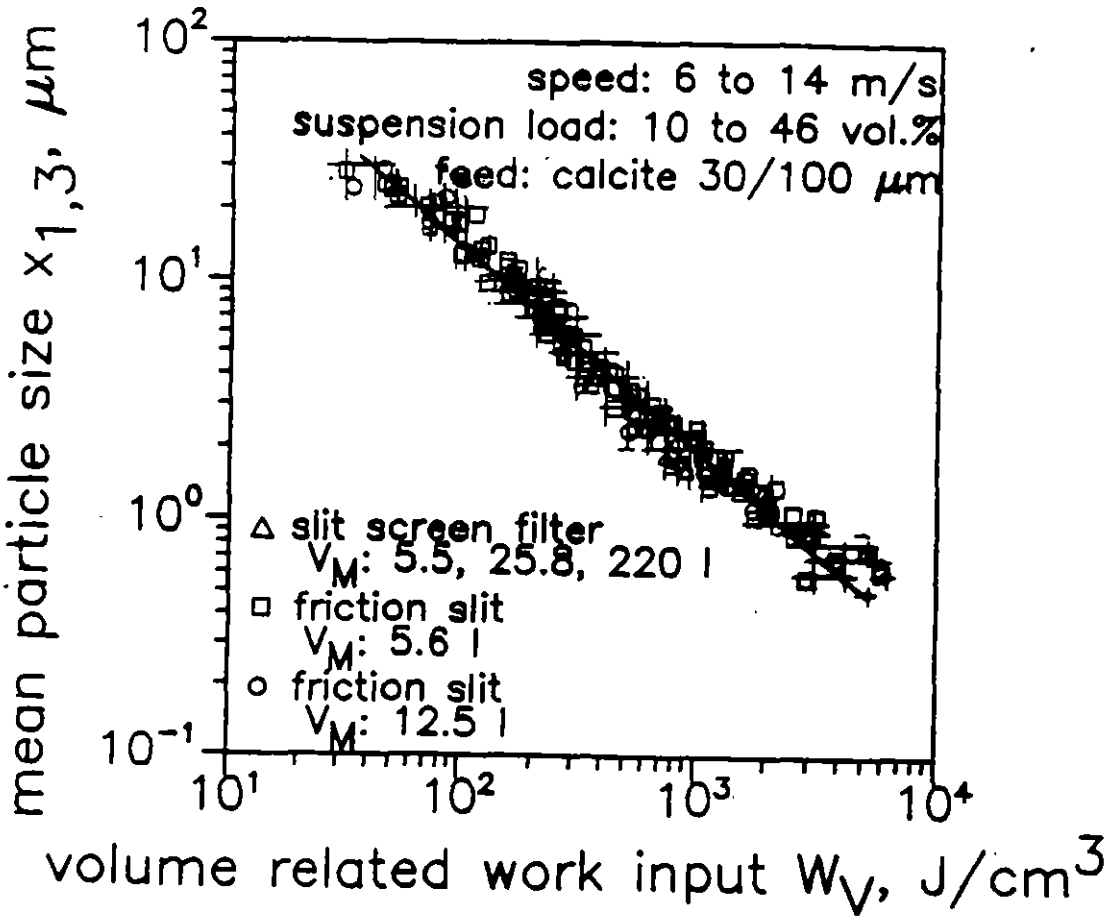

PAUL HAUSTEN GmbH, Goslar
Tel. 05321/6406 Fax 64074

STIRRED MILLS WITH DISC AND STUDS STIRRER

Sketches of usual design are shown.

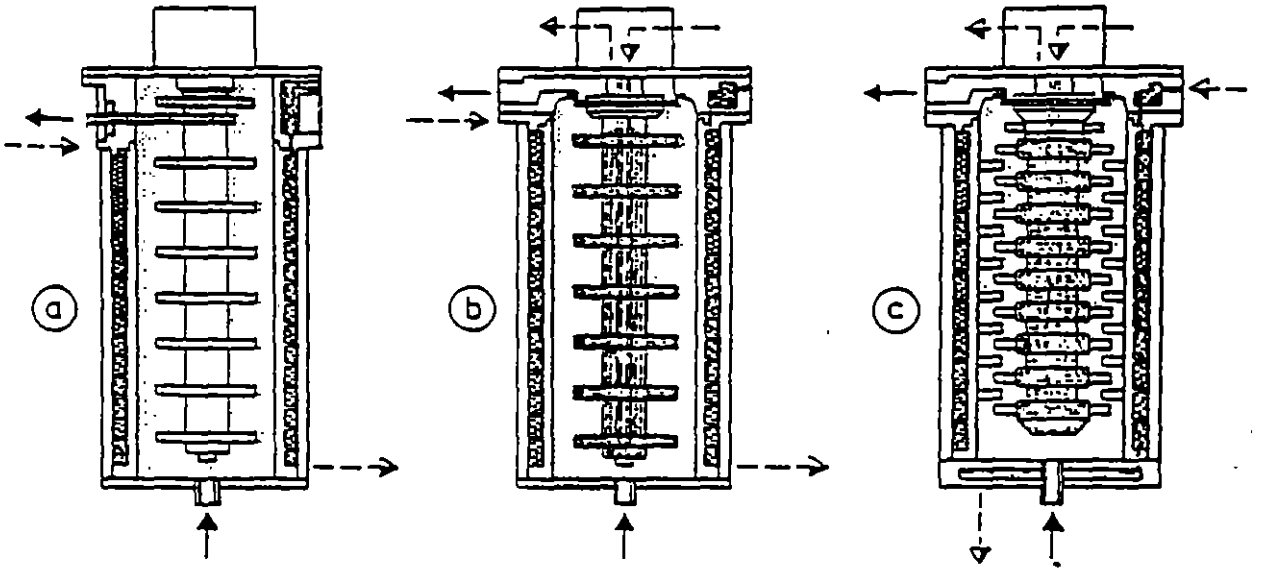

(a) disc stirrer, slit screen filter

(b) disc stirrer, friction slit

(c) stud stirrer, friction slit

mill volume : 10 .... 160 .... 1000 l

motor power : 15 .... 120 .... 280 kW

Tel.053 21/640 64 Fax 640 74

Ring Gap Mill

type Welte

The process volume is between the rotating inner body and the outer vessel. The rotor is shaped as a double cone. The process volume width is small (4 to 10 mm). The slurry is fed at the bottom center, flows upwards and leaves at the top through a friction slit.

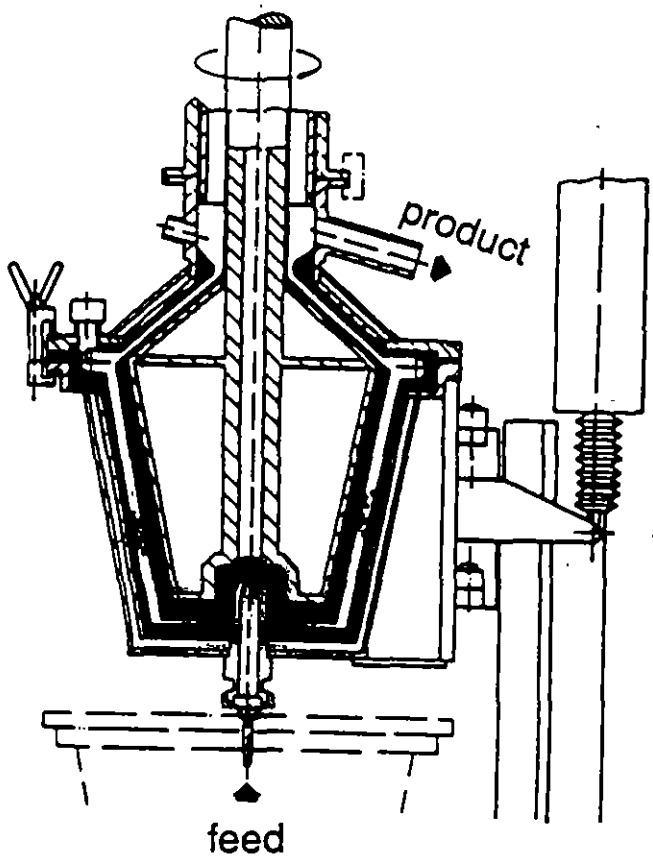

process volume : 5 .... 20 l
moter power : 10 .... 50 kW

Duplex Ring Gap Mill

type Fryma-Co Ball-Mill

The process volume is between the rotating inner body with an triangular cross section and a vessel with an corresponding shape. The gap width is small (4 to 10 mm). The suspension is fed at the bottom center, flows downwards in the inner gap space, upwards in the outer one then radial inwards and leaves at the top through a friction slit. The balls flow with the slurry and are circulated through channels connecting both gap spaces.

Tel.05321/6406 4 Fax 64074

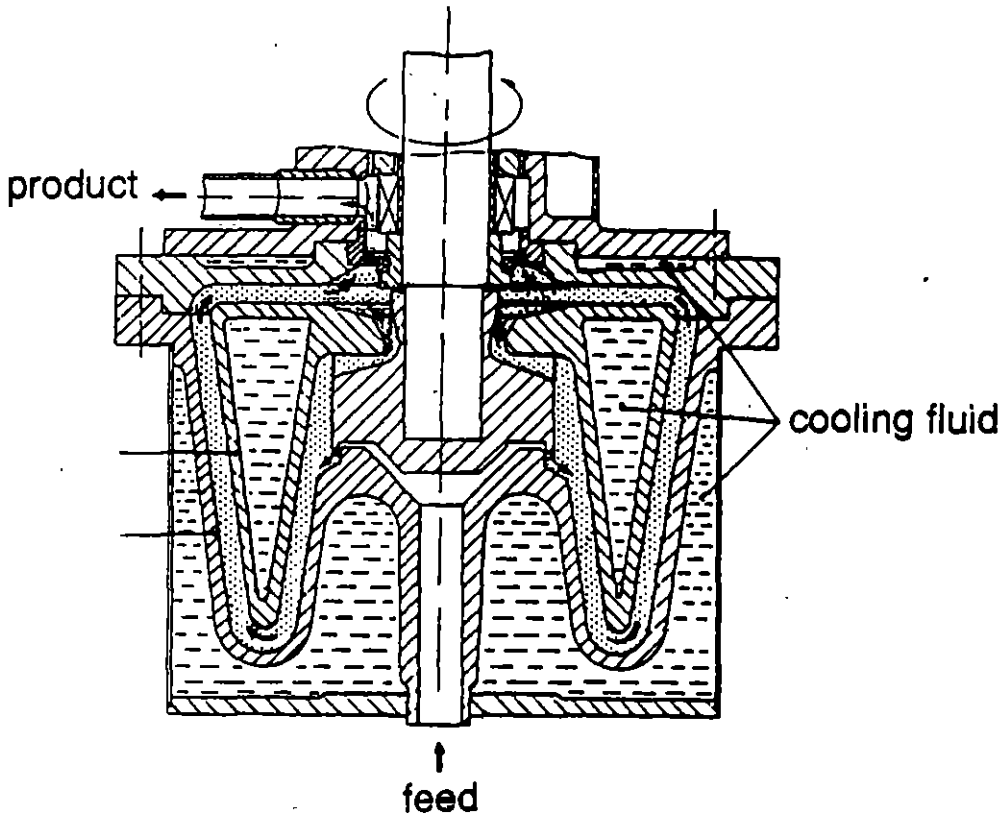

process volume : 0.5 .... 10 .... 75 l

motor power : 3 .... 50 .... 180 kW

Duplex Ring Space Mill

typ Drais PM - DCP

The width of the processing volume is small (10 to 20 mm), the middle wall rotates, the walls are equiped with studs. The slurry is fed at the top, flows downwards in the outer ring space and upwards in the inner one and leaves through a slit screen filter mounted centrally. The balls flow with the suspension and are circulated through channels connecting both ring spaces in the upper region.

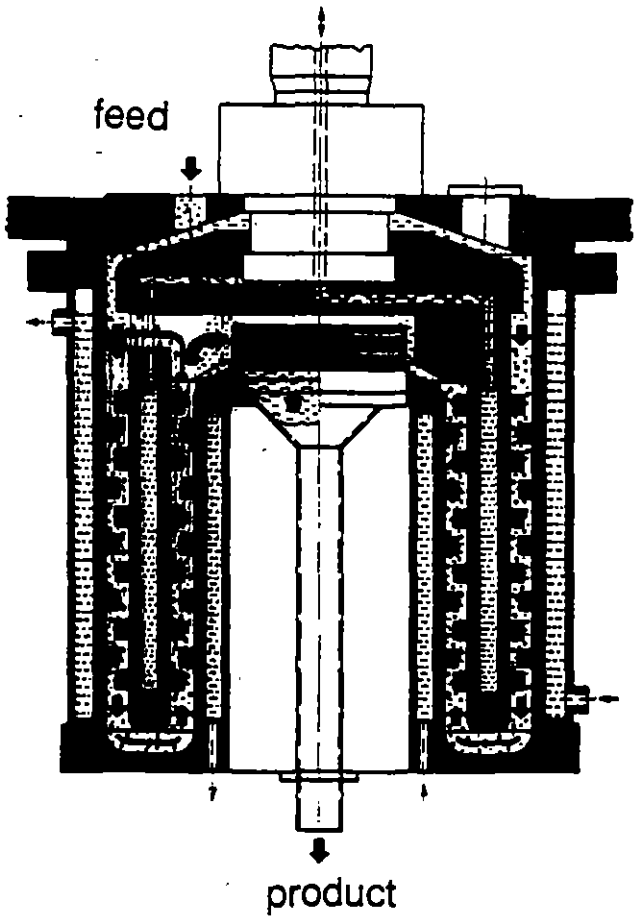

process voluem : 6 .... 50 l

motor power : 20 .... 150 kW

Tel.053 21/64 0 64 Fax 6 40 74

TOWER MILLS (1)

type MPSt Tower Mill

Tower mills consists of a big upright cylindrical vessel, a central double helix screw and a classifier at the top. The balls rises with the screw and move downwards in the outer anular space. The material and water is fed from above. The fine product flows upwards with the water to the classifier. Its underflow is recycled back to the mill. Tower mills are used for fine wet grinding of minerals and ores.

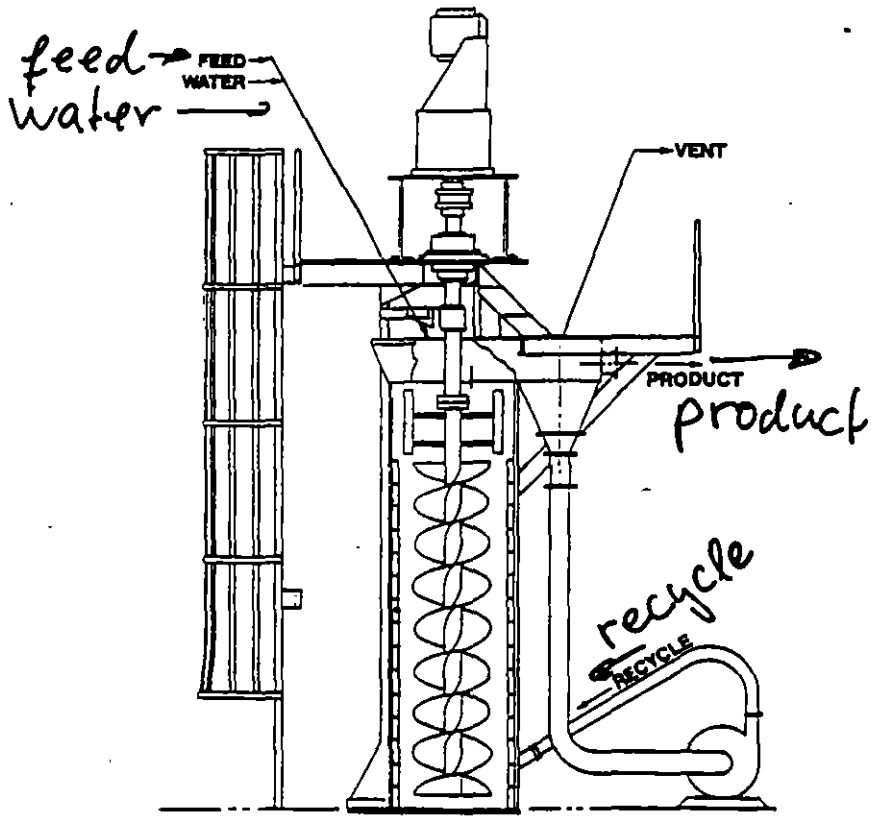

vessel height : 2600 .... 6500 mm
vessel diameter : 500 .... 1500 mm
moter power : 10 .... 300 kW

Tel.053 21/6 40 64 Fax 6 40 74

TOWER MILL (2)

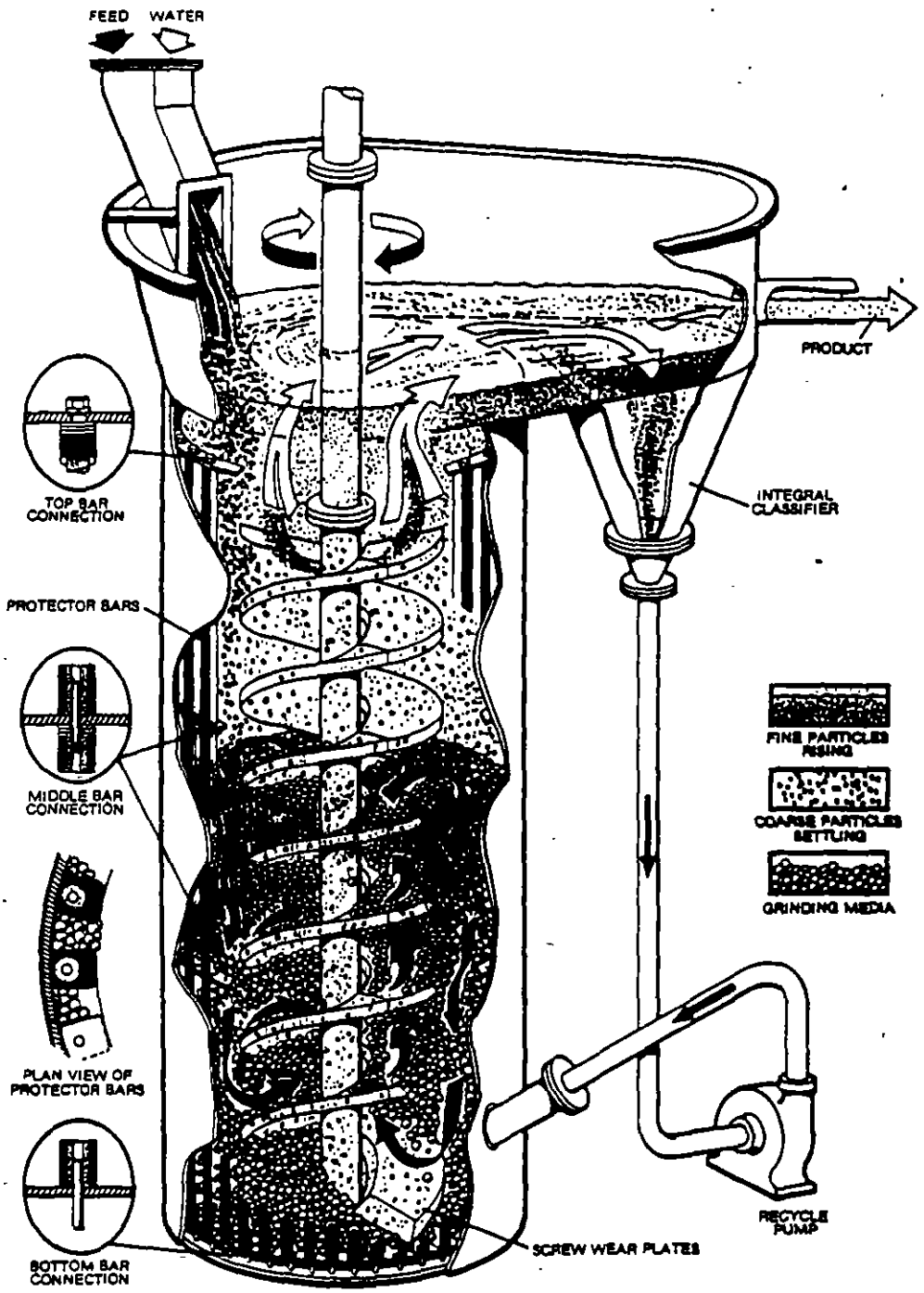

Tel.053 21/640 64 Fax 640 74

IMPACT MILLS - INTRODUCTION (1)

In impact mills the particles are stressed by collisions either against a beater, a hammer, the mill wall or against another particle. Regarding the energy transfer to the particles two main groups can be distinguished:

- **rotor impact mills,** energy transfer by a rotor,
- **jet impact mills,** energy transfer by the drag force of a high speed gas flow.

Only fine particles smaller than some hundreds micron can be easily accelerated by the drag force, therefore jet mills are used for fine and very fine grinding.

The advantages of impact mills are:

- single particle stressing therefore less energy losts by particle-particle friction and less agglomeration
- high stressing velocity which is advantageous for elastic-viscous materials
- short residence time and by that large specific throughput
- possibility to integrate an air classifier in the mill housing

Tel. 0 53 21/8 40 84 Fax 6 40 74

IMPACT MILLS - INTRODUCTION (2)

The disadvantages are:

- high wear rate, only low abrasive materials can be fed (Mohs hardness < 4), the so-called opposite jet mill may be used for some harder materials
- stressing intensity proportional to velocity square, therefore a high collision velocity needed for very fine particles, energy losts by gas ventilation
- sensitive to foreign hard bodies in the feed

Rotor impact mills have been developed in the second half of the last century.

- Ejecting rotor mill for ores (about 1860)
- Beater mill (about 1875)
- Pin mill also called desintegrator (about 1885)

IMPACT MILLS - CONTENTS

DENOTATIONS

The following denotations are used

Mill

D, B. diameter and width of rotor, h, b, d: height, width and thickness of beaters, z: number of beaters, s: gap between beater tips and mill wall, ω: angular velocity, u: peripheral velocity at the beater tips, P: power draft, T: torque, F: drag force on the rotor

Material and fluid

x: particle size, ρ_s, ρ_f: density of material and fluid, η: viscosity of fluid, $\dot{M}$: throughput, μ: volumetric material concentration in the mill, λ: mean free path of the particle in the mill, s_0= stop distance of a particle in the fluid, w_s: settling velocity of a particle

Chapter impact mechanics

m_1, m_2: mass of impacting bodies, v_1, v_2: velocity of the bodies before impact, u: velocity of the bodies at the end of the 1st impact stage, U_{el}: transferred maximum elastic energy, Y_1, Y_2: Young`s modulus of the bodies, θ: momentum of inertia of a body, c_l: longitudinal wave velocity, p_0: maximal stress in a impacted shere, α: impinging angle

TYPICAL DESIGNS OF ROTOR IMPACT MILLS

Many different types of rotor impact mills are manufactured. In respect to the design it can be distinguished as follows:

- number of rotors: one or two,mostly one rotor, some pin mills have two rotors
- orientation of rotor shaft: horizontal or vertical, mostly horizontal
- rotor impact tools: bar-shaped beaters or pins
- feed introduction: central or peripheral, mostly central
- internal classifying: screen, grates at the periphery, air classification in or outside the process volume, rotor air classifyer integrated in the mill.

Rotor diameter 150 to 1500 mm, peripheral velocity 50 to 120 m/s, motor power 10 to 200 kW.

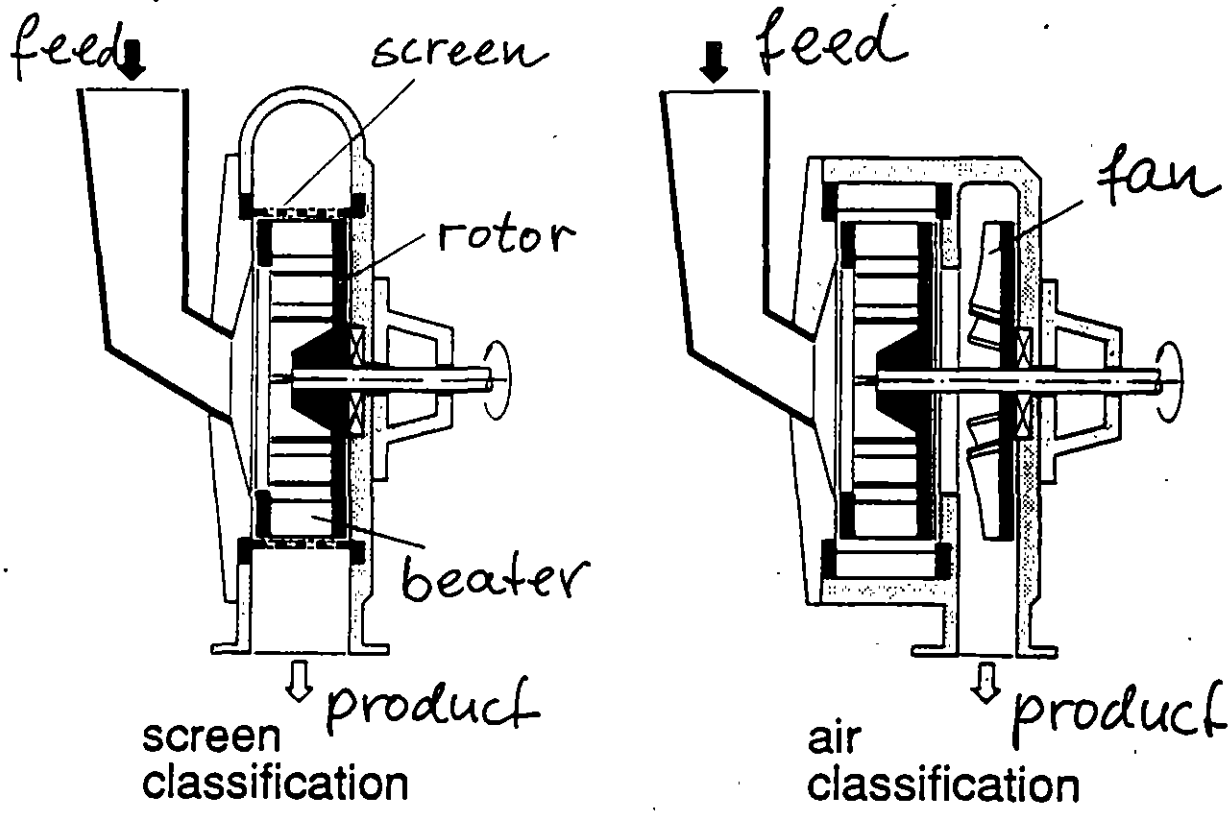

Tel.05321/6 40 64 Fax 6 40 74

IMPACT MECHANICS (1)

In impact mills the particles have to be impinged with such a high velocity that they break.

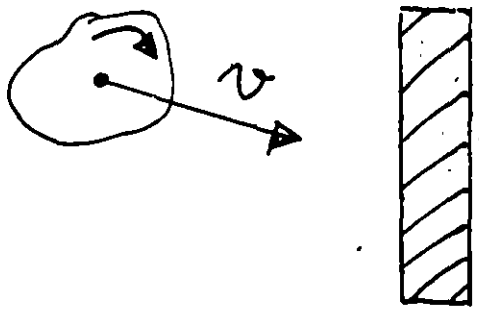

The contact-region deformes mostly inelastically. In general the impact direction is oblique and the particle rotate. Such an impact cannot be described theoretically. The simple impact mechanics considers the elastic impact of spheres without rotation (Hertz impact theory).

Impact stages

An elastic impact (without breakage) consists of two stages:

Stage 1 begins with the contact and lasts until the centers of gravity of the impacting bodies do not further move against each other.

Stage 2 follows stage 1 until the bodies part.

The maximum transfer from kinetic to elastic energy is given at the end of stage 1, then the maximum stresses arise. If cracks are not released in stage 1, the particle remaines unbroken and bounces back.

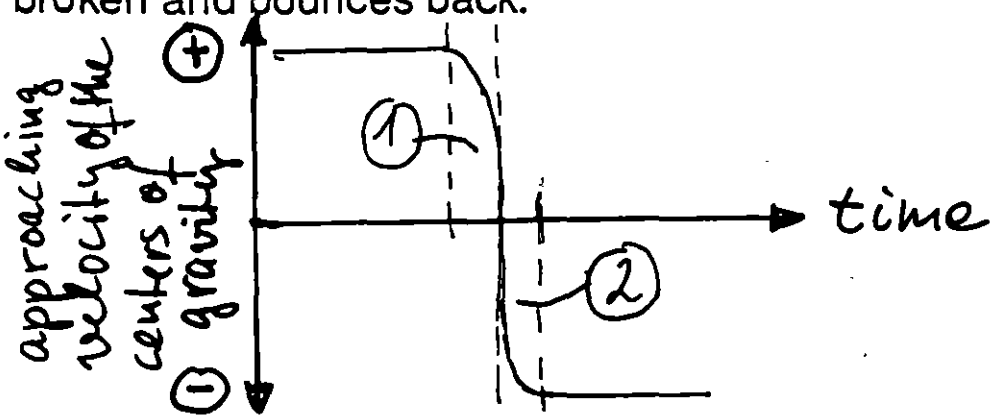

IMPACT MECHANICS (2)

Impact modes

The following modes of impacts without rotation can be distinguished in respect to the mass relation m_1 / m_2 of both bodies and the angle between their flight directions.

- $m_1 << m_2$ (particle against wall)

  straight impact: fligth direction of m_1 is equal to the plane normal of the contact point.

  oblique impact: all other impacts

- $m_1 \approx m_2$ (particle against particle)

  straight central impact: both particles approach each other along the line between the centers of gravity and the plane normals at the contact points have the same direction.

  straight eccentric impact: the flight directions are parallel or antiparallel to each other.

  oblique impact: all other impacts

In principal the probability of exact straight impacts is zero.

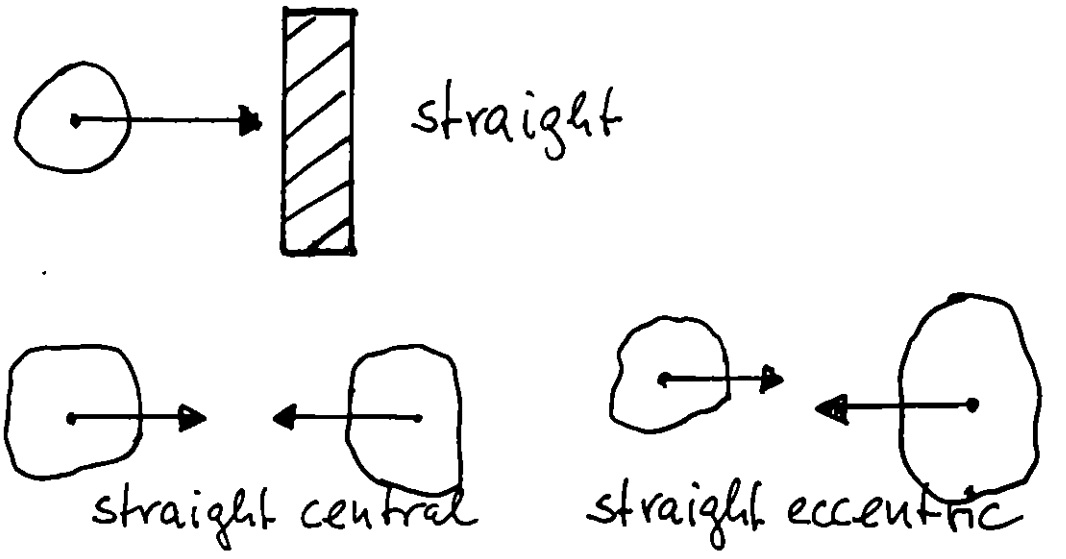

IMPACTS MECHANICS (3)

Energy transfer in straight and straight central impacts

The maximum energy transfer follows from the energy and momentum balance before the collision and at the end of stage 1 considering only the kinetic and the elastic energy.

m_1, m_2 : mass of body 1 and 2

v_1, v_2 : velocity of body 1 and 2 before collision

u : velocity of both bodies at the end of stage 1

U_{el}: elastic energy stored in both bodies at the end of stage 1

$$(1/2)\, m_1 v_1^2 + (1/2)\, m_2 v_2^2 = (1/2)\,(m_1 + m_2)\, u^2 + U_{el}$$

$$m_1 v_1 + m_2 v_2 = (m_1 + m_2)\, u$$

$$\boxed{U_{el} = (1/2)\,\{m_1 m_2 / (m_1 + m_2)\}\,(v_1 - v_2)^2}$$

particular cases:

$m_1 << m_2$,	$v_2 = 0$	$U_{el} = (1/2)\, m_1 v_1^2$
$m_1 << m_2$,	$v_1 = 0$	$U_{el} = (1/2)\, m_1 v_2^2$
$m_1 << m_2$,	$v_1 = -v_2$	$U_{el} = 2\, m_1 v_1^2$
$m_1 = m_2$,	$v_1 = -v_2$	$U_{el} = m\, v^2$

IMPACT MECHANICS (4)

Energy transfer in a straight excentric impact

The derivated equation for U_{el} can be used after replacing the body masses m_1 and m_2 by the reduced body masses m_1' and m_2'.

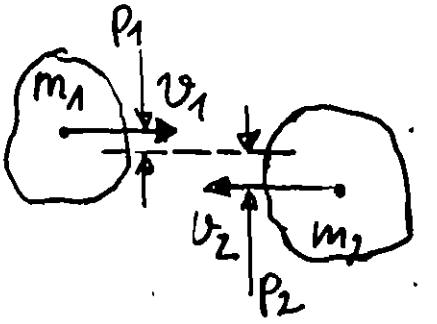

$m_1' = \{i_1^2 / (i_1^2 + p_1^2)\}\, m_1$

$m_2' = \{1_2^2 / (i_2^2 + p_2^2)\} m_2$

$i = \sqrt{\theta / m}$

θ : moment of inertia; sphere $\theta = (2 / 5)\, mr^2$, $\theta = 0.63\, r$

If two spheres collide together with $p = d / 4$ then it results

$m_1' m_2' / (m_1' + m_2') = m / 3.25 = 0.31\, m$

The elastic energy is reduced strongly be this factor 3.25.

Energy transfer in an oblique impact on a plate

The derivated equation for U_{el} can be uses as the normal component v_n of the velocity is introduced:

$v_n = v \cos\alpha$ α : impinging angle

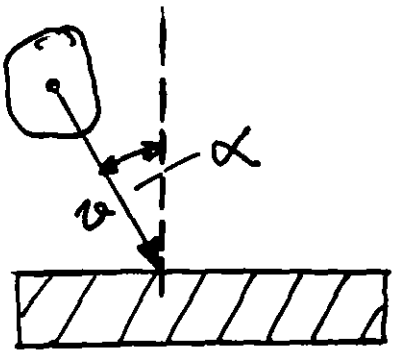

this is valid as long as

$\tan\alpha \leq (i^2 + p^2)\, \mu / i^2$

μ: coefficient of friction

α :	5°	10°	15°	20°
$(\cos\alpha)^2$:	0.99	0.97	0.93	0.88

Tel. 05321/64064 Fax 64074

IMPACT MECHANICS (5)

Energy partition

The elastic energy is transferred into both impact bodies. The partition follows from the Hertzian equation:

$$U_{el,1} / U_{el,2} = (Y_2 / Y_1) \{(1 - \nu_1^2) / (1 - \nu_2^2)\}$$

Y: Young`s modulus, ν: Poisson number. Because the Poisson number does not differ much, it can be said:

$$\boxed{U_{el,1} / U_{el,2} = (Y_2 / Y_1)}$$

$$U_{el,1} = \{ Y_2 / (Y_1 + Y_2)\} U_{el}; \quad U_{el,2} = \{Y_1 / (Y_1 + Y_2)\} U_{el}.$$

The energy fraction being tranferred to the particle raises with increasing Young`s modulus of the plate. This partition is valid for elastic behaviour before a crack is released.

Example: mineral particle with $Y_1 = 7 \cdot 10^4$ N / mm^2 against steel plate with $Y_2 = 2.1 \cdot 10^5$ N/mm^2

$U_{el,1} = 0.75\, U_{el}$ and $U_{el,2} = 0.25\, U_{el}$

IMPACT MECHANICS (6)

Maximum stress p_0 in the particle

As shown in the chapter fundamentals the maximum stress p_0 is given as:

$$p_0 / Y_{sp} = 0.87 (1 + \kappa)^{-4/5} (v / c_l)^{2/5}$$

v : collision velocity , c_l: longitudinal wave velocity, $\kappa \approx (Y_{sp} / Y_{pl})$.

particle-plate impact : $U_{el} = (1/2)\, mv^2$, $\kappa = 7/21 = 0.33$

particle -particle impact : $U_{el} = (1/4)\, mv^2$, $\kappa = 1$

The p_0-values differ in both cases by the factor 1.38.

Conclusions for impact grinding

(1) More energy is transfered to the particle as it impinges a plate with the same collision velocity than another particle. Each deviation form the straight impact reduces the energy transfer, however the particle-plate impacts are less sensitive to such deviations than particle-particle impacts. The straight central impact of two particles is very unlikely. For all these reasons particles-plate impacts should be preferred if possible.

(2) The beater material should have a high Young`s modulus beside a high hardness in order to assure that most of the energy is transferred into the particle.

tel.05321/6 40 64 Fax 6 40 74

IMPACT PROBABILITIES (1)

Particle-plate and particle-particle impact in a mill

In rotor impact mills the particles are flying around in the ring-shaped space (process volume) between the rotor and the mill wall. The flight velocities and flight directions are distributed randomly. They may impinge against the beaters of the rotor or against another particle. The question arises about the probabilities for these events which depend on the particle concentration. The govering parameter of this problem is the mean free path λ of the particles. If λ is smaller than the width s between rotor tips and wall, then particle-particle impacts are more likely than particle-plate impacts. The mean free path can be estimated analogous to the kinetic gas theory.

$$\lambda = 1 / \sqrt{2}\, \pi\, n\, x^2$$

n : number of particles per volume , N : number of partilces, V: process volume, μ: volumetric fraction of all particles in V (filling ratio)

$$n = N / V = 6\, \mu / \pi\, x^3$$

$$\lambda = x / 6 \sqrt{2}\, \mu \approx x / 10\, \mu$$

IMPACT PROBABILITIS (2)

$\lambda \approx x / 10 \mu$

The mean free path λ depends on the particle size and the filling ratio μ. For $\lambda > s$ particle-plate impacts are more likely than particle-particle impacts, therefore the filling ratio should be limited as:

$$\mu < 0.1 \, (x / s)$$

In impacts mills the gap is between 2 and 20 mm and the (x / s)-ratio at least 0.1. With a smallest particle of 50 µm the (x /s) -ratio is between 0.0025 and 0.1. The gap filling ratio should be between $2.5 \cdot 10^{-4}$ and 0.01. The finer the particle the lower μ.

Stop distance s_0

Flying particles are slowed down by the drag force and stopped after the flying path s_0:

$$s_0 = (8 / 3) \, (\rho_s / \rho_f) \times \ln\{ 1 + (x v_0 \rho_f / 48\eta)\}$$

ρ_s, ρ_f : density of solid and fluid, x: particle size, v_0 = initial velocity, η: viscosity, w_s: settling velocity

For particles smaller about 30 to 50 µm the equation can be simplified:

$$s_0 = w_s \, v_0 / g$$

example: x = 10 µm, v_0 = 100 m/s, w_s in air = 10 mm /s,

s_0 = 47 mm

Tel.05321/64064 Fax 64074

IMPACT PROBABILITIES (3)

Mean free path λ, stop distance s_0 and process vol. width s

A particle-~~plate~~ impact needs that the width s of the process volume is at least two-times smaller than s_0 and λ. The particles concentration has to be very small:

$\mu < 10^{-3}$ at x = 100 µm and $\mu < 10^{-4}$ at x = 10 µm.

The stop distance begins to dominate in the size range below 5 µm. Then it is advantageous to increase the particle concentration that particle-particle impacts become likely.

Experiences show that grinding in rotor impact mills is limited at 5 to 10 µm.

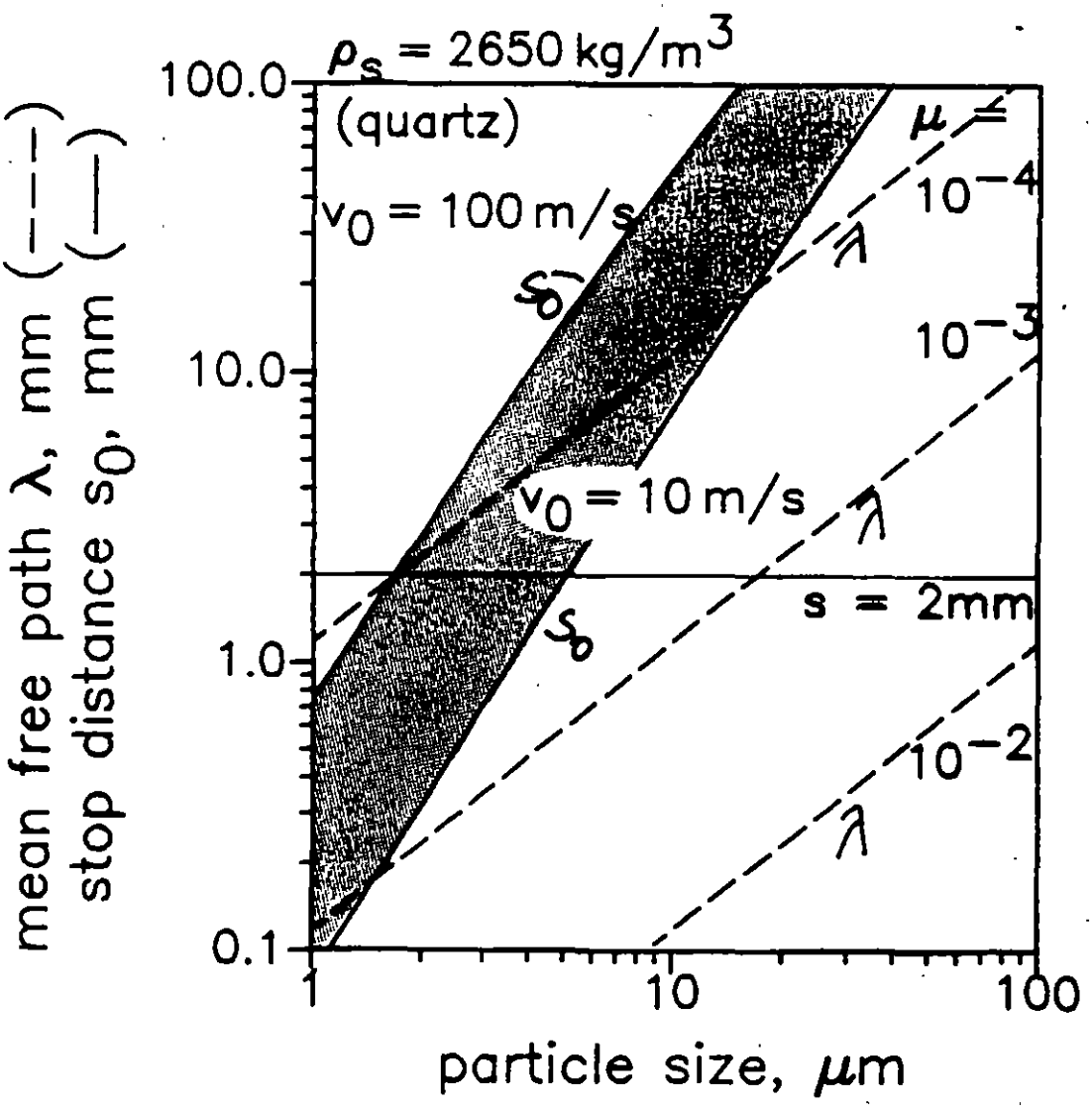

IMPACT PROBABILITIES (4)

Penetrating into the beater space

Particles in the process volume between beater tips and mill wall have to penetrate into the beater space to be impacted and/or accelerated. This is only possible, if they bounce back from the wall. The probability P for penetrating follows from geometrical considerations.

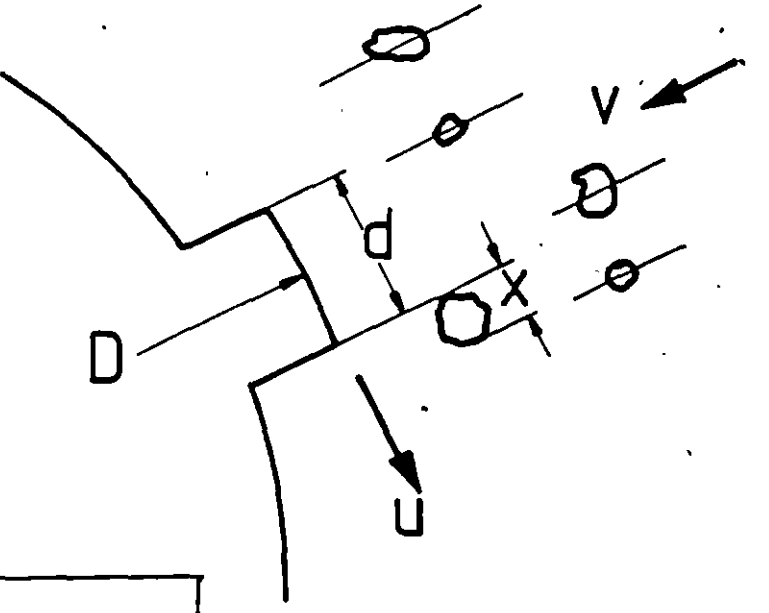

D : diameter of beater circle
z : number of beaters
d : thickness of beaters
x : particle size
u : peripheral rotor velocity
v : radial particle velocity

$$P = 1 - \{ zx / \pi D \} \{ 1 + (d / x) + (u / 2v) \}$$

if $(ux / 2 dv) << 1$ then

$$P = 1 - (zd / \pi D)$$

The penetrating probability increases with raising radial particle velocity and declining number of beaters. However the acting beater surface increases with z therefore, an optimum number exists. Often mills are equipped with too many beater.

POWER DRAFT OF ROTOR IMPACT MILLS (1)

The power draft is an essential characteristic of a machine. The general background of an equation for rotor impact mills is discussed.

$$P = T\,\omega = 2\,\pi\,n\,T = 2\,u\,T / D$$

The rotor works like a fan. The torque is caused by the drag force F which depends on the particular design of the rotor, the size and shape of the mill volume and the wall structure of the housing. Most essential are those parts of the rotor transferring the energy to the fluid, e. g. the beaters in a so-called turbo rotor mill. Their surface A_B has to introduced into the equation. The flow is turbulent, therefore the drag force proportional to the square of the rotor speed u.

$$F = \text{const}\ \rho^*\ A_B\ u^2$$

$\rho^* = \rho_f + \mu\rho_s$: density of the gas-particle mixture in the mill

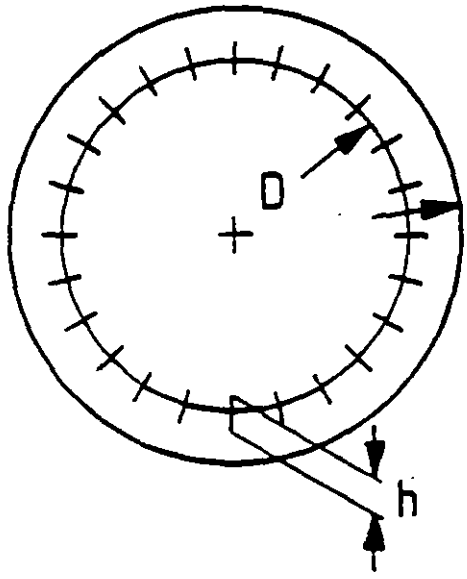

Tel. 05321/64064 Fax 64074

POWER DRAFT OF ROTOR IMPACT MILLS (2)

$P = 2\,u\,T / D$ $\qquad T = F\,D / 2$

$P = u\,F = \text{const}\ \rho^*\ u^3\ A_B$

$$\boxed{P = \text{const}\,(1 + \mu\,(\rho_S / \rho_f))\ \rho_f\ u^3\ A_B = p(\rho_f\ u^3\ A_B)}$$

The power factor p depends on the particular design, the density ratio (ρ_S / ρ_f) and the material concentration μ in the mill. In usual operation p is between 0.003. and 0.012.

The material concentration μ in the mill is not known, μ depends on the throughput $\dot{M}$ and the classifier cut which determines the fineness of the product. In general μ raises with increasing $\dot{M}$ and fineness. Furthermore the breakage behaviour influences μ that it increases as the material is less grindable. The size-reduction effect increases with the speed, because of that μ decrases as u is raised. This interrelation can cause that P seems not to be proportional to u^3.

POWER DRAFT OF ROTOR IMPACT MILLS (3)

The surface A_B of all beater is given:

$$A_B = z\ h\ b$$

In principle P is proportional to z if the beaters mainly determine the drag force. The number of beaters can influence the size-reduction effect and by that the value of μ.

Because of the complex interrelation between the material concentration μ and the operation condition it is difficult to set up a general power equation.

Beater Mill with Screen

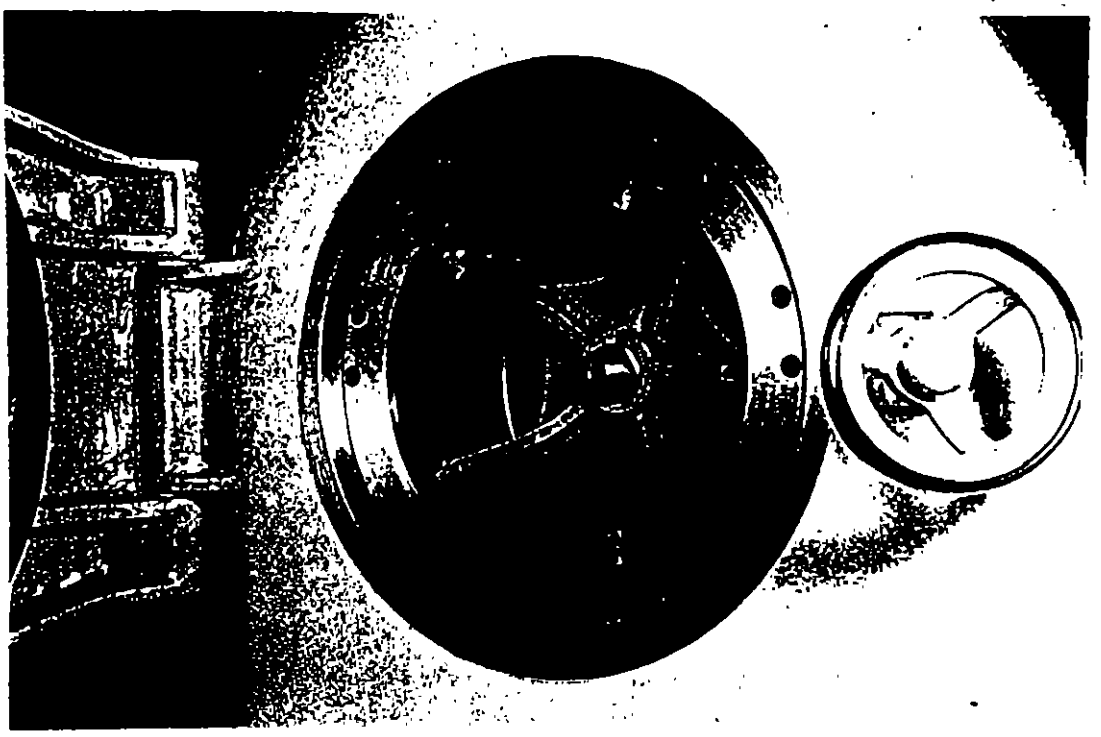

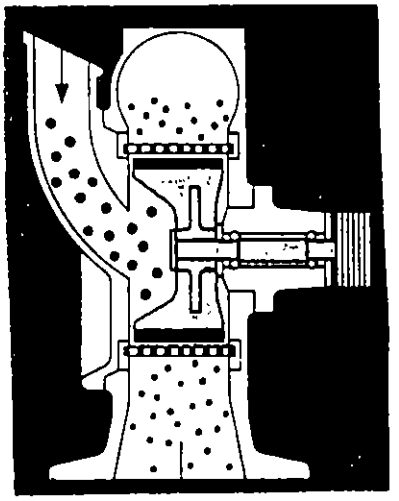

chamber Ø	mm	600	800	900	1200
chamber width	mm	200	300	430	600
motor power	kW	45	63	90	160

Beater Mill with Screen

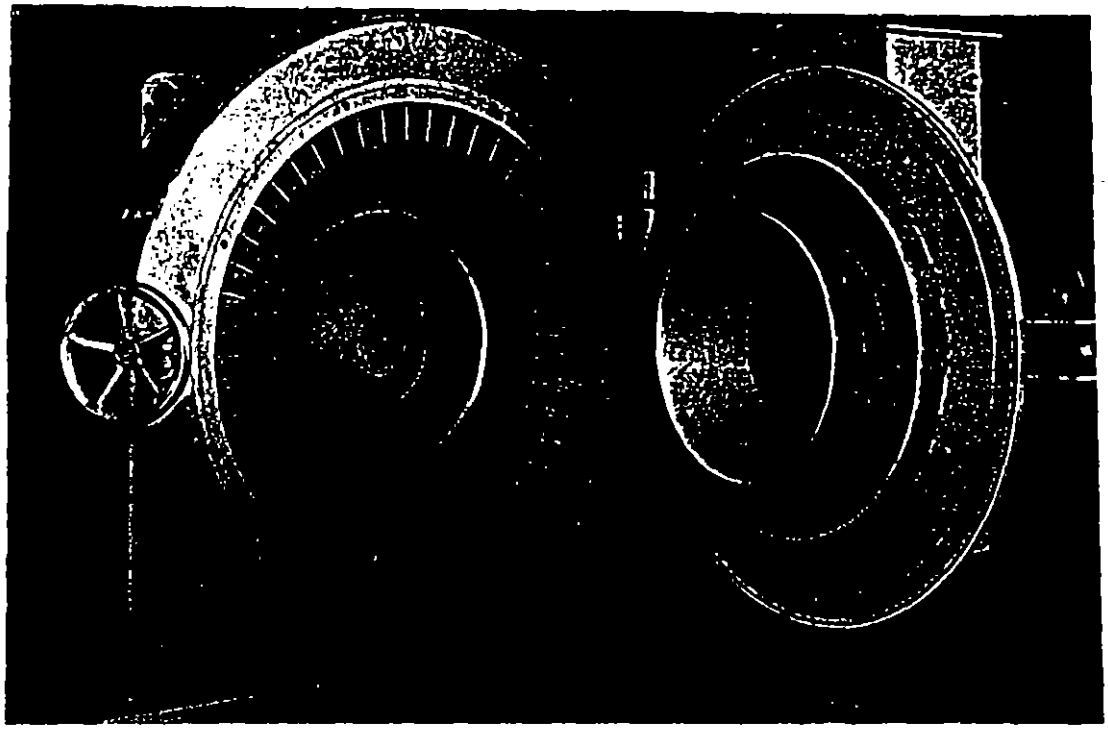

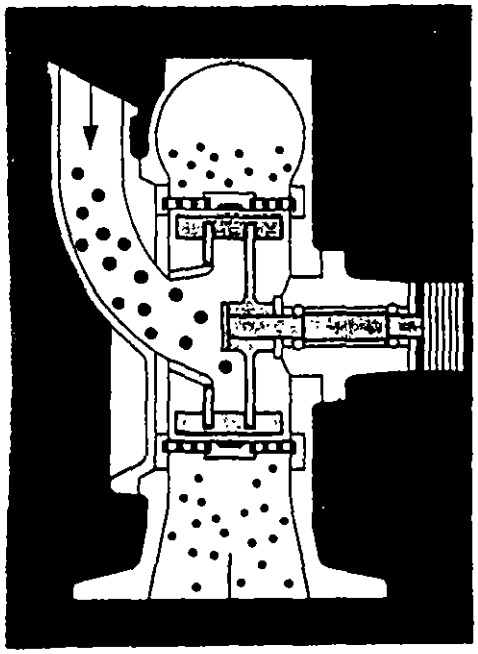

chamber Ø	mm	600	800	1200	1500
chamber width	mm	100	150	200	230
motor power	kW	45-55	75-110	132-160	200-300

Tel.053 21/6 40 84 Fax 6 40 74

Rotor Impact Mill with Five Rings of Beaters

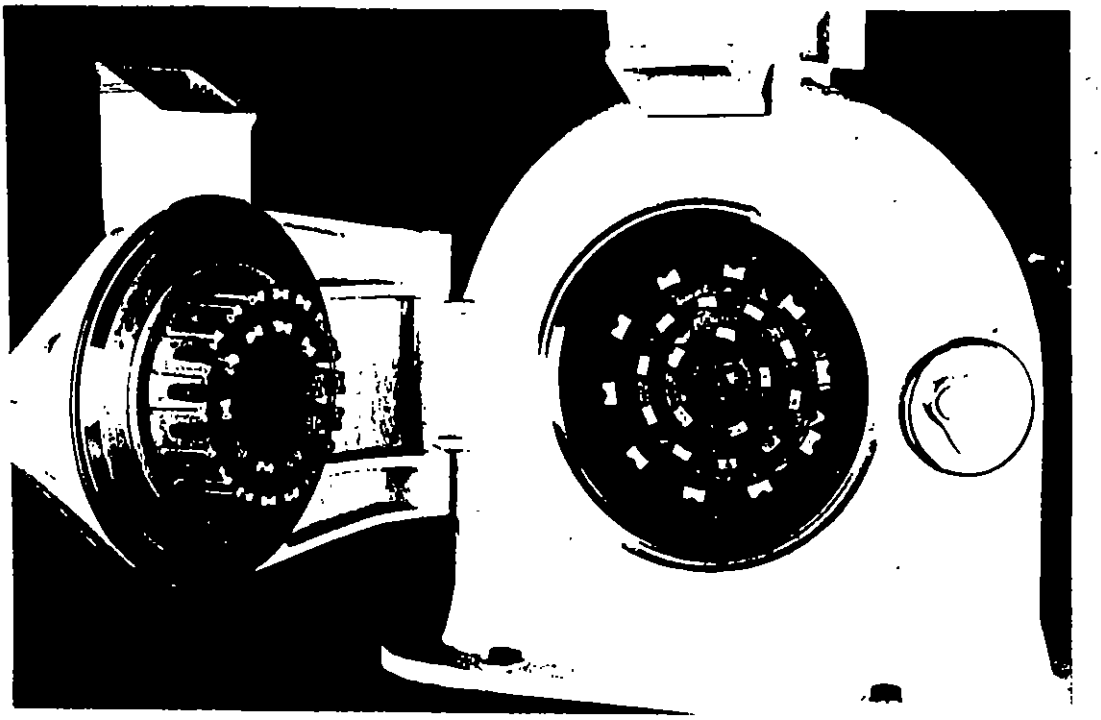

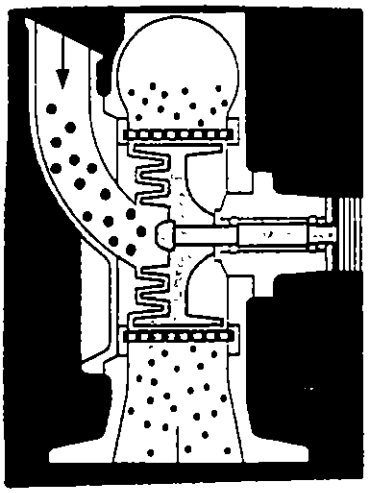

chamber Ø	mm	315	450	630	1000
maximum speed	Rpm	3500	2700	1700	3600
motor power	kW	22	55	75	110

Tel. 05321/64064 Fax 64074

Hammer Mill

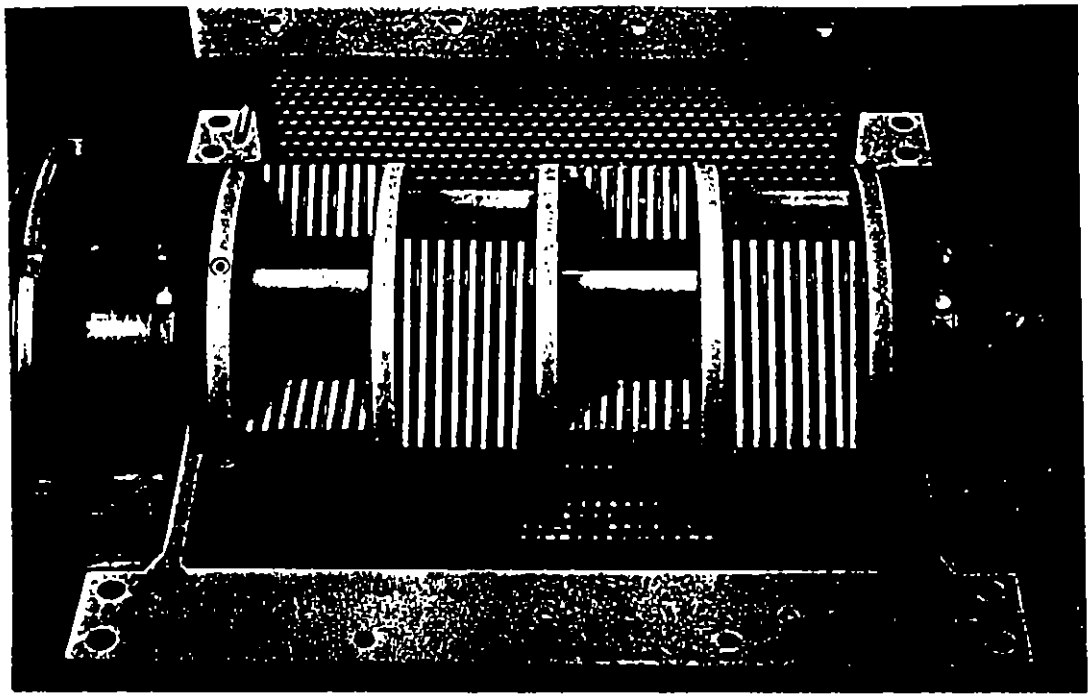

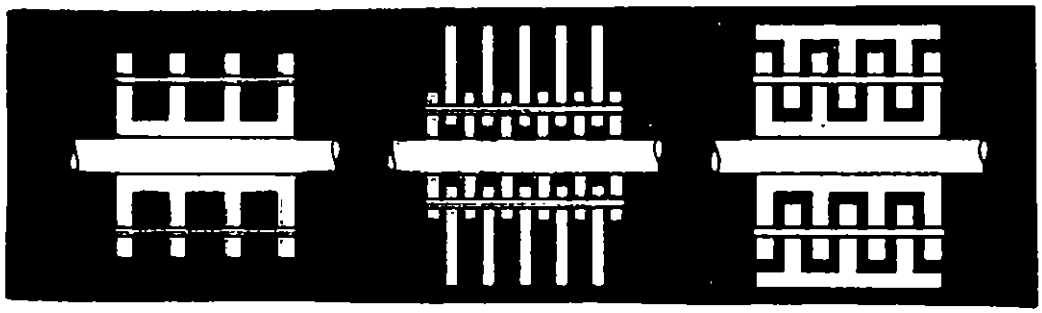

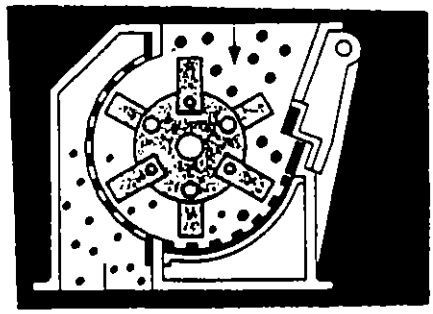

Rotor Ø	mm	220	400	600	600	800
Chamber width	mm	240	500	300	600	1200
motor power	kW	3	18-22	22-30	30-45	75-110

Tel.05321/64064 Fax 64074

Beater Mill with V-Shaped Grinding Zone and rotating Classifying Slit

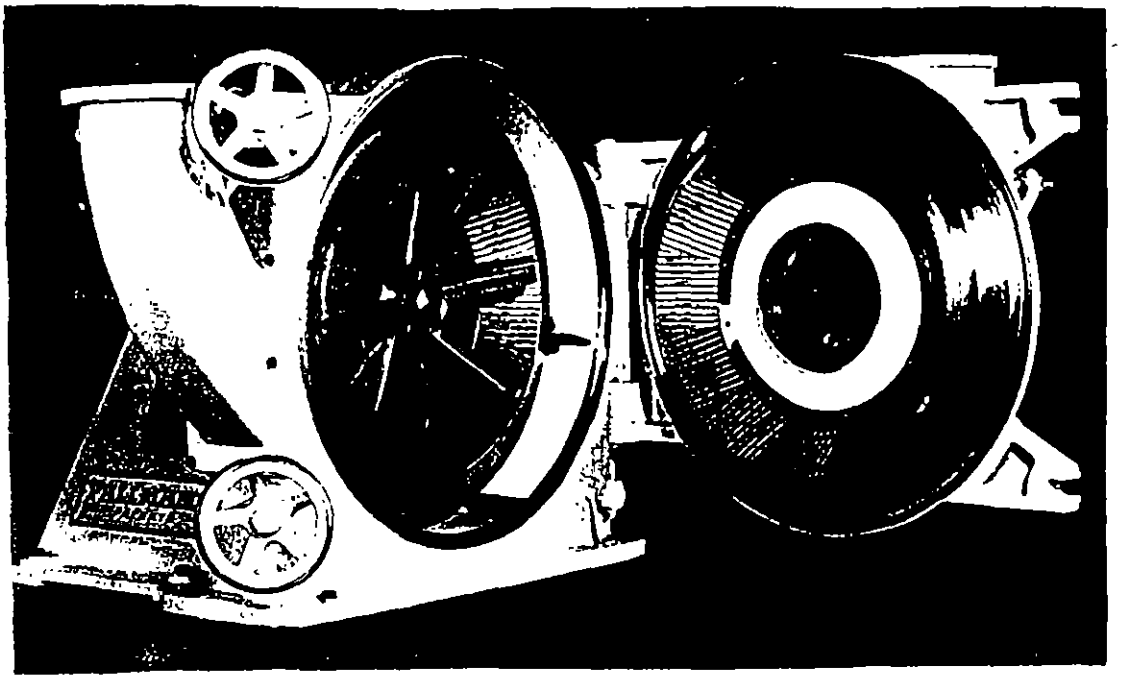

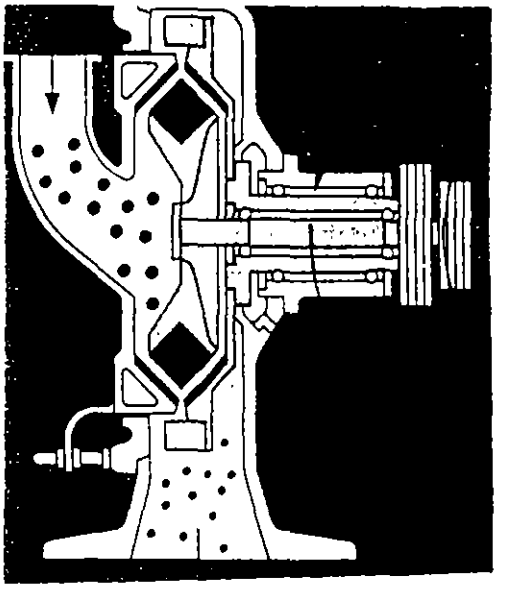

chamber Ø	mm	400	600	800	1200
rotor motor power	kW	15	30	45	75
motor power for rotating mill wall	kW	7,5	11	18,5	22

Beater Mill with V-Shaped Grinding Zone and Air Classifying

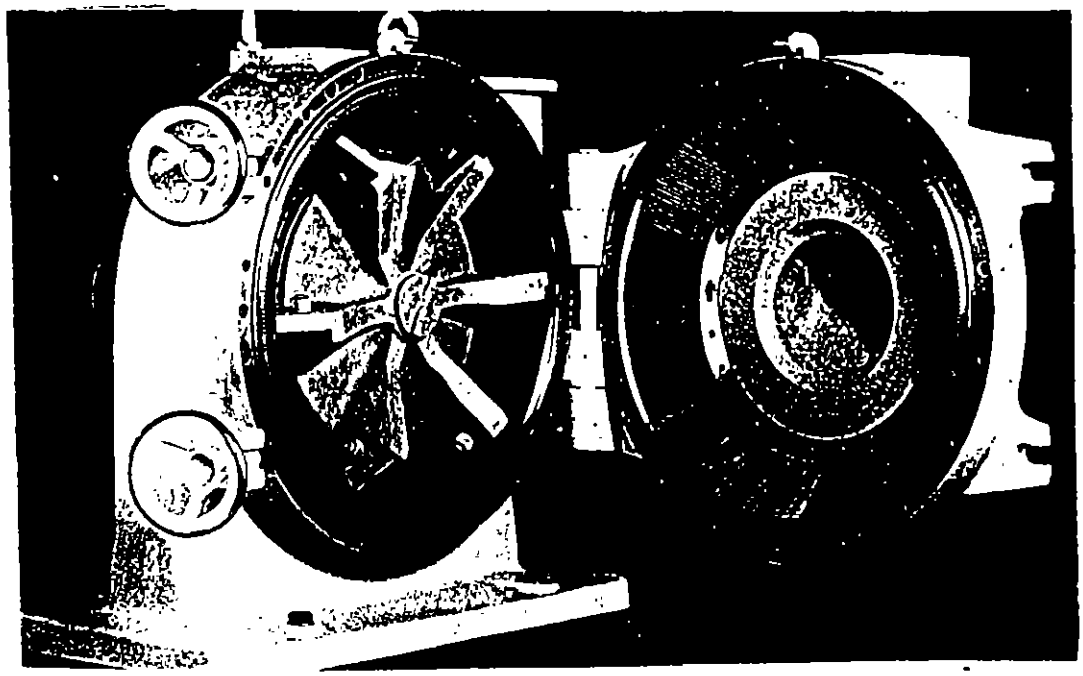

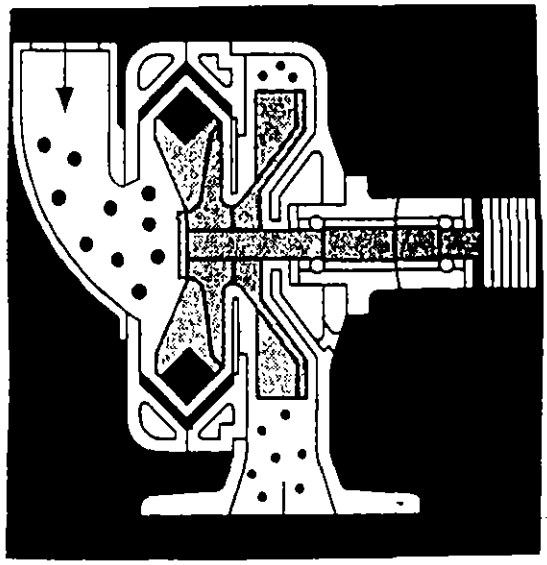

chamber Ø	mm	400	600	800	1200
rotor motor power	kW	15	30	45	75

ACM Mill with Classifier

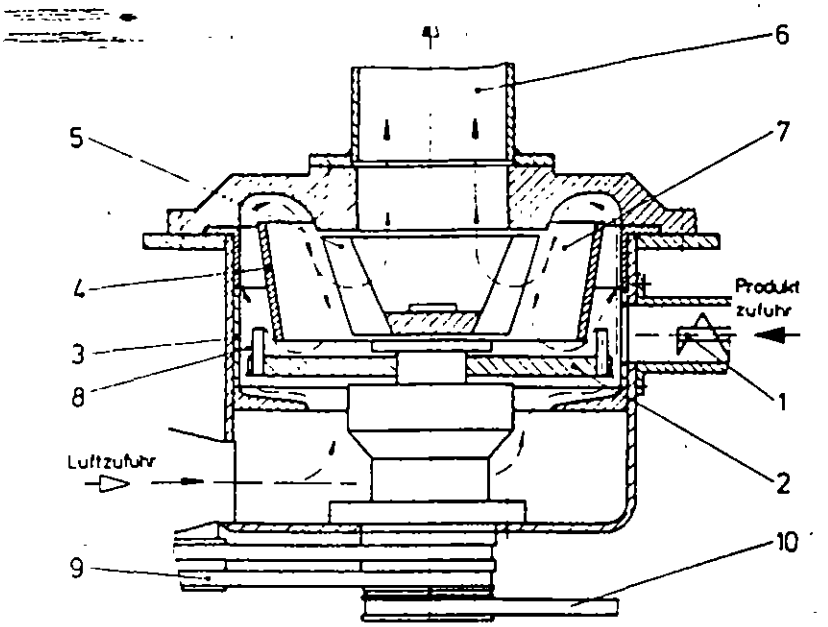

1 screw feeder
2 rotor with pins
5 classifier rotor
6 outlet
7 classifing zone
8 grinding zone
9 pin rotor drive
10 classifier drive

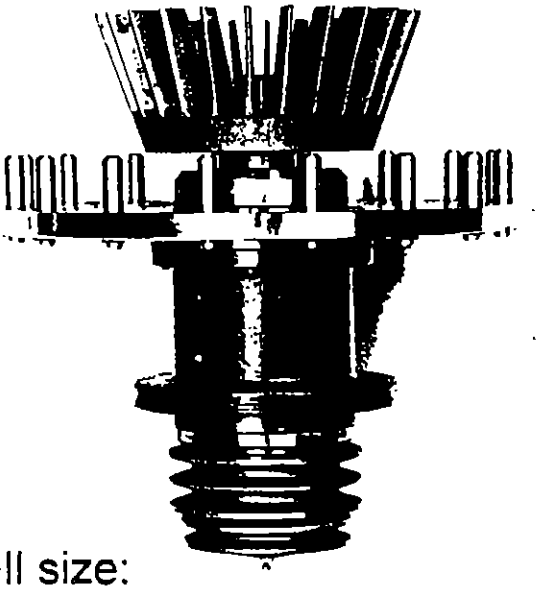

Maximum mill size:
mill motor power 200 kW, classifier motor power 30 kW
maximum throughput 10 t/h

Tel.05321/64064 Fax 64074

Pin Mill with One Rotor

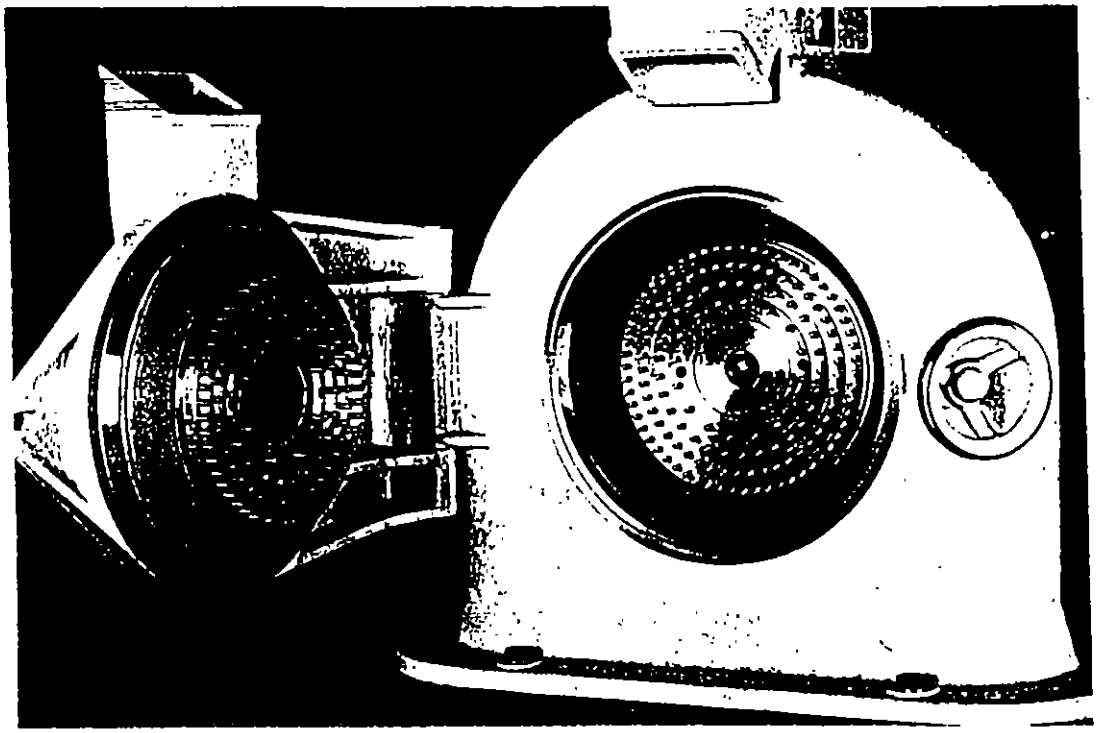

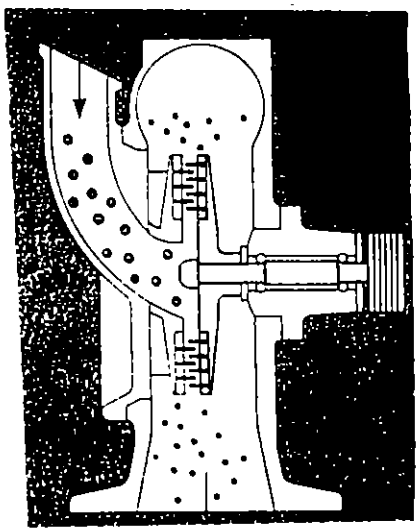

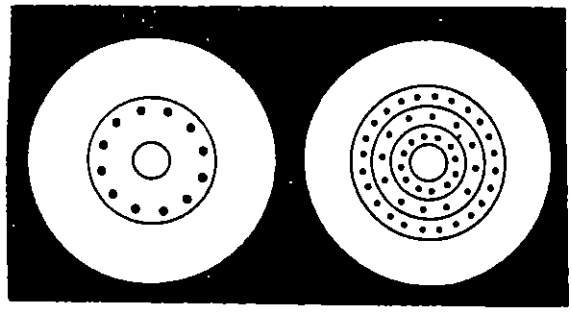

chamber Ø	mm	315	450	630
maximum speed	Rpm	10000	7500	4500
motor power	kW	22	45	55

tel.0b321/b4U b4 fax b4U /4

Pin Mill with Two Rotors

The two rotors rotate in opposite direction, the collision velocity is increased

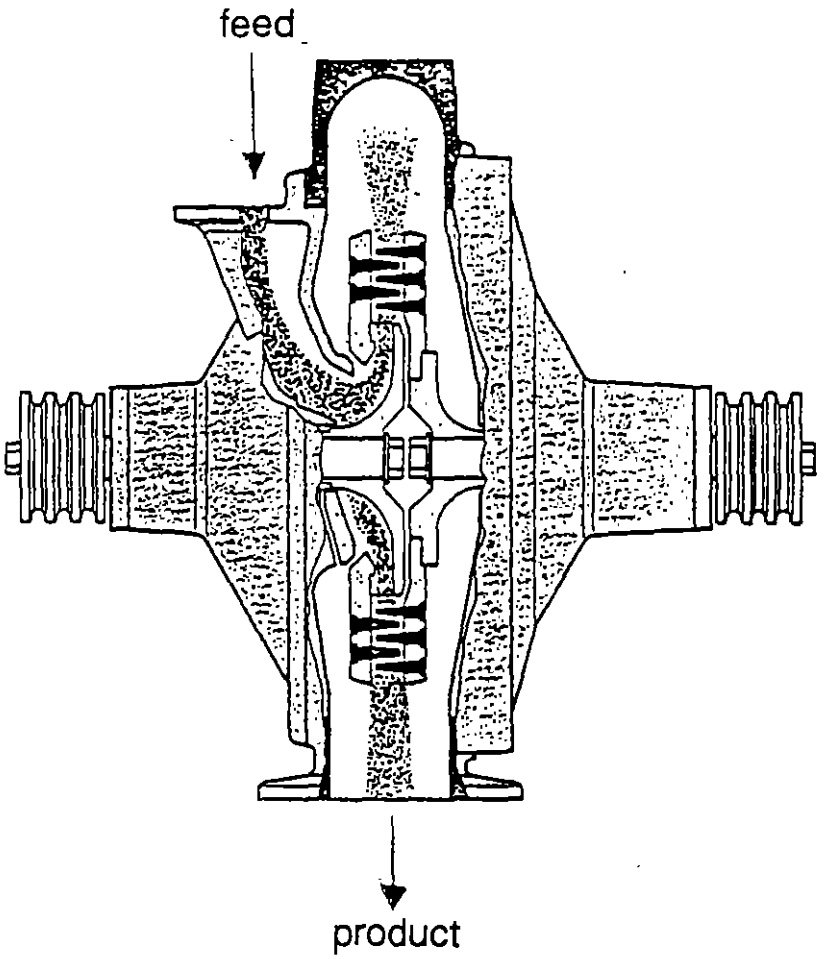

rotor diameter	315	450	630 mm
maximum speed	10000	7500	4500 rpm
motor power	2 x 22	2 x 45	2 x 55 kW

Tel.05321/6401 Fax 64074

Narrow Gab Rotor Impact Mill

gap width: 1 mm

maximum peripheral velocity: 120 m/s

fineness: minus 20 µm

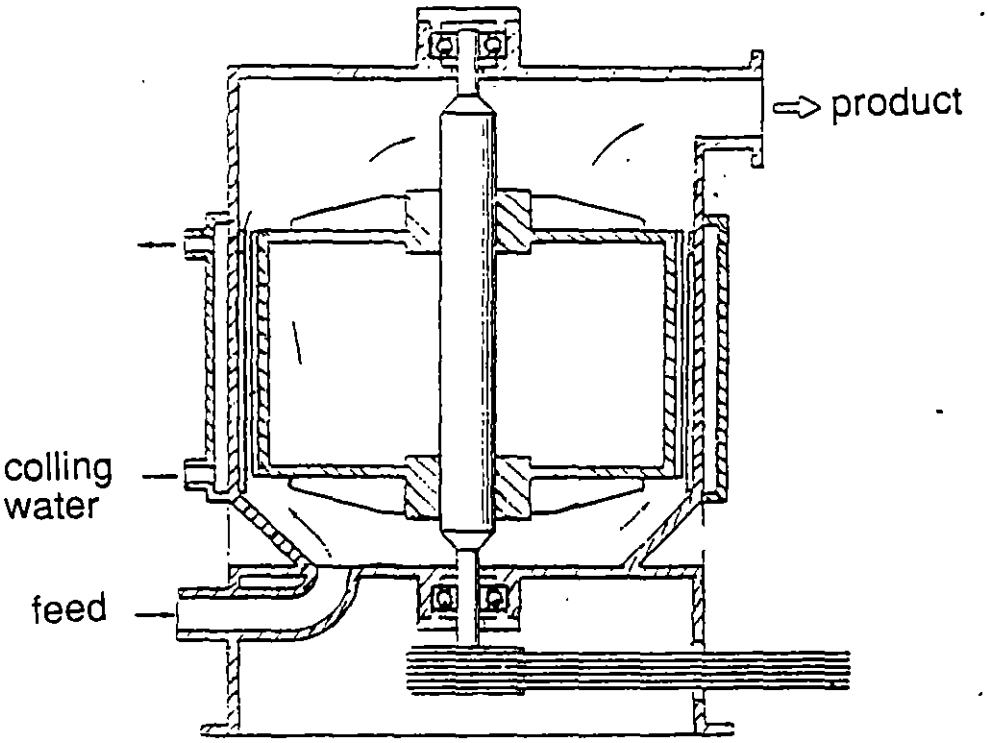

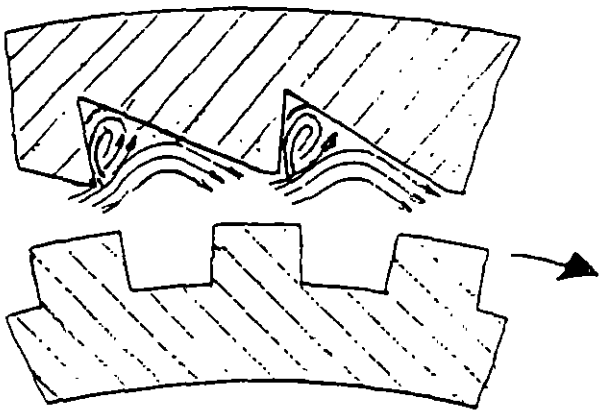

High Speed Rotor Impact Mill

maximum peripheral velocity: 200 m/s

gap width: 2 mm

fineness: minus 10 µm

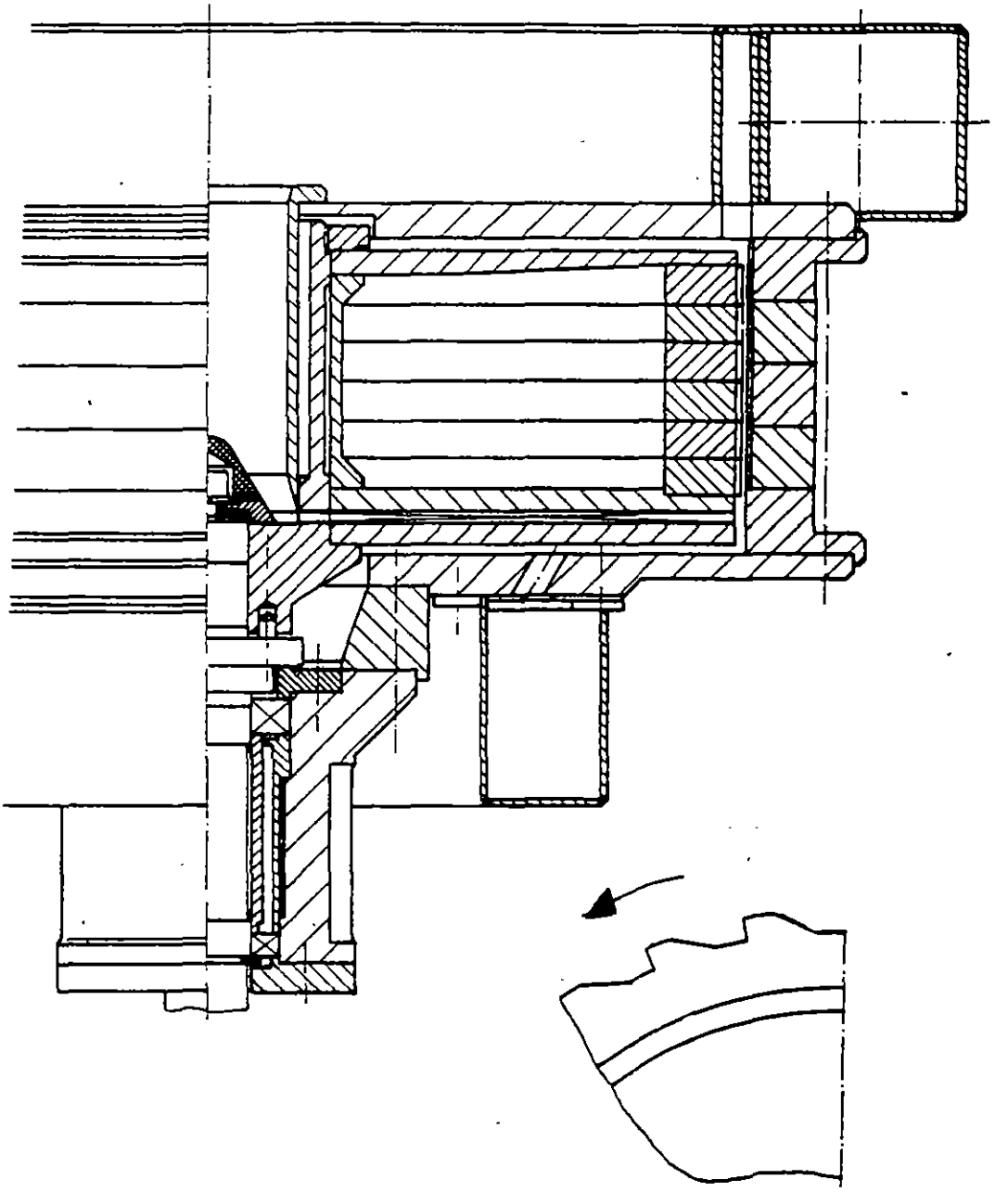

JET IMPACT MILLS (1)

In jet impact mills the particles are accelerated by drag forces in high speed jets and collide against each other. Particle-wall impacts are avoided to reduce wear. The energy consumption is much higher than with rotor impact mills, therefore jet mills are used only for high value substances to grind them from 100 to 300 µm below some ten micron or even very fine below some micron.

In some cases jet mills replace rotor impact mills for materials which can explode (chemical stubstances) because rotor mills are to consider being a potential spark source.

The flow pattern has to be such that an iterior turbulence region exists with a high particle concentration. Jet mills posses always an integrated air classification. The jet velocity is between 300 and 600 m/s if supplied with air or about 1000 m/s if supplied with steam. The air pressure is between 6 and 10 bar and the steam pressure between 15 and 30 bar.

Four different types of jet mills are manufactured:

- spiral jet mills
- oval tube jet mills
- opposite jet mills
- fluidized bed jet mills

JET IMPACT MILLS (2)

Spiral jet mill

The mill consits of a flat circular chamber. The obliquely orientaded nozzles are mounted in an interior ring dividing the chamber. The pressurized fluid (gas or steam) enters the outher chamber part, flows through the nozzles, creates a spiral flow and leaves the chamber through the central opening. The material is fed with an injector mounted between the nozzle ring and the outlet.The particles moving in a ring shaped region because of the centrifugal and radial drag forces. The spiral flow causes a classification. The particles stay in the chamber until they are broken down to the required fineness.

Chamber diameter 100 to 500 mm, throughput 5 to 100kg/h

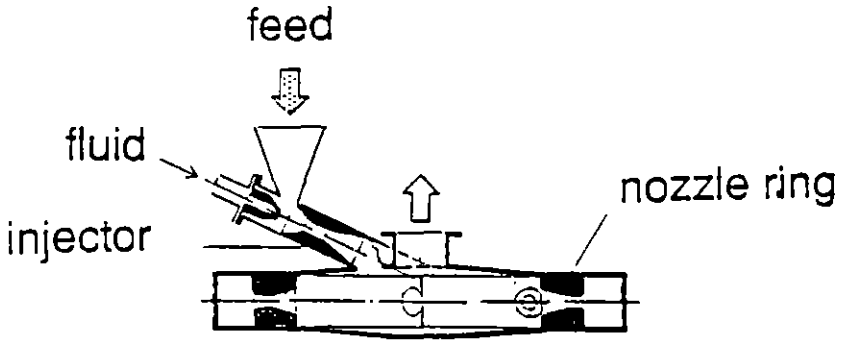

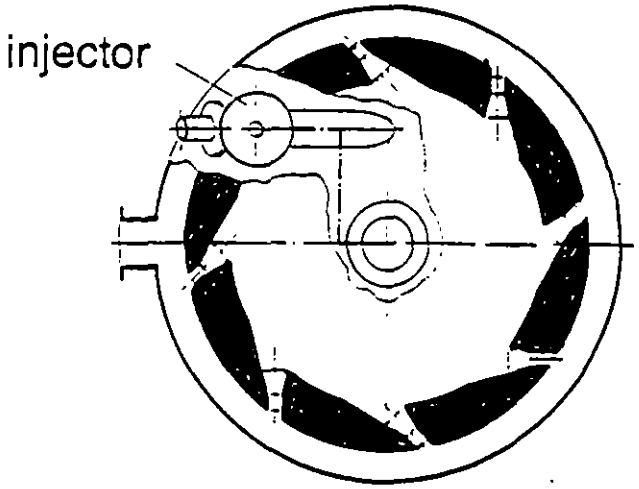

JET IMPACT MILLS (3)

The size cut x_c the classification can be estimated as

$$x_c = \text{const} \sqrt{\eta D / \rho_S v}$$

η: viscosity, ρ_S: particle density, D: outled diameter, v: radial fluid velocity at D. The constant depends on the particular design and is usually between 0.2 and 0.4, however it is to determine experimentally.

A spiral jet mill itself is relatively small, however the surrounding equipments take much space. The flow sheet of the worst case comprises: filter (1), compressor (2), cooler (3), liquid separater (4), pressure vessel (5), pressur filter (6), dryer (7), feeder (8), mill (9), cyclone (10), filter (11), eventually water jet ejector (12).

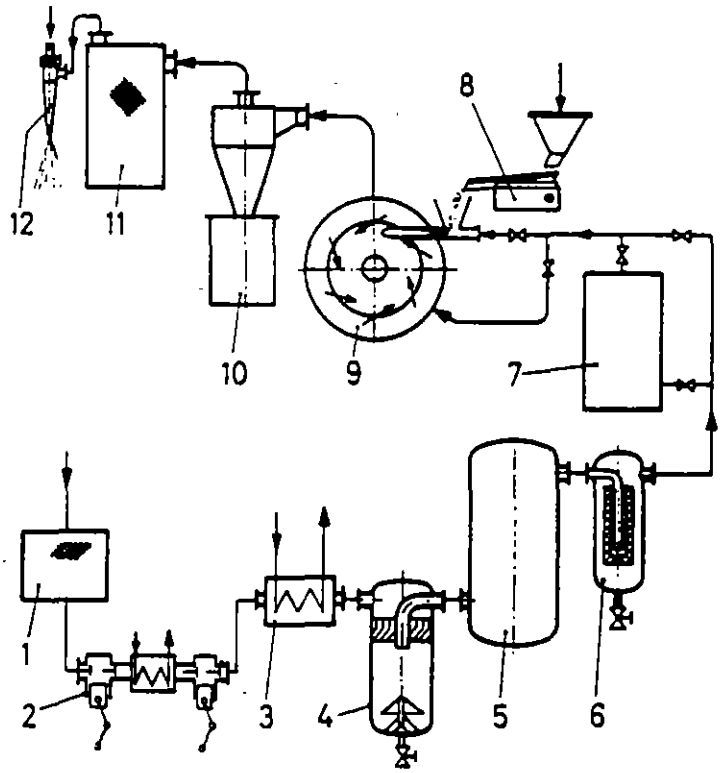

JET IMPACT MILLS (4)

Oval tube jet mill

The mill consits of tube bended to an oval.The pressurized fluid (air or steam) flows into the tube through nozzles mounted at the lower bend and causes a high turbulent flow in this region and also a circulating flow in the tube and leave it through a classifier in the upper region. The material is feed with an injector short above the nozzles. The separation cut x_c can be estimated with the relation:

$$x_c = \text{const} \sqrt{\eta\, b / \rho_S\, v}$$

η: viscosity, ρ_S, particle density, b: width of the flow before the classifier, v: fluid velocity before the classifier. The constant depends on the particular design and is usually between 6 and 9, however it is to determine experimentally.

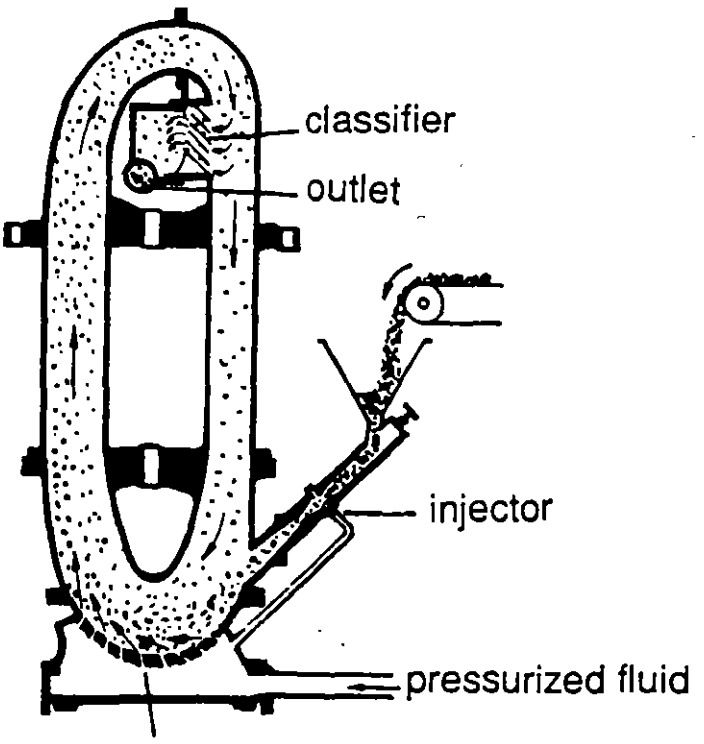

JET IMPACT MILLS (5)

Opposite jet mill

In this mill two flow tubes are directed against each other. The particles are fed into these tubes, are accelerated and collide in the mill chamber. The air flows to a rotor separator and the rejected coarse particles are recirculated to the flow tubes a schematical sketch is shown. This mill type was not very successful in technical application, however modification may improve the performance.

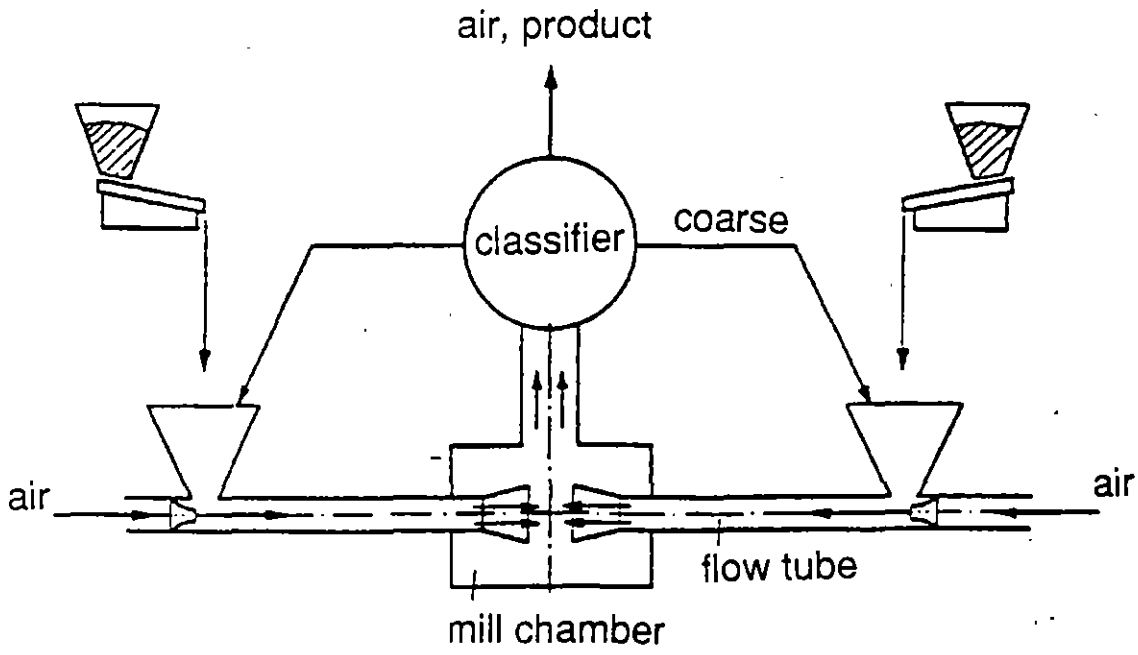

Tel.05321/64064 Fax 64074

Opposite Jet Mill

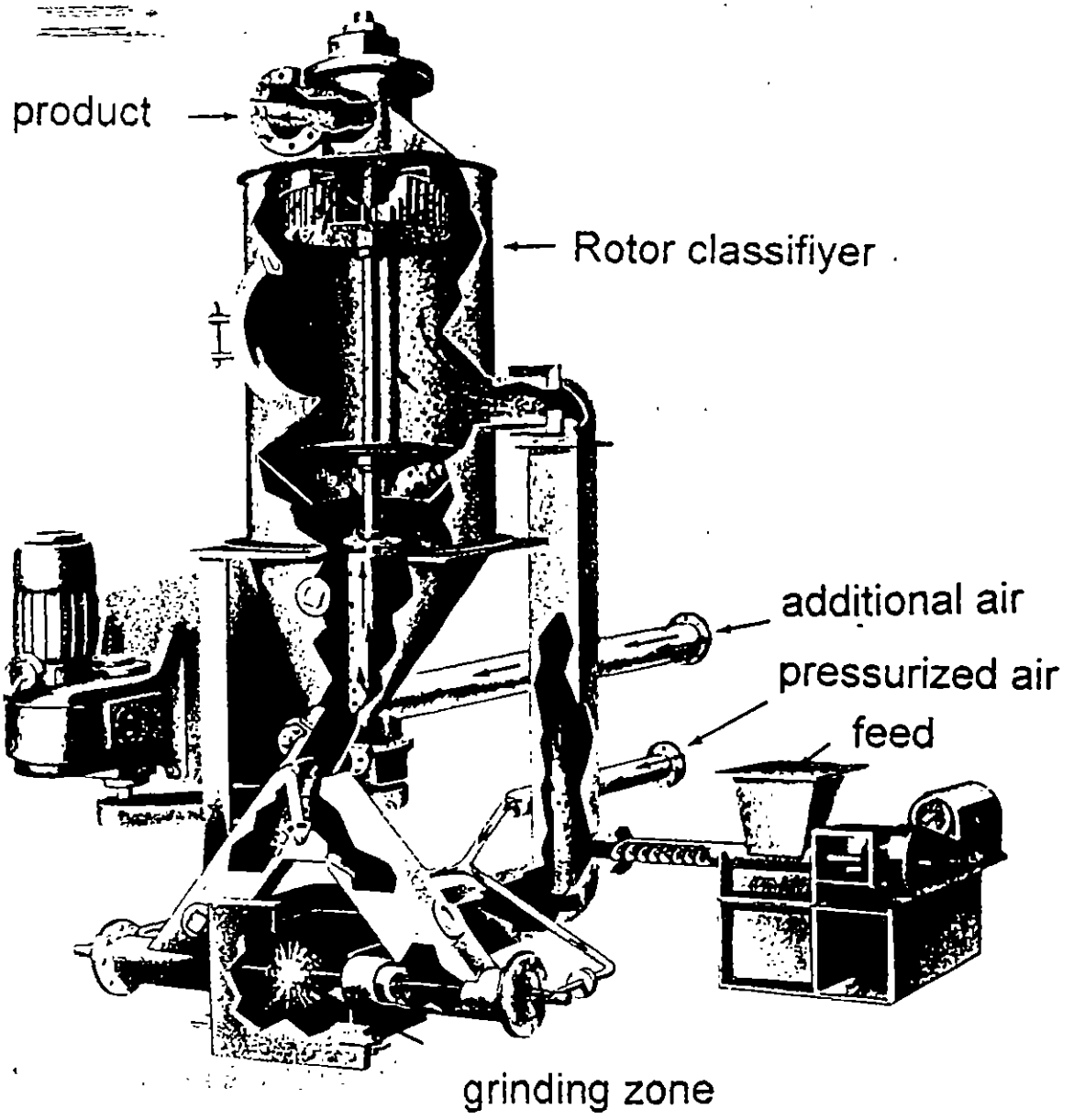

maximum throughput	12 t/h
maximum air flow	120 m^3/min
air pressure	7 bar

JET IMPACT MILLS (6)

Fluidized bed jet mill

The particular feature of this mill is that in the lower part of the mill vessel a particle bed is fluidized by 3 to 7 jets (number depending on the mill size). The particles are forced to collide strongly in order to be broken. The fine particles are carried upward to one or more rotor classifiers. Such mills are manufactured with a vessel diameter between 200 and 1000 mm, the throughput depends strongly on the material grindability and the required fineness and is between 5 and 1000 kg/h.

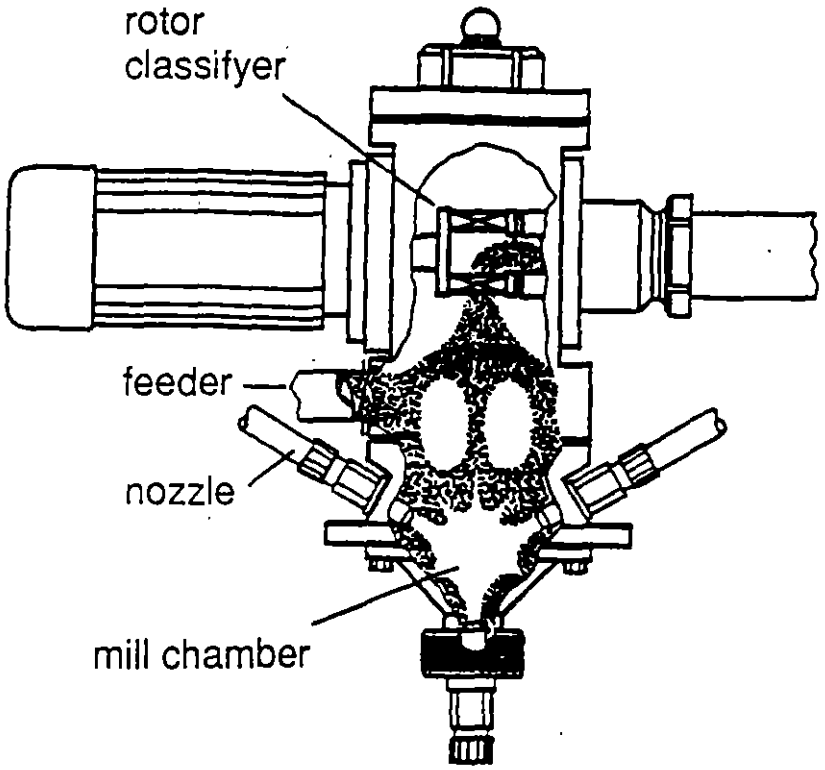

FACULTAD DE INGENIERIA U.N.A.M.
DIVISION DE EDUCACION CONTINUA

AVANCES EN LAS TECNICAS DE REDUCCION DE TAMAÑO Y CLASIFICACION DE PARTICULAS FINAS

ANEXO

PROFESOR KLAUS SCHONERT

1996

Palacio de Mineria Calle de Tacuba 5 Primer piso Deleg Cuauhtemoc 06000 Mexico, D.F. APDO. Postal M-2285
Teléfonos 512-8955 512-5121 521 7335 521-1987 Fax 510-0573 521-4020 AL 26

Eccentric Vibration Mill

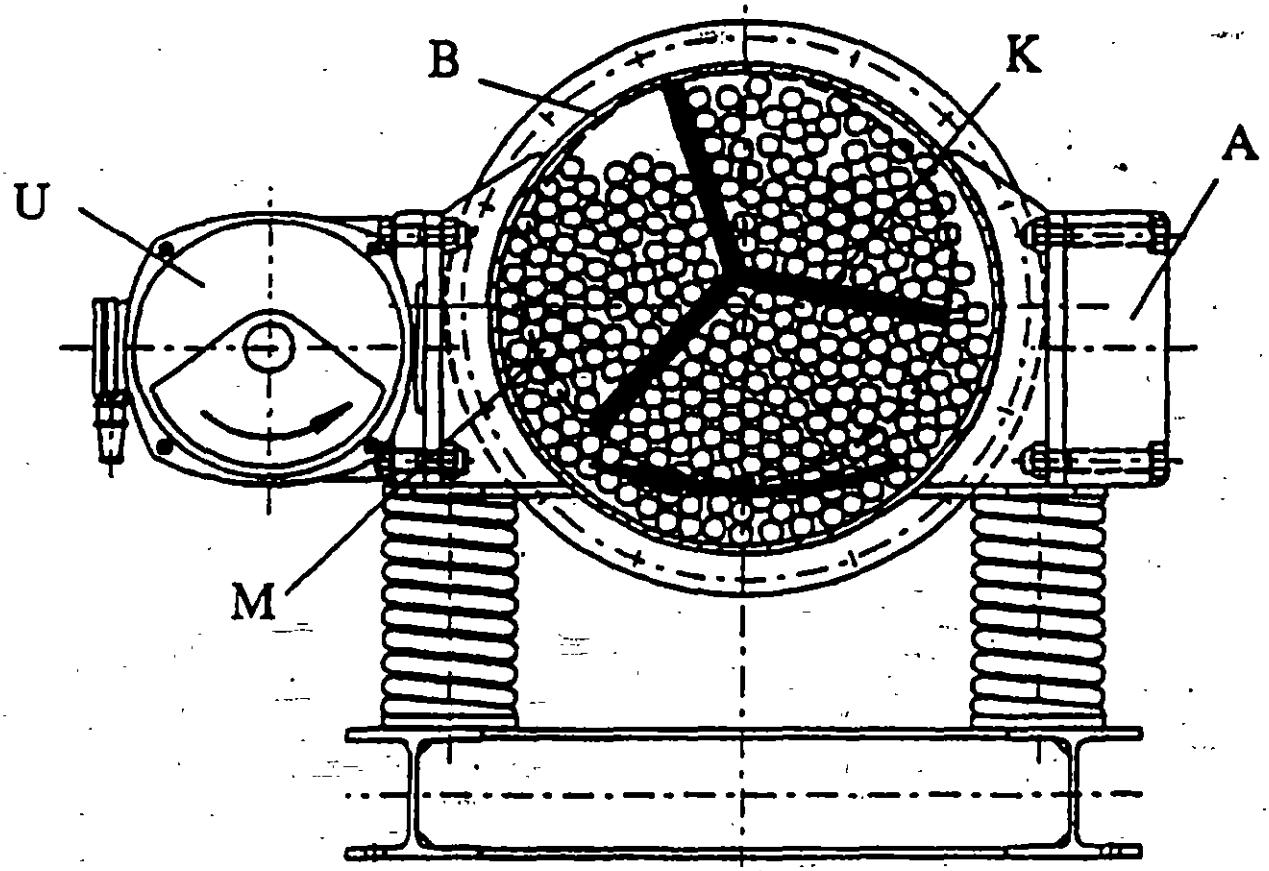

A: counter mass, B: mill vessel, M: Grinding balls,
K: cross-shaped momentum activator,
U: motor with eccentric weigth

mill diameter:	230 to 850 mm
mill length:	450 to 1360 mm
motor power:	1 to 40 kW
throughput:	0,2 to 4 t/h

Drag Coefficient for Spheres

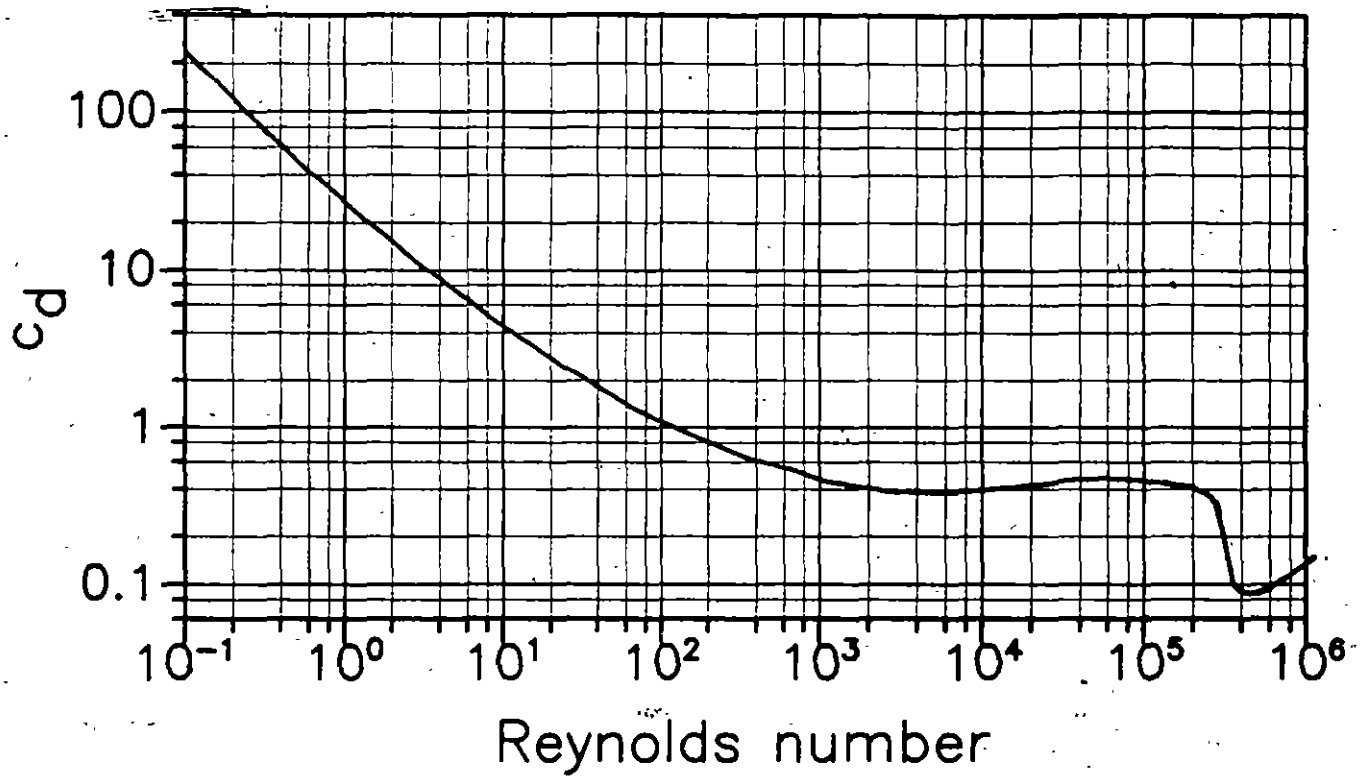

Ball Bearing Mill

type "Peters EM Mill"

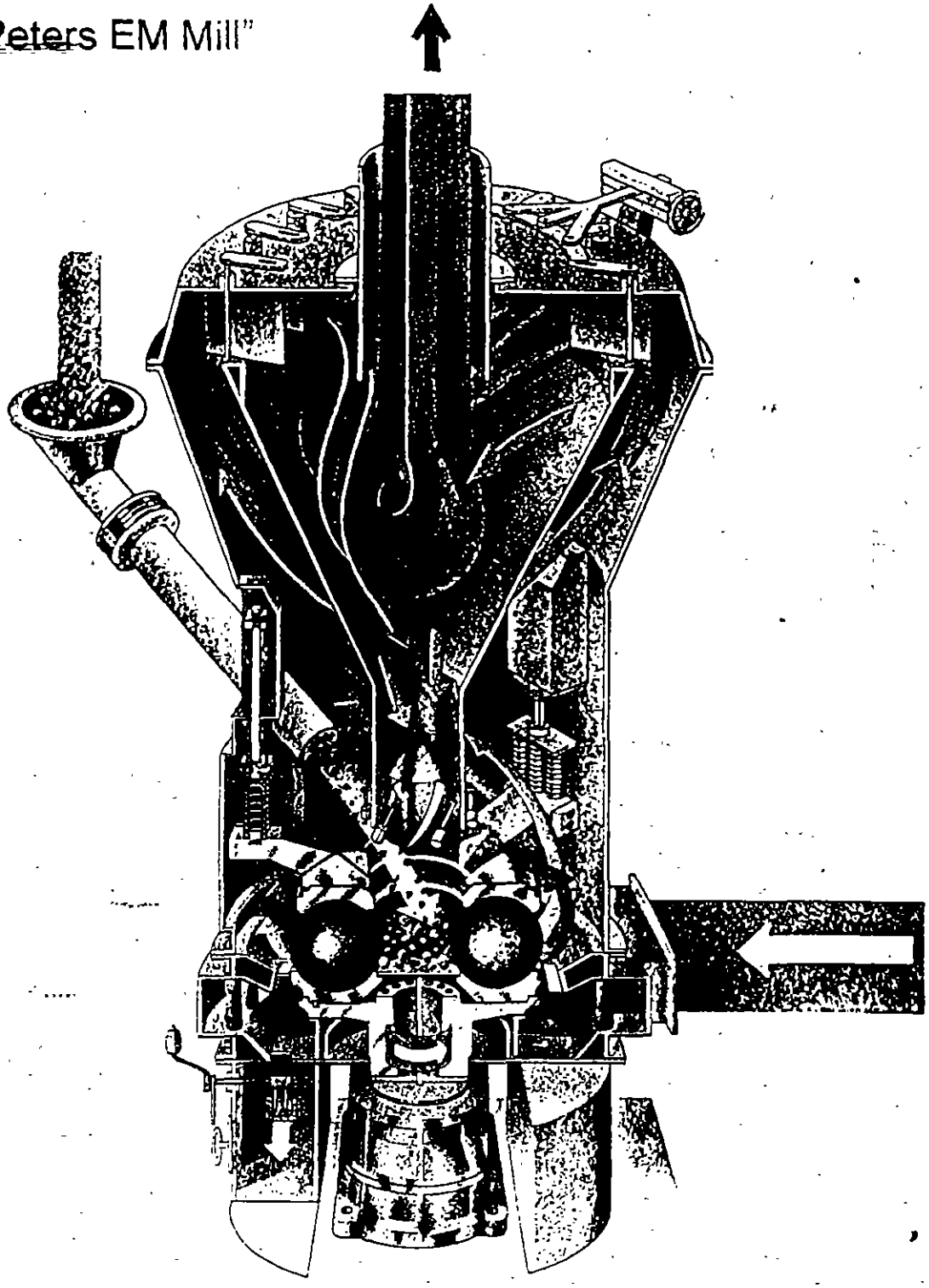

ball diameter:	500 to 1150 mm
number of rolls:	5 to 9
table motor power:	55 to 900 kW
throughput:	5 to 65 t/h (limestone)

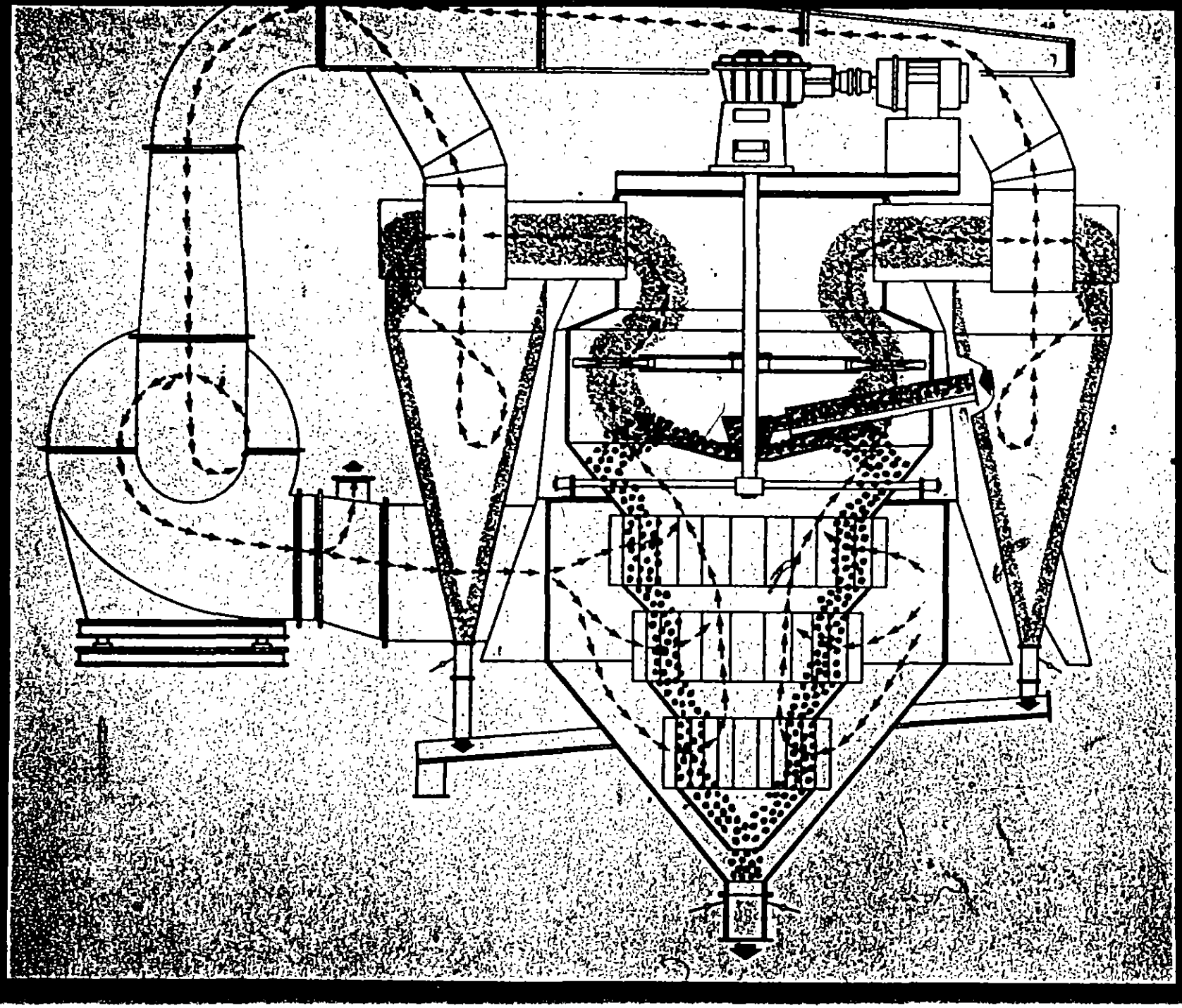

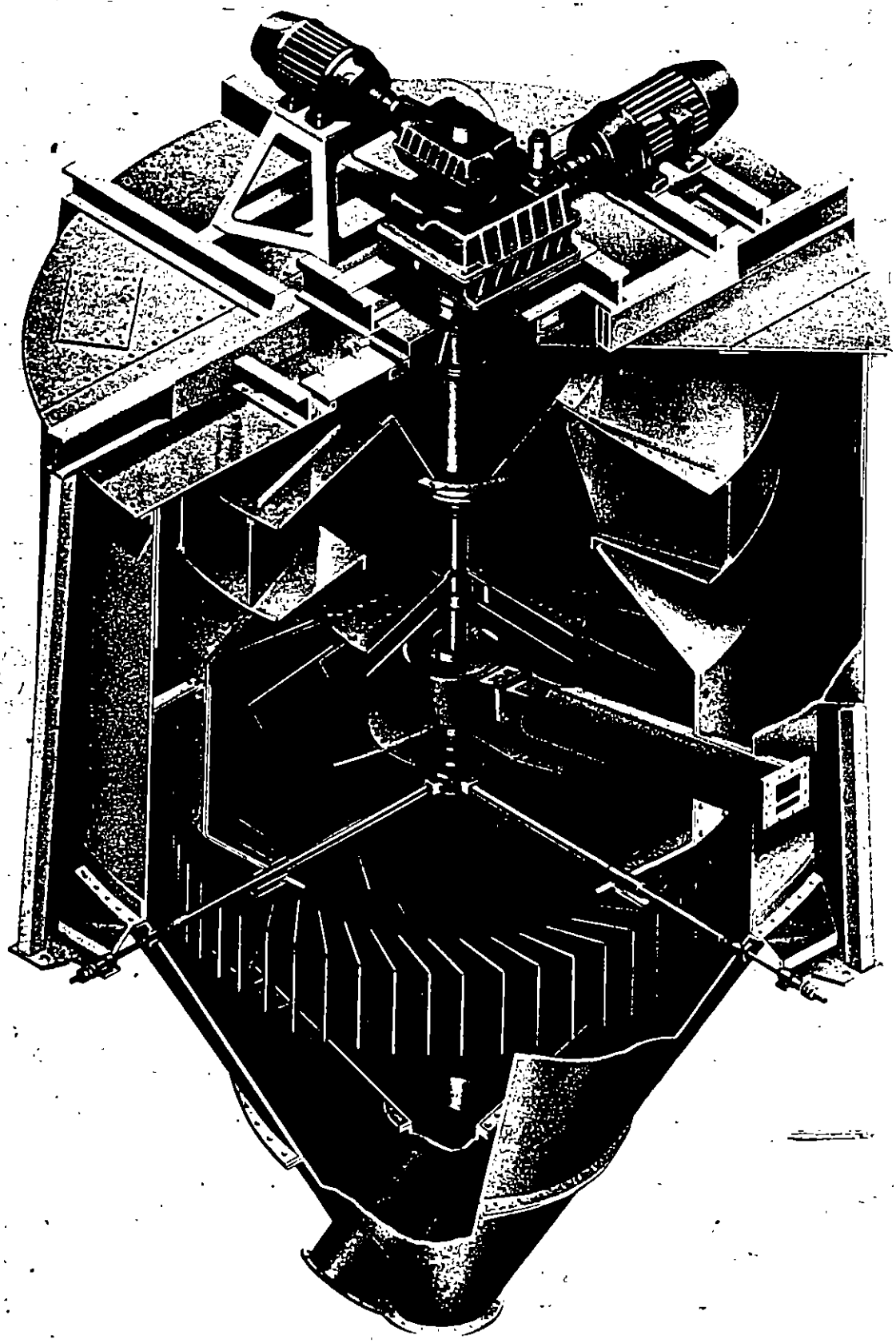

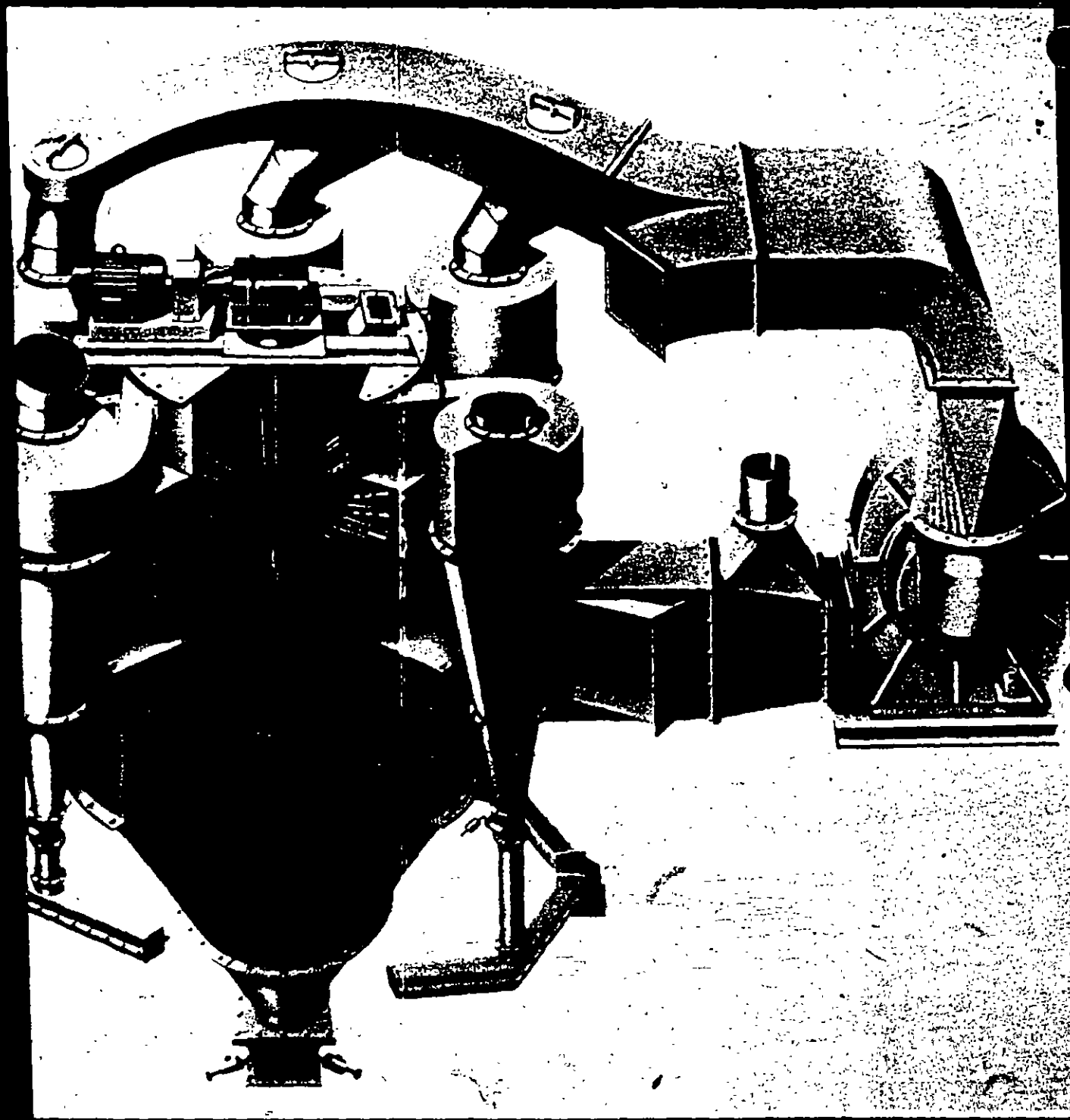

Zyklon - Umluftsichter

0-573

HUMBOLDT WEDAG

Schema Mikroplex-Spiralwindsichter MP, MPS

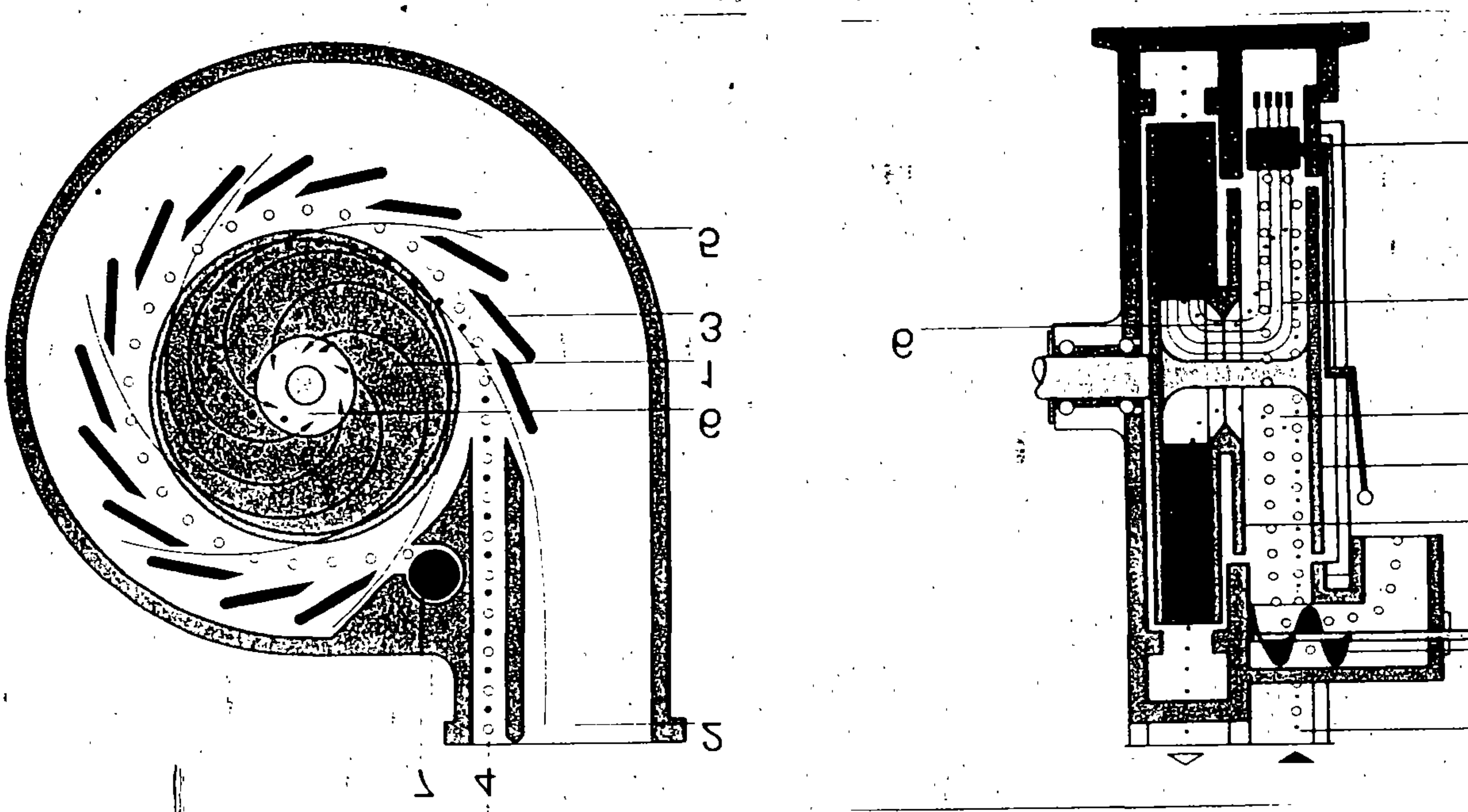

ALPINE

Multi Rotor Air Classifier

size, cm	mm	100-400	150-250	120-300	120-800	500-900	500-1000	500-1500
rotor diam.	mm	400	500	800	800	900	1200	1500
rotor speed	rpm	11200	9000	4000	5400	5000	4800	4500
number of rotors		1 or 4	1 or 4	1 or 6	1 or 4	1	1	1
motor power of one rotor	kW	3	8	11	15	55	90	45

Rotor Air Classifier

size cut: 20 to 200 µm

maximum rotor speed: 40 m/s

maximum throughput 240 t/h

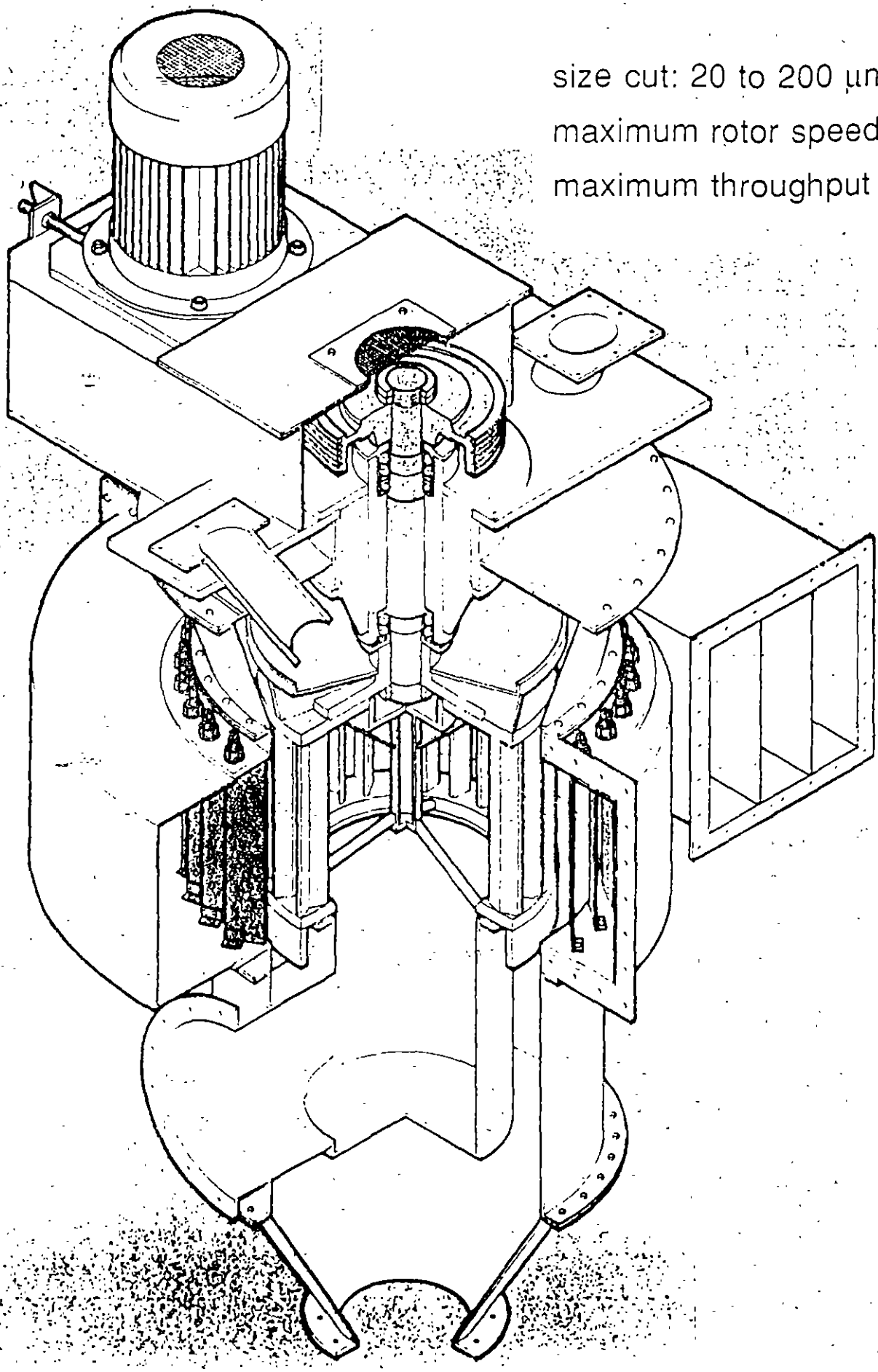

Classifying Decanter

classification in the microrange

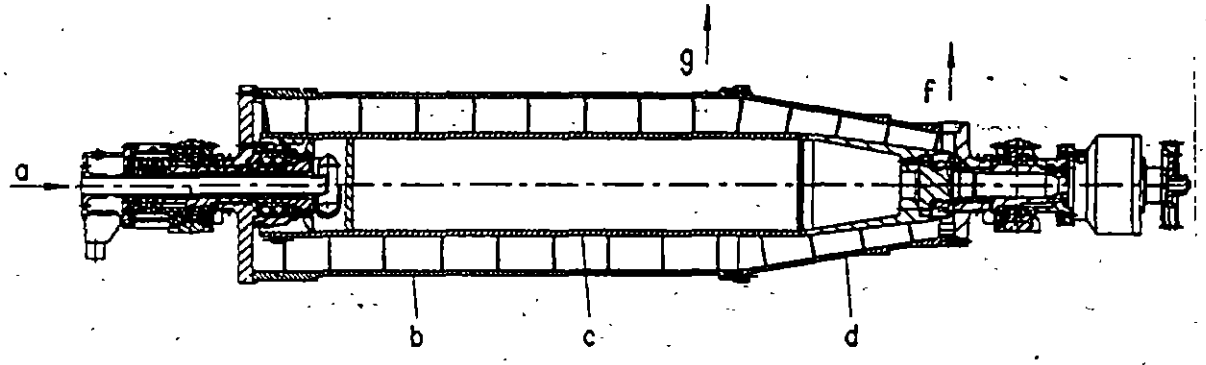

(a) feed
(b) centrifuge body
(c) rotating screw for transporting the coarse product
(d) conė
(f) fine product
(g) coarse product

centrifugal acceleration	100g to 2000g
suspension throughput	500 to 2500 l/h
solid feed load	up to 30 mass%
maximum speed	4500 rpm

Tel. 05321/64064 Fax 64074

Classifying Decanter

classifying in the microfine range

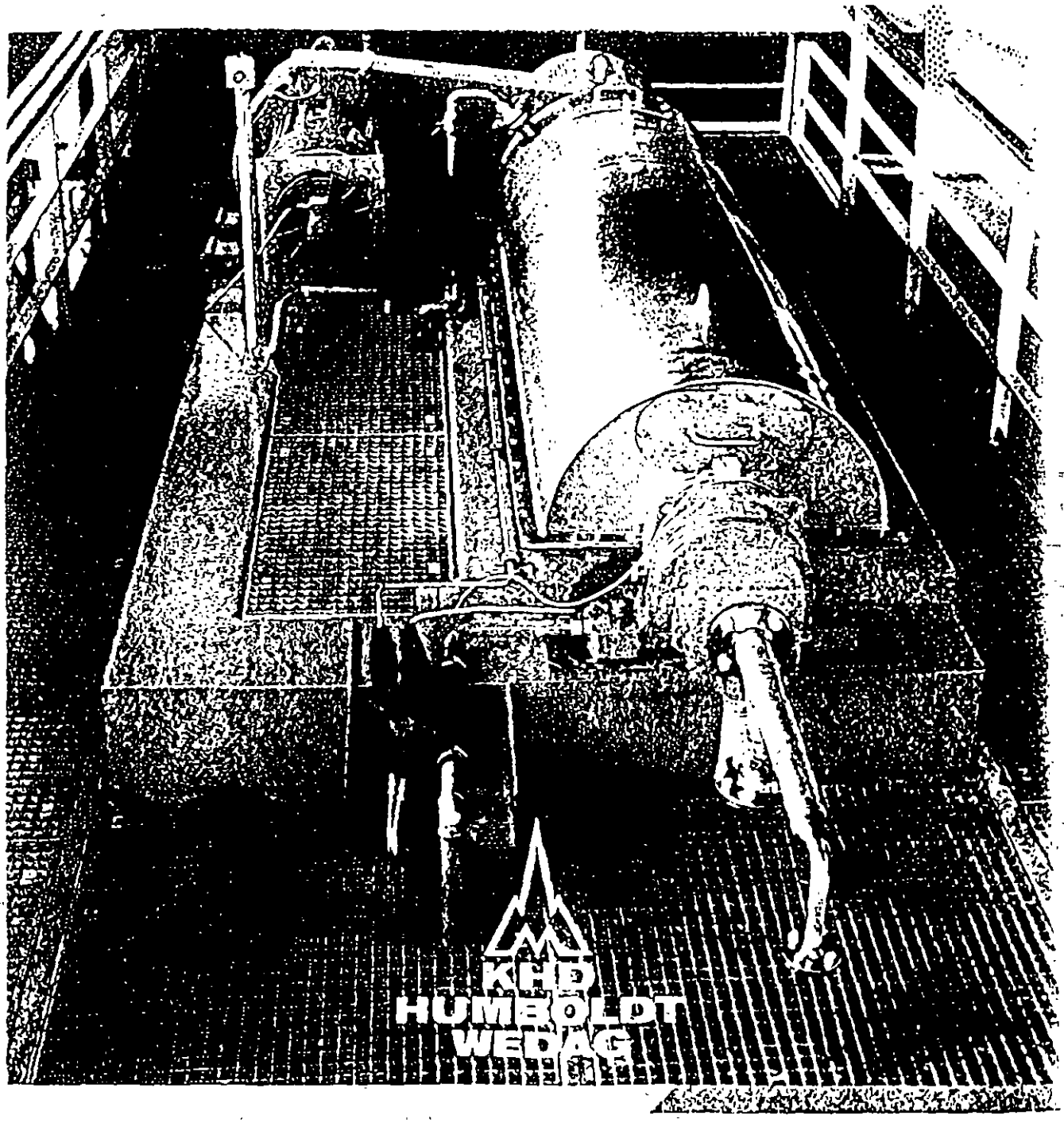

PAUL RAUSCH GMBH, BONN
Tel.0 53 21/6 40 64 Fax 6 40 74

Tel.05321/64064 Fax 64074

DEVICE (1)

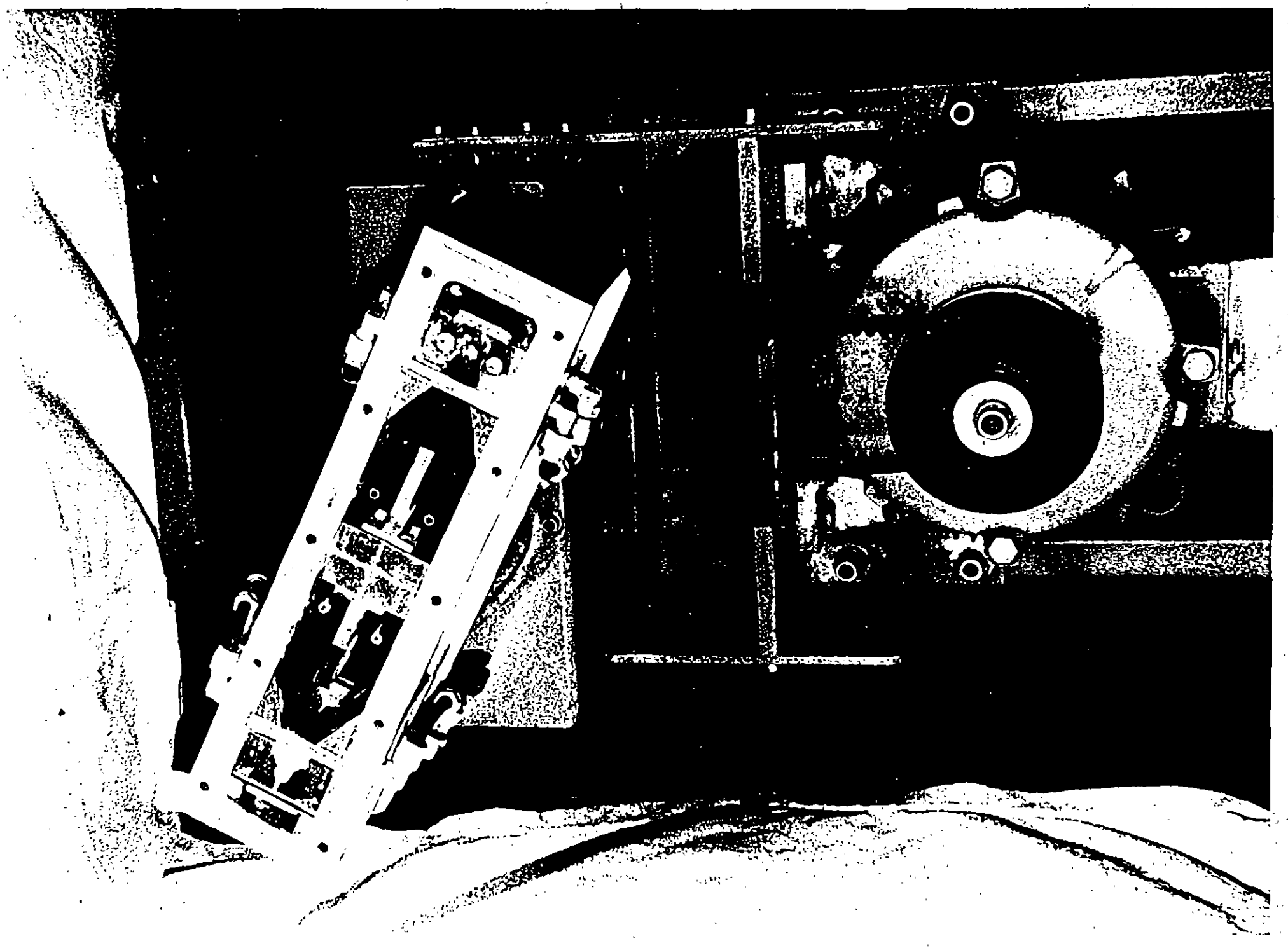

PAUL HAUSEN Bonn, Bosial
Tel. 05321/64064 Fax 64074

DEVICE (2)

cross-sections of the rotor

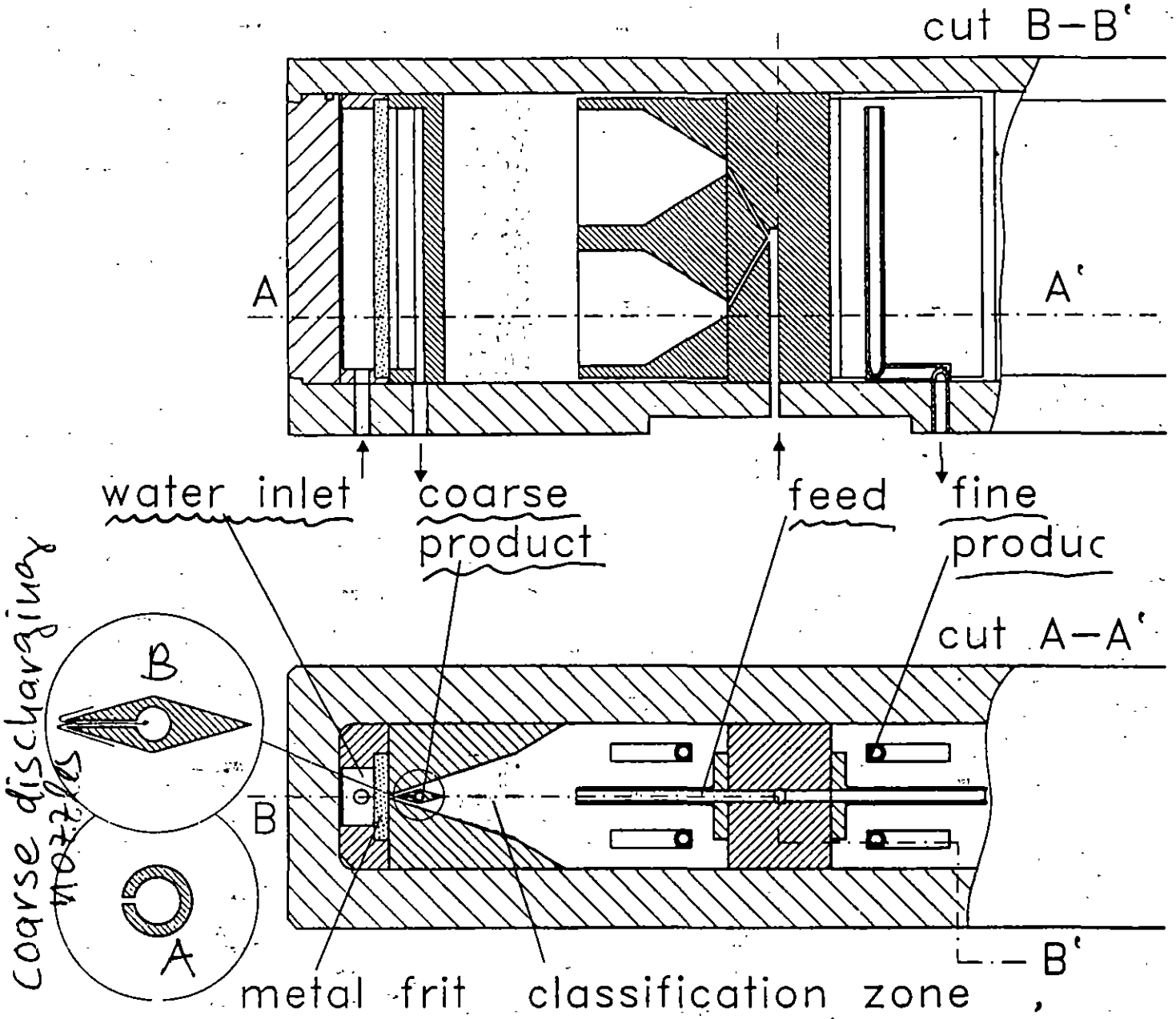

exterior diameter of the classification zone 230 mm

outer width of the classification zone 15 mm

centrifugal acceleration 200 ... 1000g

EXPERIMENTAL PROGRAM

Feed material	:	quartz and calcite - 20 µm
Feed solids load δ_F	:	10, 20 and 30 vol.%
		21, 35 and 53 mass%
Cut size	:	1 to 5 µm
Acceleration	:	300g to 900g

Size analysis with Sedigraph

Q_F, Q_{fi}, Q_{co}	:	psd. of feed and the fine and coarse product
x_{th}	:	theoretical size cut
T(x)	:	classification efficiency curve
x_t	:	experimental size cut, $T(x_t) = 0,5$
$\kappa = x_{25}/x_{75}$	:	separation sharpness

$R_{fi} = f\, Q_{fi}(x_t) / (Q_F(x_t)$: recovery of fine particles

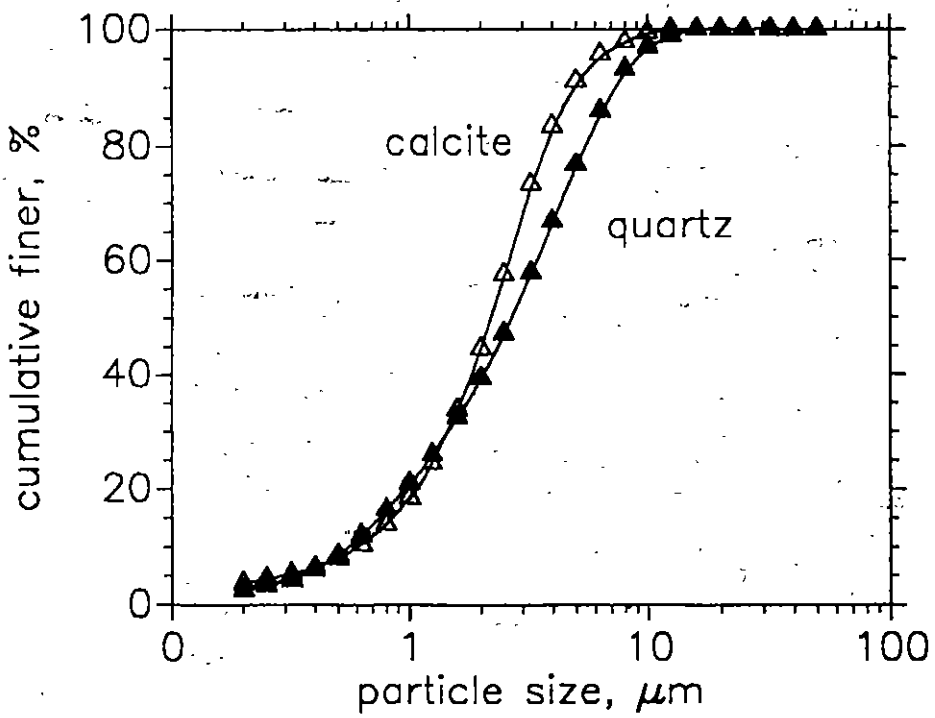

CENTRIFUGAL ACCELERATION

coarse discharging nozzle B

calcite -20 µm, δ_F = 10 vol.%, x_{th} = 1.4 µm

$\dot{V}_F$ = 60 ml/min, $\dot{V}_{co}$ = 150; 300; 450 ml/min

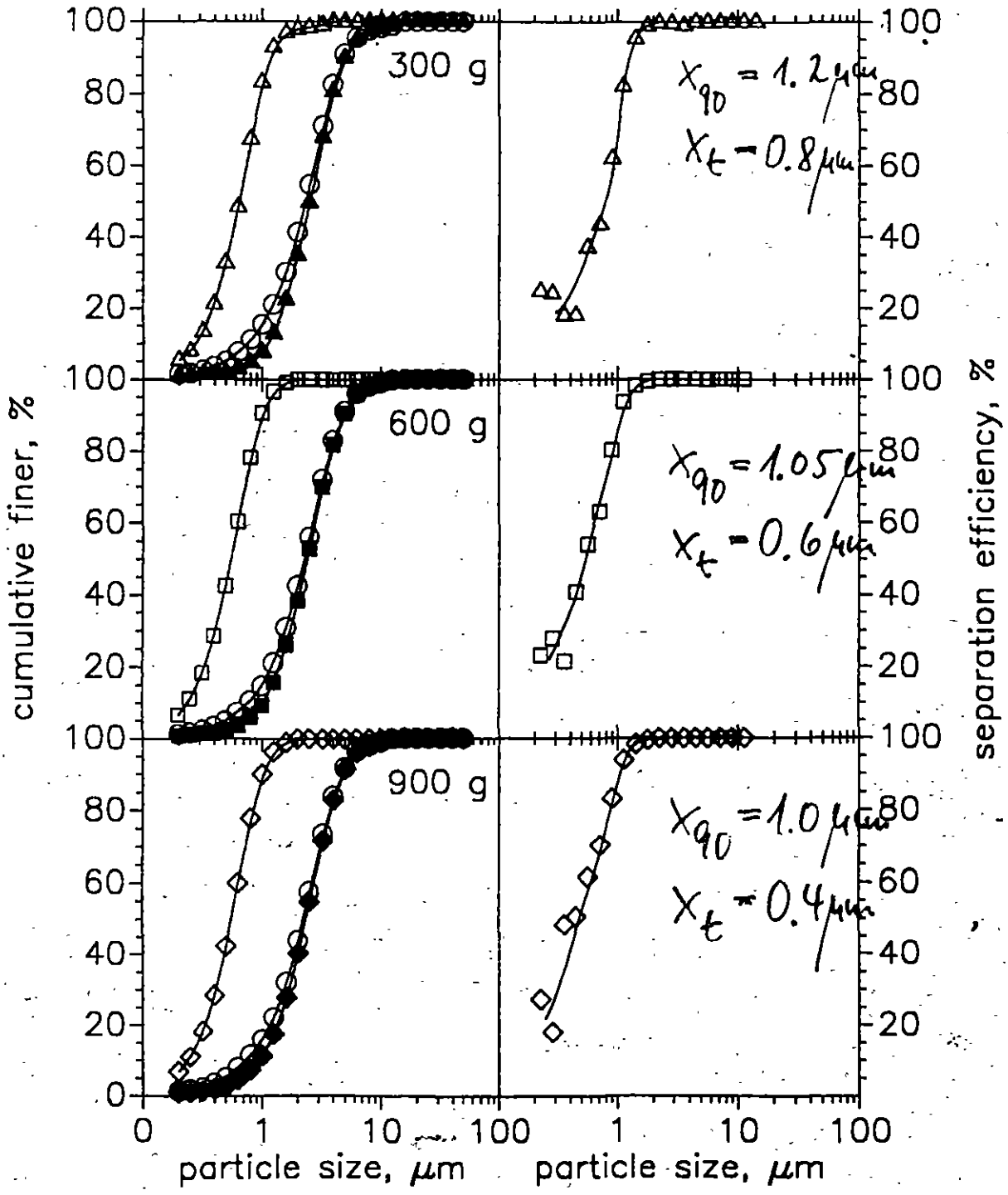

Tel.05321/6406 4 Fax 64074

FEED SOLIDS LOAD

coarse discharging nozzle B
quartz -20 µm, a = 300g, x_{th} = 3.2 µm
$\dot{V}_F$ = 30 ml/min, $\dot{V}_{co}$ = 70 ml/min

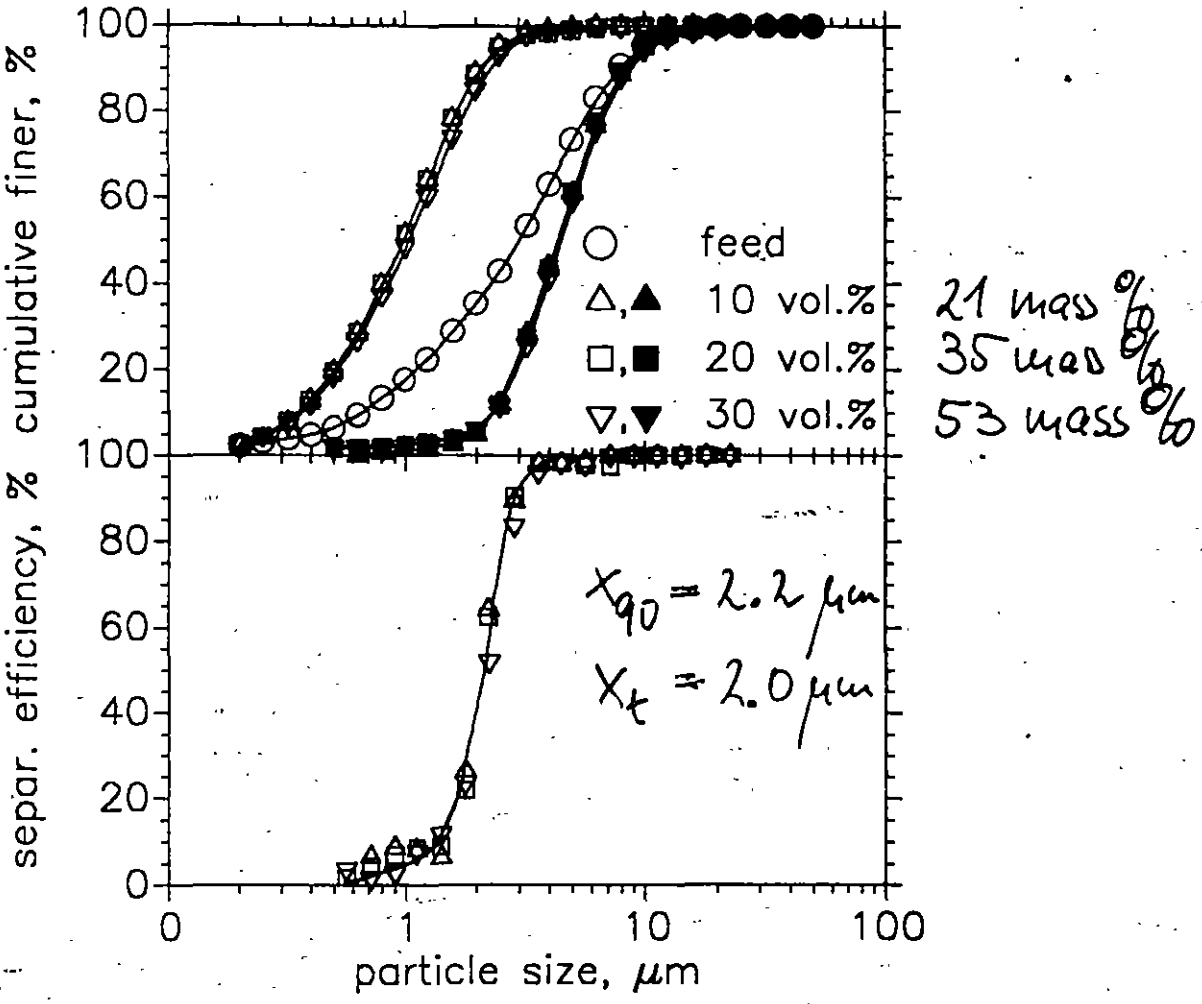

Solids load of feed (δ_F), coarse product flow (δ_{co}) and fine porduct flow (δ_{fi})

δ_F	δ_{co}	δ_{fi}	
10	3.4	1.9	%
20	5.4	2.1	%
30	10.8	2.2	%

Tel.05321/6406 4 Fax 6 40 74

COMPARISON OF DIFFERENT CLASSIFIERS (1)

Centrisizer (KHD), a = 500g
Hydroplex (Hosokawa Alpine), a = 625g
Fryma Classifier, a = 600g
Clausthal Centrifuge, a = 300g
Calcite finer 20 to 30 µm

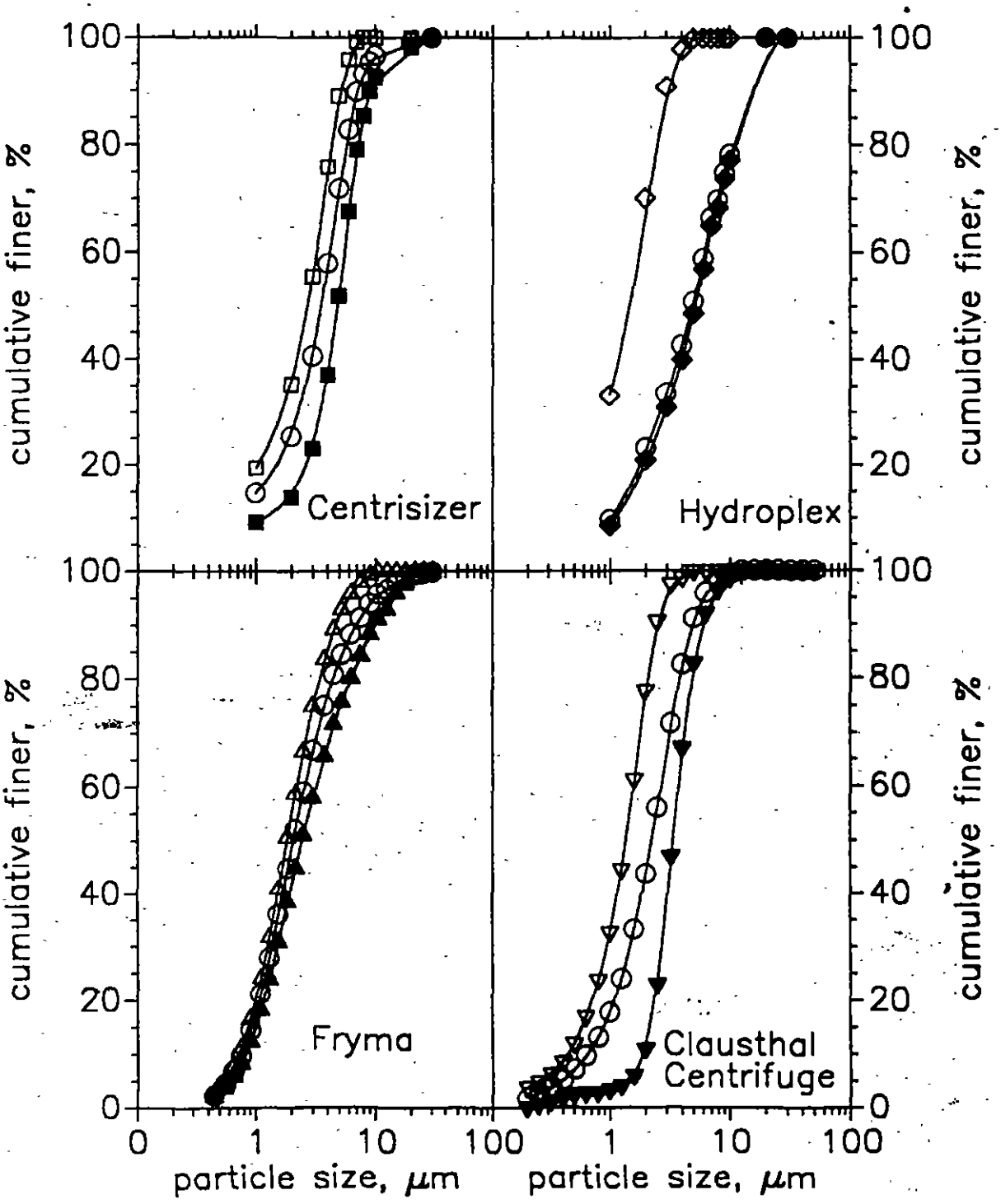

Tel.05321/6 40 64 Fax 6 40 74

COMPARISON OF DIFFERENT CLASSIFIERS (2)

Centrisizer (KHD), a = 500g
Hydroplex (Hosokawa Alpine), a = 625g
Fryma Classifier, a = 600g
Clausthal Centrifuge, a = 300g
Calcite finer 20 to 30 µm

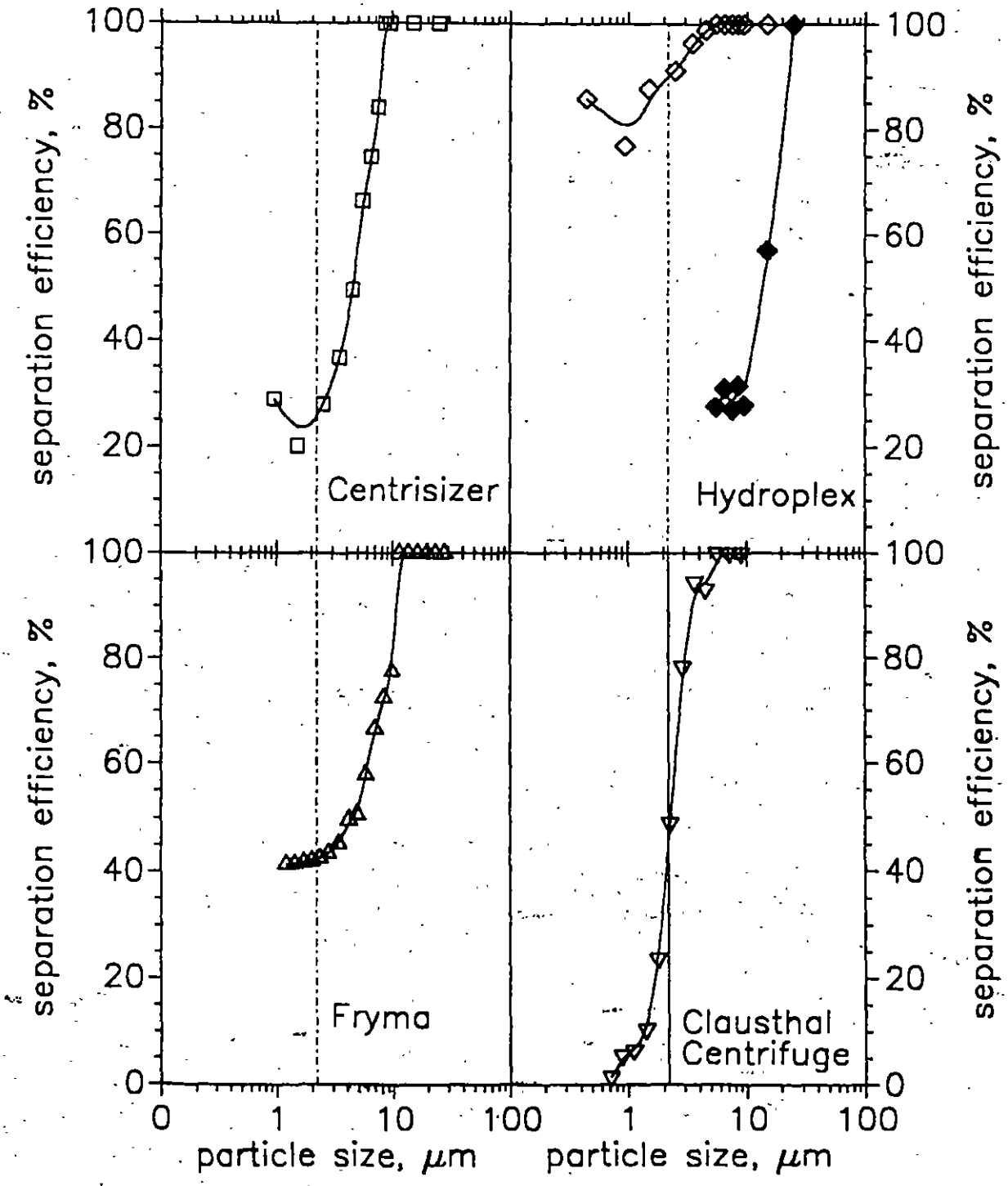

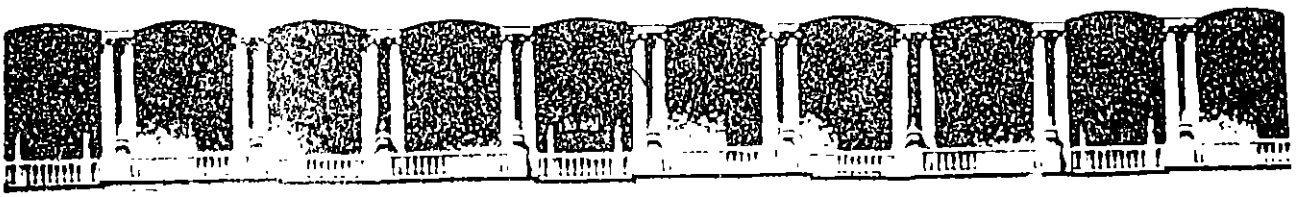

FACULTAD DE INGENIERIA U.N.A.M.
DIVISION DE EDUCACION CONTINUA

AVANCES EN LAS TECNICAS DE REDUCCION DE TAMAÑO Y CLASIFICACION DE PARTICULAS FINAS
DEL 30 DE SEPTIEMBRE AL 4 DE OCTUBRE DE 1996
DIRECTORIO DE PROFESORES

ING. JOSE IGNACIO FLORES GOMEZ
GERENTE GENERAL
REGIO CAL, SA DE CV
CERRO DE LAS MITRAS No 2350
OBISPADO
64060 MONTERREY, NUEVO LEON
91 83 48 25 00

ING. LUIS ANTONIO GARCIA GARCIA
ESTUDIANTE
FACULTAD DE QUIMICA, UNAM
CIUDAD UNIVERSITARIA
COYOACAN
04510 MEXICO D.F.
682 71 11

ING. SALVADOR GARCIA GARCIA
INVESTIGADOR DE LABORATORIO
SERVICIOS CONDUMEX, SA DE CV
CARRETERA A SLP KM 9.6
PARQUE INDUSTRIAL JURICA
76100 QUERETARO, QUERETARO
91 42 18 18 02

ING. CARLOS EDUARDO GARZA GONZALEZ VELEZ
JEFE DEL DEPTO DE YACIMIENTOS
FACULTAD DE INGENIERIA, UNAM
CIRCUITO ESCOLAR, CU
COYOACAN
04510 MEXICO D.F.

ING. HOMERO GEORGE TELLEZ
ESTUDIANTE
FACULTAD DE INGENIERIA, UNAM
MAYAS M 101 No 40
AJUSCO COYOACAN
04300 MEXICO D.F.
618 67 60

RAFAEL GONZALEZ LOPEZ

ING. JOSE LUIS JIMENEZ MENDOZA
PROFESOR DE TIEMPO COMPLETO
FACULTAD DE INGENIERIA, UNAM
CIRCUITO ESCOLAR, CU
COYOACAN
04510 MEXICO D.F.
622 09 18

ING. ISRAEL LUCAS LAGUNAS
ESTUDIANTE
FACULTAD DE QUIMICA, UNAM
RIO COLORADO No 10
PUENTE BLANCO IZTAPALAPA
09770 MEXICO D.F.
693 14 73

ING. MIGUEL MARQUEZ MARTINEZ
PROFESOR
FACULTAD DE INGENIERIA, UNAM
CIUDAD UNIVERSITARIA
COYOACAN
04510 MEXICO D.F.
622 08 55

ING. JOSE NOEL MENERA GOMEZ
ESTUDIANTE
FACULTAD DE QUIMICA, UNAM
VIOLETA MZ 188-B LT 19
HANK GONZALEZ IZTAPALAPA
09700 MEXICO D.F.
691 53 82

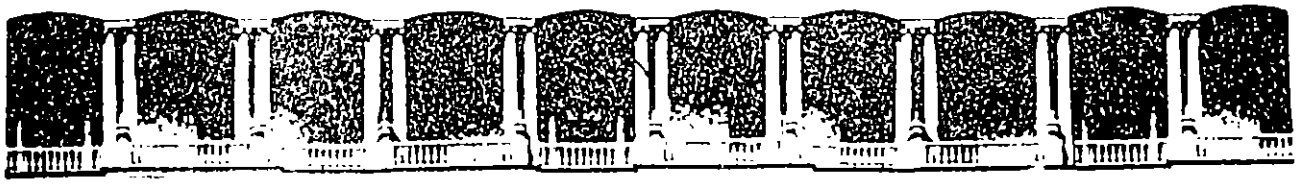

FACULTAD DE INGENIERIA U.N.A.M.
DIVISION DE EDUCACION CONTINUA

AVANCES EN LAS TECNICAS DE REDUCCION DE TAMAÑO Y CLASIFICACION DE PARTICULAS FINAS
DEL 30 DE SEPTIEMBRE AL 4 DE OCTUBRE DE 1996
DIRECTORIO DE PROFESORES

ING. HOMERO MONJARDIN LOPEZ

SERVICIOS CORP. FRISCO
JAIME BALMES No 11-C
LOS MORALES POLANCO MIGUEL HIDALGO
11510 MEXICO D.F.
626 77 99 EXT 173

ING. MARISA ISABEL MUÑOZ OCHOA
ING. METALURGISTA
CONSEJO DE RECURSOS MINERALES
AV. INDUSTRIAS No 6
PARQUE INDUSTRIL ROBINSON
CHIHUAHUA, CHIHUAHUA
20 05 77

ANGEL NAVA CARRILLO

ING. JOSE LUIS NAVARRO REYNA
JEFE DEL DEPTO DE GEOLOGIA Y G
FACULTAD DE INGENIERIA, UNAM
CIRCUITO INTERIOR, CU
COYOACAN
04510 MEXICO D.F.
622 08 54

ING. JUAN LUIS REYES BAHENA
PROFESOR INVESTIGADOR
INSTITUTO DE METALURGIA
SIERRA LEONA No 550
LOMAS 2da SECCION
78210 SLP, SLP
25 43 26

ING. FRANCISCO JAVIER REYES CARMONA
ACADEMICO
INSTITUTO POLITECNICO NACIONAL
U PROF ADOLFO LOPEZ MATEOS EDIF 7
ZACATENCO GUSTAVO A MADERO
07320 MEXICO D.F.
729 60 00 EXT 54408

SALVADOR RODRIGUEZ

ING. JUAN CARLOS RUIZ MENDEZ
ENCARGADO DE EXP. METALURGICA
CONSEJO DE RECURSOS MINERALES
Cda DE SANTA ROSA No 4
LOMAS DE CHAPULTEPEC MIGUEL HIDALGO
11000 MEXICO D.F.
520 24 11 520 24 13

ING. JOSE ISRAEL SALAZAR RAMIREZ
JEFE DE DEPTO
INDUSTRIA MINERA MEXICO
DOMICILIO CONOCIDO
FRACC. MORALES A.P. 1305
78180 SLP, SLP
13 95 15 EXT 1803

ING. CARLOS SANCHEZ RUELAS
SUPERINTENDENTE DE AREA
INDUSTRIAL MINERA MEXICO
DOMICILIO CONOCIDO
FRACC. MORALES A.P. 1803
78180 SLP, SLP
13 95 15 EXT 1700

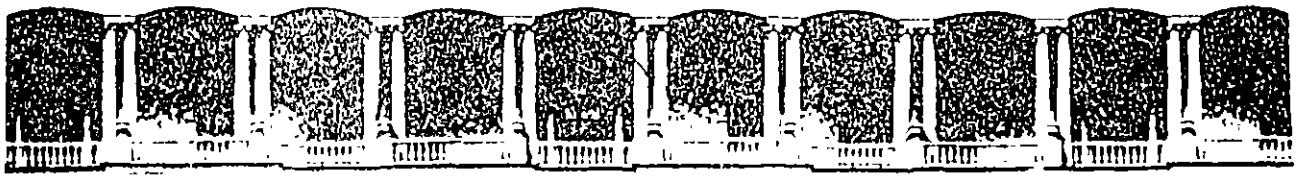

FACULTAD DE INGENIERIA U.N.A.M.
DIVISION DE EDUCACION CONTINUA

AVANCES EN LAS TECNICAS DE REDUCCION DE TAMAÑO Y CLASIFICACION DE PARTICULAS FINAS
DEL 30 DE SEPTIEMBRE AL 4 DE OCTUBRE DE 1996
DIRECTORIO DE PROFESORES

CLAUDIA SANTOS MARTINEZ

ING. LUIS TREVIÑO VILLARREAL
INGENIERO DE PROCESO
CEMEX CENTRAL
AV. CONSTITUCION No 444 PTE
CENTRO
64000 MOTERREY, NUEVO LEON
351 51 00

ING. MIGUEL VERA OCAMPO
FACULTAD DE INGENIERIA, UNAM
CIUDAD UNIVERSITARIA
COYOACAN
04510 MEXICO D.F.
622 09 18

ING. ROBERTO ESTEBAN VILLAPANDO CORTES

ZARAGOZA No 138
ROMERO DE TERREROS COYOACAN
04360 MEXICO D.F.
658 57 63

ING. LEONEL VILLAVICENCIO LOPEZ
GERENTE PLANTA
REGIO CAL, SA DE CV
CERRO DE LAS MITRAS No 2350
OBISPADO
64060 MONTERREY, NUEVO LEON
348 25 00